REPORT DOCUMENTATION PAGE

Form Approved
OMB No. 0704-0188

1. AGENCY USE ONLY *(Leave blank)*	2. REPORT DATE	3. REPORT TYPE AND DATES COVERED
	9 Jan 97	

4. TITLE AND SUBTITLE
A Case Study of the Low-Level Jet During An Episode of Spring Convection

5. FUNDING NUMBERS

6. AUTHOR(S)
Christopher Scott Donahoe

7. PERFORMING ORGANIZATION NAME(S) AND ADDRESS(ES)
Texas A&M University

8. PERFORMING ORGANIZATION REPORT NUMBER
96-123

9. SPONSORING/MONITORING AGENCY NAME(S) AND ADDRESS(ES)
DEPARTMENT OF THE AIR FORCE
AFIT/CI
2950 P STREET
WPAFB OH 45433-7765

10. SPONSORING/MONITORING AGENCY REPORT NUMBER

11. SUPPLEMENTARY NOTES

12a. DISTRIBUTION AVAILABILITY STATEMENT
Unlimited

12b. DISTRIBUTION CODE

13. ABSTRACT *(Maximum 200 words)*

14. SUBJECT TERMS	15. NUMBER OF PAGES
	102
	16. PRICE CODE

17. SECURITY CLASSIFICATION OF REPORT	18. SECURITY CLASSIFICATION OF THIS PAGE	19. SECURITY CLASSIFICATION OF ABSTRACT	20. LIMITATION OF ABSTRACT

A CASE STUDY OF THE LOW-LEVEL JET DURING AN EPISODE OF SPRING CONVECTION

A Thesis

by

CHRISTOPHER SCOTT DONAHOE

Submitted to the Office of Graduate Studies of
Texas A&M University
in partial fulfillment of the requirements for the degree of

MASTER OF SCIENCE

August 1996

Major Subject: Meteorology

A CASE STUDY OF THE LOW-LEVEL JET DURING AN EPISODE OF SPRING CONVECTION

A Thesis

by

CHRISTOPHER SCOTT DONAHOE

Submitted to Texas A&M University
in partial fulfillment of the requirements
for the degree of

MASTER OF SCIENCE

Approved as to style and content by:

Dusan Djuric
(Chair of Committee)

Louis J. Wicker
(Member)

Vatche P. Tchakerian
(Member)

Gerald R. North
(Head of Department)

August 1996

Major Subject: Meteorology

ABSTRACT

A Case Study of the Low-Level Jet During an Episode of Spring Convection.

(August 1996)

Christopher Scott Donahoe, B.S., St. Louis University

Chair of Advisory Committee: Dr. Dusan Djuric

Circulation and transport of the low-level jet (LLJ) were examined for a case of severe convection that occurred in Spring 1995. Radiosonde observations and Eta model output on constant pressure and isentropic surfaces allowed a detailed examination of the relationship between the LLJ and a subtropical jet (STJ) streak. Height falls associated with a lee cyclone caused an ageostrophic and isallobaric wind that strengthened the LLJ.

The smaller horizontal resolution of Eta model grids and hourly forecasts allowed a detailed examination of the LLJ evolution and transport methods. The model's accurate placement of terrain provided realistic plots of the LLJ at the commonly used 850 mb level. The radiosonde observations, when interpolated to grid points, yielded suspicious results over higher terrain. The hourly forecast of transport variables revealed a step-by-step progression of convection along ridges of equivalent potential temperature advection.

The evolution of the LLJ appeared to be influenced by a thermally indirect circulation (TIC) induced in the exit region of a STJ streak. A low-level isallobaric wind responding to a leeside trough and cyclogenesis also effected the LLJ. The TIC is part of the ageostrophic circulation in the exit region of the streak. The low-level isallobaric wind coincided with a trough moving east over the northern Great Plains and a deepening trough in the lee of the Rockies.

Results of the case study for the LLJ evolution showed 1) The LLJ developed beneath a STJ streak exit region as the lower branch of an indirect circulation. 2) A strong cross-contour ageostrophic wind in the lower troposphere aided in accelerating the LLJ. 3) The LLJ strengthened in response to a isallobaric wind associated with lee

cyclogenesis. 4) LLJ speed and magnitude decreased during a transition between the large scale forcing mechanisms as the ageostrophic circulation, cross-contour ageostrophic wind, and isallobaric wind all weakened. 5) Eta model hourly forecasts fairly well predicted heat and water vapor transport, offering an hourly look at convective movement.

ACKNOWLEDGMENTS

The author would like to thank Dr. Dusan Djuric for his guidance and patience in the preparation of this paper. I would like to thank Dr. James McGuirk for his recommendations in leading me toward meaningful objectives during the proposal stage. Dr. Lou Wicker's offer to substitute for an absent committee member was instrumental in completing this work.

I am also grateful for Mr. Robert White and Dr. Michael Morgan's assistance in using the department computer resources. The research works of Captain Richard Ritz and Dr. Salvador Organista laid the groundwork for this study. Mr. Paul Janish from the National Severe Storms Laboratory provided the model data used for this research. Lastly, I thank the United States Air Force for funding this research at this fine institution.

TABLE OF CONTENTS

CHAPTER		Page
I	INTRODUCTION	1
	A. Objectives	2
	B. Research Procedure	3
II	LITERATURE REVIEW	4
III	THE ETA MODEL	9
	A. Analysis and Initialization	9
	B. Numerics and Physical Package	12
	C. Previous Objective Verification	13
IV	WEATHER PATTERN	16
	A. Surface Weather	16
	B. Stages of the Wind Event	21
	C. Low-level and Upper-level Wind Maxima	22
	D. Low-level Temperature and Water Vapor Distribution	28
	E. Low-level Troughs and Ridges	31
	F. Low-level Properties on Isentropic Charts	34
V	LOW-LEVEL JET EVOLUTION AND INTERACTION WITH A SUBTROPICAL JET STREAK	38
	A. Upper-level Jet Streak Tendencies	38
	B. Wind Divergence and Convergence Patterns	40
	C. Low-level Ageostrophic Wind	46
	D. Ageostrophic Circulation	54
	E. Vertical Motion	55

CHAPTER Page

VI TRANSPORT OF HEAT AND MOISTURE BY THE LOW-LEVEL JET 69

A. Temperature Advection 69
B. Mixing Ratio Transport 75
C. Equivalent Potential Temperature Advection 77
D. Transport on Isentropic Surfaces 84

VII ETA MODEL PERFORMANCE 88

A. Low-Level Jet 88
B. Upper-level Jets 91
C. Heat and Water Vapor Transport 94

VIII CONCLUSIONS AND DISCUSSION 96

A. Summary of Conclusions 96
B. Discussion of Research 98

REFERENCES 100

VITA 102

LIST OF FIGURES

FIGURE		Page
1	Eta model soundings available for this study	10
2	Radiosonde soundings available for this study	11
3	Surface weather chart for 1200 UTC 5 May 1995	17
4	Surface weather chart for 1200 UTC 6 May 1995	18
5	Surface weather chart for 1200 UTC 7 May 1995	20
6	Wind magnitude and streamlines at 850 mb; isotachs in m s^{-1} for stages A-D of the LLJ at 1200 UTC 5 May, 1200 UTC 6 May, 0000 UTC 7 May, and 1200 UTC 7 May respectively	23
7	Dallas-Fort Worth sounding at 1200 UTC 7 May 1995	24
8	Wind magnitude and streamlines at 850 mb, 300 mb, 250 mb and 200 mb on 1200 UTC 7 May 1995	26
9	Time-height cross section of wind magnitude for Corpus Christi, Waco, and Dallas, Texas and Lawton, Oklahoma from 1200 UTC, 5 May 1995 to 1200 UTC, 8 May 1995	27
10	Meridional cross section of wind magnitude during stages A-D of the LLJ	29
11	Temperature and wind magnitude at 850 mb for stages A-D of the LLJ	30
12	Mixing ratio and wind magnitude at 850 mb for stages A-D of the LLJ	32
13	Height contours and wind magnitude at 850 mb for stages A-D of the LLJ	33
14	Isobars and wind magnitude on 301 K isentropic surface for stages A-D of the LLJ	35
15	Wind magnitude and streamlines on 301 K isentropic surface for stages A-D of the LLJ	37
16	Height, wind magnitude, and streamlines at 200 mb during stages A-D of the LLJ	39
17	Wind divergence and wind magnitude at 850 mb during stages A-D of the LLJ	42
18	Wind divergence at 200 mb and wind magnitude at 850 mb during stages A-D of the LLJ	43

FIGURE Page

19 Meridional vertical section of wind divergence and wind magnitude during stages A-D of the LLJ 45

20 Ageostrophic wind, height, and wind magnitude at 850 mb during stages A-D of the LLJ 48

21 Isallobaric wind, height, and wind magnitude at 850 mb during stages A-D of the LLJ 50

22 Isallobaric wind divergence and wind magnitude at 850 mb during stages A-D of the LLJ 52

23 Isallobaric wind and 12 hour height change at 850 mb during stages A-D of the LLJ 53

24 Meridional vertical section of the ageostrophic circulation and wind magnitude during stages A-D of the LLJ 56

25 Vertical motion (omega) and wind magnitude at 850 mb during stages A-D of the LLJ 57

26 Vertical motion (omega) at 500 mb and wind magnitude at 850 mb during stages A-D of the LLJ 59

27 Vertical motion (omega) at 300 mb and wind magnitude at 850 mb during stages A-D of the LLJ 61

28 Meridional vertical section of vertical motion (omega) and wind magnitude during stages A-D of the LLJ 62

29 Zonal vertical section of vertical motion (omega) and wind magnitude during stages A-D of the LLJ 64

30 Q-Vectors and wind magnitude at 850 mb during stages A-D of the LLJ 65

31 Q-Vector divergence and wind magnitude at 850 mb during stages A-D of the LLJ 67

32 Q-Vector divergence at 500 mb and wind magnitude at 850 mb during stages A-D of the LLJ 68

33 Vertical sections of temperature advection by the observed wind and wind magnitude between 1000 mb and 500 mb during stages A-D of the LLJ 72

FIGURE		Page
34	Temperature advection by the observed wind and wind magnitude at 850 mb using Eta model output. Panels 1-4 display output at 0000 UTC, 0200 UTC, 0300 UTC, and 0400 UTC on 6 May respectively	74
35	Flux of mixing ratio by the southerly wind component and southerly wind component magnitude at 850 mb using Eta model output	76
36	Mixing ratio advection by the observed wind and wind magnitude at 850 mb during stages A-D of the LLJ using Eta model output	78
37	Equivalent potential temperature advection by the observed wind and wind magnitude at 850 mb during stages A-D of the LLJ	80
38	Combination of zonal and meridional vertical sections of equivalent potential temperature advection by the observed wind and wind magnitude during stages A-D of the LLJ between 1000 mb and 500 mb	81
39	Equivalent potential temperature advection by the observed wind and wind magnitude at 850 mb using Eta model output. Panels 1-4 display output at 0000 UTC, 0200 UTC, 0300 UTC, and 0400 UTC on 6 May respectively	83
40	Meridional vertical sections of equivalent potential temperature advection by the observed wind and pressure between 300 K and 310 K isentropic surfaces during stages A-D of the LLJ	85
41	Parcel trajectories on the 301 K isentropic surface. All six trajectories begin at 0000 UTC on 4 May and progress at 12 hour segments represented by dots	87
42	Wind magnitude at 850 mb during stages A-D of the LLJ for radiosonde and Eta model output	89
43	Wind magnitude at 200 mb during stages A-D of the LLJ for radiosonde and Eta model output	92
44	Wind divergence at 200 mb during stages A-D of the LLJ for radiosonde and Eta model output	93
45	Equivalent potential temperature advection at 850 mb during stages A-D of the LLJ for radiosonde and Eta model output	95

CHAPTER I

INTRODUCTION

Severe convection occurred over the southern Great Plains between 5 and 8 May 1995. A strong, southerly low-level jet (LLJ) developed during the period but deviated from the classical pattern for LLJ formation. The LLJ developed under a subtropical jet (STJ) streak exit region while the closest cyclone system was located over northeast Nevada. As a leeside cyclone developed, the LLJ speed increased, and the LLJ became better defined as did the low-level equivalent potential temperature (θ_e) advection and mixing ratio flux. The LLJ studied differs in formation and oscillation tendencies from the classical pattern. A typical diurnally oscillating LLJ, influenced by topography, extends vertically between 400-800 meters in the planetary boundary layer but is not forced by synoptic scale processes. Although our LLJ appears to exhibit a diurnal oscillation, it extends above 3000 meters at times and is forced by large-scale mechanisms.

Water vapor transport from the Gulf of Mexico provides most of the "fuel" for severe convection in the Great Plains. The progression of humid air northward is controlled by the LLJ. This LLJ is a mesoscale phenomenon not easily predicted by larger scale numerical forecast models. A better understanding of the LLJ is needed in order to improve our ability to predict convective events in the United States. If the mechanisms that cause and influence the LLJ are better understood and modeled, more accurate short range local forecasts of heavy convective rainfall can be expected.

For the last two years, the National Centers for Environmental Prediction (NCEP) has provided mesoscale forecast guidance for North America using the Eta model. This new numerical weather prediction model replaced the Limited-Area Fine-Mesh Model (LFM) with hopes of improving the overall forecast skill, specifically in quantitative

---

The style is that of the *Monthly Weather Review*.

precipitation forecasts. The numerical weather prediction models are especially important for forecasting severe weather potential in the south central United States. The principal stimulation for this work is the availability of the hourly output from the Eta model. This allows examination of the hourly progression of the LLJ evolution and transport variables.

A. Objectives

The goal of this research is to document a case of an apparent diurnally oscillating LLJ that formed under the exit region of a STJ streak over a three day period in early May 1995. The LLJ was also synoptically forced by a cyclone system west of the Rockies and strengthened in response to the leeside low development. This stronger, low-level wind speed maximum aligned low-level heat and humidity to produce a favorable environment for severe convection in the southern Great Plains.

The hypothesis is that the LLJ initially formed because of an indirect circulation initiated by a STJ exit region then strengthened due to synoptic influences from a trough advecting east over the northern Great Plains and a newly formed lee cyclone. The weakening of the LLJ was not a diurnal oscillation but a transition period of the large scale forcing mechanisms.

The first objective of this research is to give a synoptic overview of the weather pattern that led to the development of the LLJ. The second objective is to demonstrate the early LLJ development is coupled with a STJ streak exit region and show its influences on heat and moisture transport as influenced by a cyclone west of the Rocky Mountains prior to the strongest synoptic forcing. The third objective is to describe the apparent diurnal tendencies, peak LLJ development and intensification that was aided predominately by a newly formed lee cyclone but also formed under a STJ streak. As Uccellini and Johnson (1979) found, the LLJ can form in the lower portion of an indirect circulation underneath the exit region of an upper-level jet (ULJ) streak. A diagnosis of the ageostrophic and isallobaric wind should show the connection between the cyclone

influences, the STJ streak, and the LLJ intensification. As the fourth objective, the Eta model will be evaluated for its jet streak evolution and transport methods. An attempt will be made to show the role of the LLJ in the transport of warm, moist air essential for the occurrence of heavy convective rainfall.

B. Research Procedure

To accomplish the goal of this research four objectives were stated. For the first objective:

1. NCEP weather charts, radiosonde observations and Eta model soundings will be used to show positions of jet streams, pressure centers and fronts. These data will permit the development of constant pressure and isentropic charts as well as vertical sections.

The second, third, and fourth objectives will be completed by using:

2. Vertical sections of radiosonde observations and model output that allow a complete examination of the factors leading to the LLJ development and intensification. Some of these factors include inversions, diurnal variations of heating and cooling on sloped terrain, a deepening cyclone and changing height gradients, a STJ streak occurring east of the Rocky Mountains, and the LLJ and STJ regions intersecting southeast of a surface cyclone.

3. Skew T-log p diagrams that will indicate locations and altitudes of inversions associated with the LLJ.

4. Gridded radiosonde and model data from which the ageostropic and isallobaric wind fields are computed. It is expected that the isallobaric wind field should be similar to the cross-contour ageostrophic wind except for its smaller magnitude (Chen, et al. 1994). This may be a major factor in strengthening the LLJ and ULJ. The gridded model output will also show the hourly progression of heat and water vapor transport by the LLJ using θ_e advection and mixing ratio flux.

CHAPTER II

LITERATURE REVIEW

The low-level jet and its role in convection has been a topic of research over the last four decades. Blackadar (1957) first noted that a wind speed maximum is frequently observed at night below 1 km, and the maximum speed is usually located at the top of a nocturnal inversion.

Bonner (1968) was one of the pioneers in studies of the LLJ. He defined this wind maximum as a LLJ when the wind speed reached at least 12 m s^{-1} and decreased to half its maximum value all under 3 km. His statistical analysis concluded that a large number of low-level speed maxima occur over the Great Plains, with the largest number taking place from Texas to Nebraska. He also showed the importance of their rapid transport of heat and moisture from the Gulf of Mexico into areas of convective storms that produce heavy rainfall. More specifically, he found that diurnal oscillations in the jet speed are responsible for the nighttime maximum in thunderstorm activity observed across the Great Plains. Bonner concluded that the lower tropospheric synoptic conditions creating a strong pressure gradient across the Great Plains are necessary for the LLJ formation.

Browning and Pardoe (1973) reported that the LLJ is embedded within a convective boundary layer, reaching its maximum velocity between 900 and 850 mb. This showed the importance in using vertical cross-sections to analyze this feature since its maximum values were between mandatory reporting levels. They also found the LLJ to form a tongue of warm, moist air.

Until the middle 1970s, scientists focused their research on the LLJ and its development within the lower-troposphere, but more recently there have been studies that related the LLJ to upper-level and synoptic scale features. Uccellini and Johnson (1979) showed that the LLJ often appears beneath the exit region of upper-tropospheric jet

streak. This study also showed the LLJ increased the lower-tropospheric heat and moisture transport into the inception area of the severe convective storms.

Uccellini (1980) expounded on his earlier work by proposing that a LLJ beneath the exit region of an ULJ is embedded in the lower branch of an indirect circulation, and the development of the LLJ is largely due to an increased lower tropospheric isallobaric wind component. This isallobaric wind accounts for the net mass adjustments above the planetary boundary layer (PBL) and should be an important topic of studies since it appears to be a key feature in the forcing of lower tropospheric wind maximum. In twelve of fifteen cases, the upper flow pattern consisted of a trough over the southwestern United States, and ULJ streaks propagating from the Rocky Mountains into the Great Plains. This pattern is responsible for leeside cyclogenesis or leeside troughing that produces the pressure gradient required for the LLJ development. Verifying Bonner's earlier work, Uccellini found when a blocking ridge is over the Great Plains region the LLJ is characterized by a diurnal oscillation, as the wind speed reaches maximum intensity by early morning and is associated with the development of a nocturnal temperature inversion. Considering the larger picture, Uccellini showed that the LLJ often appears with a cyclone in the lee of the Rocky Mountains and points out that the development of the LLJ occurs in response to the isallobaric forcing during cyclogenesis.

Djuric and Damiani (1980) agreed that the LLJ is the most important mechanism for supplying warm, humid air for middle-latitude storms. They found the formation of most LLJs take place when a short wave trough coupled with the ULJ appears east of the Rockies. This lee troughing is of fundamental importance for the production of a low-level wind maximum. In its early stages, the LLJ developed on the west side of a polar anticyclone, usually above the planetary boundary layer. They also showed that in its advanced stage the LLJ is situated in the warm sector of the cyclone showing up as a warm, moist tongue extending northward from the Gulf of Mexico.

Djuric (1981) using a one layer, one dimensional model to produce a LLJ, supported the hypothesis that a nearby pressure fall was the direct cause of the LLJ. The

LLJ started as an isallobaric wind near the region of pressure falls and expands to cover a large area, verifying the need for an inversion. Djuric and Ladwig (1983) agreed that synoptic-scale processes in the atmosphere may cause the LLJ that the PBL processes then modify.

More recently, Chen and Kpaeyeh (1993) in a synoptic scale study of the LLJ over the Great Plains found many severe storms and much of the precipitation in the area occurred where the intersection between the ULJ and LLJ is located. The low-level circulation generated by the LLJ transported heat and water vapor toward the severe convection regions. However, they state the development of a baroclinic short wave east of the Rockies is a triggering mechanism for the LLJ. In our case, the LLJ is already in place when the short wave trough east of the Rockies develops.

Chen and collaborators Chen et al. (1994) were the first to distinguish between two different types of low-level wind speed maxima. The first is a boundary layer jet (BLJ) that has strong vertical wind shear and possesses a remarkable diurnal variation. The BLJ reaches its maximum intensity by early morning then breaks down in the afternoon. Second, they address the LLJ that occurs between 900-600 mb and is usually associated with fronts and cyclones.

The following references help describe how transport by the LLJ affected convective regions. Bonner (1968) was one of the first to show rapid ascent of air on a synoptic scale can be expected downstream from the jet maximum and this ascent may be an important factor in nocturnal thunderstorms. Thus, lifting associated with the LLJ combined with the vertical motion of the surface boundary. The vertical motion is especially important when a rapid influx of moisture reaches the frontal surface.

Miller (1972) found that because of forced ascent when the low level warm, moist flow overruns the surface front, there is an increase in potential instability in the low level air moving north under the cool air aloft and storms develop. Frontal lifting of the warm moist air triggers the initial outbreak of thunderstorm activity.

Martin et al. (1995) found a warm front circulation may cause a gradual vertical protrusion of high θ_e air originally confined to the low levels. Vertical circulation

associated with the front can create a convectively unstable region in the mid levels required for rainbands to form.

In a conceptual model of areas favorable for heavy convective rainfall, Glass et al. (1995) found convergence, humidity and temperature advection were maximized along and north of a surface boundary where the LLJ and positive 850 mb θ_e advection are coupled. This study was based on the LFM forecasts that occurred every 12 hours and had a grid spacing of 153-180 km. This pattern of new cell growth will normally remain until the LLJ veers shifting the convergence and advection pattern. The LLJ serves to maximize positive low level θ_e advection along and north of the boundary. Cells continuously develop in this region where the LLJ and θ_e advection are coupled.

In summary, it has been shown that a low-level wind maximum often exists at night above a nocturnal inversion. Most authors state the diurnal oscillations of the boundary layer wind maximum are responsible for many nighttime thunderstorms over the Great Plains. The diurnally oscillating BLJ reaches a maximum between 950-900 mb in the early morning. Diurnal heating and cooling on sloped terrain influences this jet. There is also a LLJ that exists from 900-650 mb that is forced by cyclogenesis and intensified by an increase in the low-level isallobaric wind. More of a distinction needs to be made between the two types of low-level wind maxima described by Chen.

The LLJ often appears beneath the exit region of an ULJ. The LLJ beneath this exit region is embedded in the lower branch of an indirect circulation. This intersection is also the site of many severe storms and heavy precipitation. The LLJ has proven invaluable in transporting lower level water vapor and heat into convective regions. The literature also shows that air rapidly ascends downstream from the LLJ maximum while crossing over a surface frontal region. Heavy convective rains are found on the cold side of this boundary. The LLJ helps maximize the positive low-level θ_e advection along and north of the boundary.

Some questions still need to be addressed. Does the subtropical jet exit region cause a different ageostrophic circulation for LLJ development? Is the exit region the primary forcing mechanism for the LLJ formation since the cyclone system is west of the

Rockies at its inception? What are the roles of the ageostrophic and isallobaric wind during the apparent LLJ diurnal oscillation? What happens to the wind maximum features during this transition period between forcing mechanisms? How does the transition effect heat and moisture transport?

CHAPTER III

THE ETA MODEL

The 80 km resolution, 38-level version of the Eta model, replacing the Limited-area Fine-mesh Model (LFM) became operational in June 1993 providing forecast guidance over North America (Black, 1994). The implementation is known as the 'Early' or 80-km version of the Eta model. Mesinger et al. (1988) replaced the aging sigma coordinate system with improved quasi-horizontal coordinates to eliminate the problems with the sloping coordinate surfaces. The Eta model also differs substantially from the Nested Grid Model (NGM) in structure, numerics, and physical parameterizations with the aim of producing an overall improvement in forecast skill, particularly in quantitative precipitation forecasting Black et al. (1993).

This study used Eta model sounding data provided by the National Severe Storms Laboratory. The data sets consist of 461 Eta model hourly soundings around North America that are available hourly for 48 hours from the initialization time. These sounding locations allowed examination of the LLJ using the soundings in Mexico and off the Texas coast. For this case, the sounding locations provided a high concentration of data over the southern Great Plains (Fig. 1). Figure 2 shows the sparsely scattered radiosonde locations around the United States. The 0000 UTC and 1200 UTC Eta soundings for each day were available from 0000 UTC on 5 May 1995 to 0000 UTC on 8 May 1995. The National Severe Storm Forecast Center is currently testing the mesoscale resolution (48 km) version of the Eta model for future production.

A. Analysis and Initialization

Initial conditions for the 80 km Eta model are provided by an analysis scheme based upon optimum interpolation. The first guess is provided by the Global Data Assimilation System (GDAS) using the National Center for Environmental Prediction

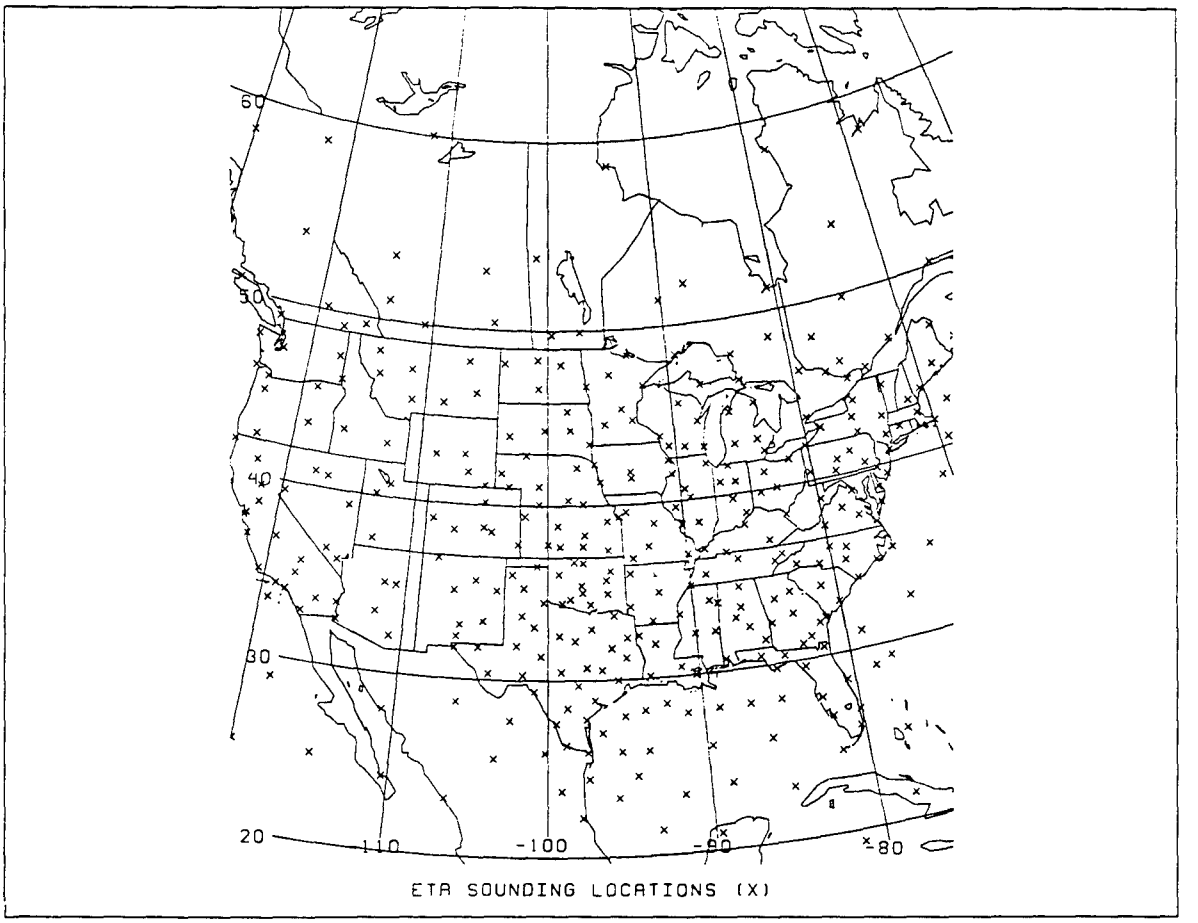

Fig. 1. Eta model soundings available for this study.

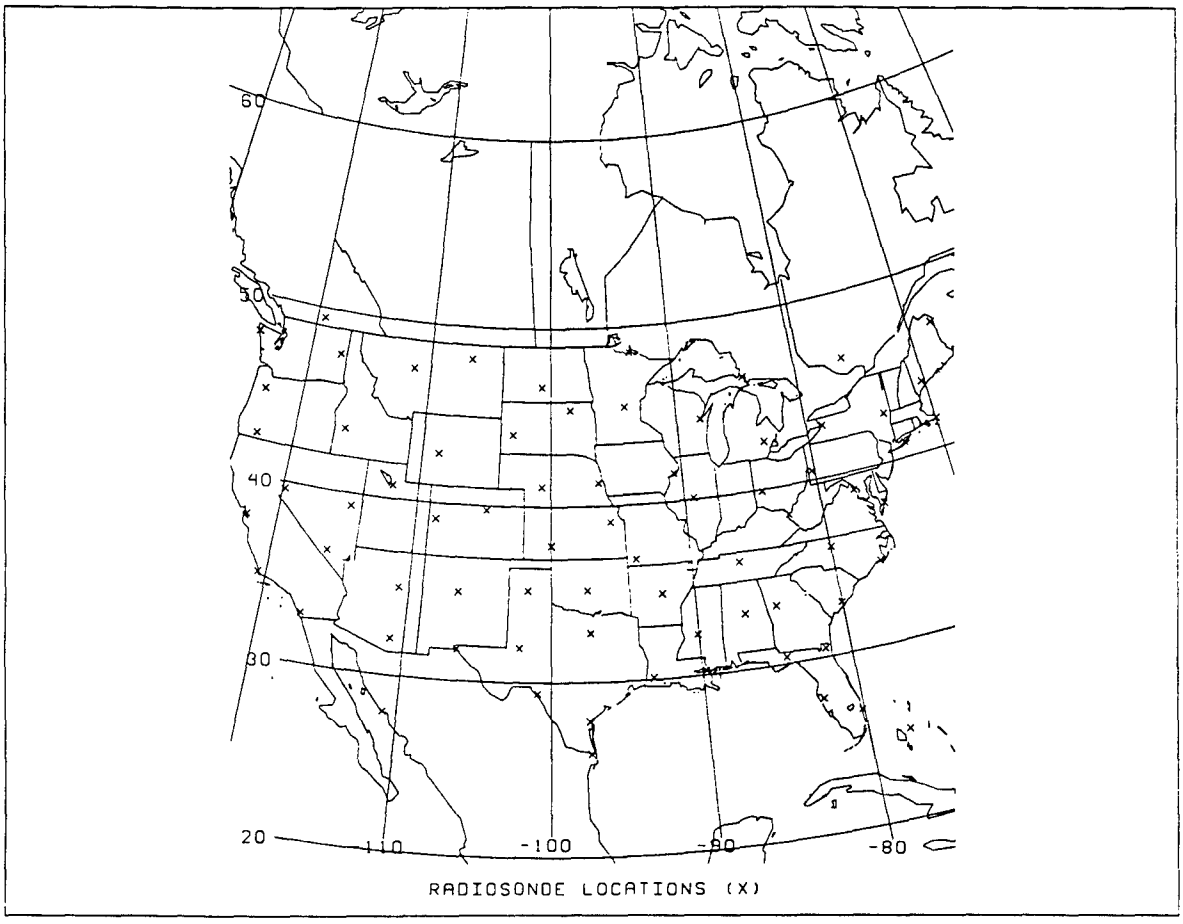

Fig. 2. Radiosonde soundings available for this study.

(NCEP) 6 hour global spectral model forecast. The initialized fields are either mandatory pressure levels or the NGM's sigma levels. The analysis includes data from soundings (height and wind), wind profilers, domestic aircraft and all available surface land and marine reports. The initial conditions are obtained by interpolating these fields from the analysis grid to the model grid. After all available observations are processed (data cutoff = T00 + 75 minutes), the first guess is interpolated to the observation location and the observed increments are computed. The boundary conditions are derived from NCEP's aviation forecasts starting 12 hours earlier.

B. Numerics and Physical Package

The model vertical coordinate (called the Greek letter eta) is a generalization of the terrain-following sigma coordinate. The eta coordinate system is actually a variation of the commonly used sigma coordinate system employed at the NCEP in the NGM and the global spectral model. The resultant eta surfaces tend to be quasi-horizontal, thus eliminating errors in pressure gradient force computation over steeply sloped terrain which occur in sigma coordinates (Black et al. 1993). Both coordinate systems are normalized and pressure-based, but the Eta model is normalized with respect to the mean sea-level pressure whereas the sigma is normalized with respect to the surface pressure. In regions where the ground elevation changes rapidly, the horizontal variation of sea-level pressure is much less than that of surface pressure. This means the sigma surfaces must slope steeply just as the ground does. The lack of slope on the eta surfaces produces a significant improvement when computing the pressure-gradient force near steeply sloping terrain. Because of this, the model's topography is in the shape of steps.

The horizontal resolution is approximately 80 km in the 'Early' version of the Eta model. This means that the distance between a mass point and its nearest mass point neighbor is about 80 km. The grid's central point is currently located at 52°N and 111°W. The 'equator' across the center of the forecast domain minimizes the

convergence of meridians. It has the numerically advantageous effect of minimizing the difference in Δx and Δy.

The horizontal grid resolution of the model ranges from 87.7 km at the center of the domain to 79.6 km on the northern and southern boundaries. The vertical resolution of the model is in 38 layers with the lowest layer of the model over the ocean having a thickness of 20 meters for a standard atmosphere. The layers thicken gradually with height into the middle troposphere then begin to thin with respect to mass approaching the upper domain.

The Eta model is a quasi-hemispheric primitive equation model with a semi-staggered grid. This means that the grid values are predicted on alternate points to those of all the mass variables (temperature, specific humidity, surface pressure). Mesinger (1984) found that it is possible to get a quasi-horizontal coordinate surface that does not suffer the problems of the sigma coordinate system. This new coordinate system (eta) is specified as:

$$\eta = (p-p_t)/(p_s-p_t)\,\eta_s \qquad (1)$$

where

$$\eta_s = (p_{rf}(Z_s - p_t)/(p_{rf}(0) - p_t) \qquad (2)$$

In these equations, p is for pressure, the subscripts t and s represent the top and ground surface values of the model atmosphere, Z is the geometric height, and $p_{rf}(Z_s)$ is a reference pressure as a function of Z_s, the ground reference height.

C. Previous Objective Verification

Before replacing the LFM, numerous agencies performed various objective verifications with the Eta model. The Meteorological Operations Division, the Weather Forecast Branch, the Monitoring and Aviation Branch, and the Severe Local Storms Unit of the then National Meteorological Center (NMC) all conducted extensive evaluations

of the LFM and Eta model. For comparison's sake, the LFM had 7 layers and a horizontal resolution of 190.5 km while the Eta model has 38 layers and a 80 km resolution.

Overall, the Eta model proved superior to the LFM in forecasting the synoptic-scale fields. The Eta model outperformed the LFM in predicting most meteorological variables used by forecasters in quantitative precipitation forecasting.

Despite the overall better performance of the Eta model in forecasting synoptic-scale features, the model had problems forecasting the evolution of intense cyclones. The Eta model overforecast the strength of the 850 mb wind. The Eta model appeared most likely to overpredict the 850 mb wind in the warm sector ahead of a cold front or to the east and north of a strong cyclone. The Eta model also experienced problems with the boundary-layer fields. The Eta model average boundary-layer wind at 0000 UTC increased from 10.6 kt to 13.3 kt, a significant difference when the wind speed should be lower. Even so, the Eta model forecasts had significantly less error in the wind fields than the LFM winds. The low-level winds tended to be too strong, indicating circulations that are too vigorous. There is a need to develop a good wind forecast product from the Eta model for low-level significant weather forecasting for aviation applications.

In summary for the NMC tests, the 850 mb Eta forecasts were too wet ($0.5\ g\ kg^{-1}$) and too warm (1.5-2.0 °C); low-level wind speeds were too strong; mid-level heights were too low as a result of temperatures being too cold in the lower troposphere and jet stream wind speeds were too low.

Janish et al. (1995) performed an evaluation of model strengths and weaknesses during periods of offshore and return flow using the NGM and the Eta model. Differences between 48 hour Eta model forecasts of mixing ratio and verifying analysis are generally less than $1.0\ g\ kg^{-1}$ except for the Texas coast. However, the axis of accurate moisture amounts is confined to the LLJ region exclusively. The Eta model also overforecast the LLJ strength over Texas while not resolving the upward slope of the LLJ from the Gulf of Mexico, inland, and it advanced the LLJ axis eastward too rapidly.

This study will try to answer the following questions concerning the Eta model. Does the Eta model adequately develop the LLJ and subtropical jet? Does the Eta model develop the LLJ at the proper altitude and show its upward slope heading north from the Gulf of Mexico? How does the Eta model handle heat and moisture transport in the vicinity of the LLJ?

CHAPTER IV

WEATHER PATTERN

A. Surface Weather

The month of May 1995 started with a strong cold front that passed through stations as far south as Brownsville, Texas and reached a few hundred miles into the Gulf of Mexico. This Canadian air mass left an anticyclone over the eastern Great Plains during the start of this case study.

Figure 3 shows a weak occluded front extending from a 1000 mb low in east central Nevada on 5 May at 1200 UTC. The front stretched southeast through Utah and into eastern Arizona. Only some isolated rainshowers in southern Nevada and California were associated with the low at this time. A 1025 mb high pressure was entrenched over the eastern Great Plains causing light northeasterly flow as far south as Waco, Texas. The only thunderstorms occurring were in eastern New Mexico and into the Texas Panhandle.

The low pressure center, now 998 mb, had moved to northeastern Nevada by 6 May at 0000 UTC with its front progressing into western New Mexico (not shown). A sharp dewpoint gradient began to develop in western Texas as the southeast flow developed from the Gulf of Mexico. This warm, humid air is seen in the dewpoint reaching over 21°C into east central Texas. A warm front could be seen between the converging southeast and northeast flows in this region. Thunderstorm activity had spread into north central Texas and southern Oklahoma. During the period 5 May at 1200 UTC and 6 May at 1200 UTC, these thunderstorms produced over two inches of rain in west Texas and over three inches in the Dallas-Fort Worth Metroplex.

Figure 4 shows the low center, now 997 mb, moved into southwest Montana by

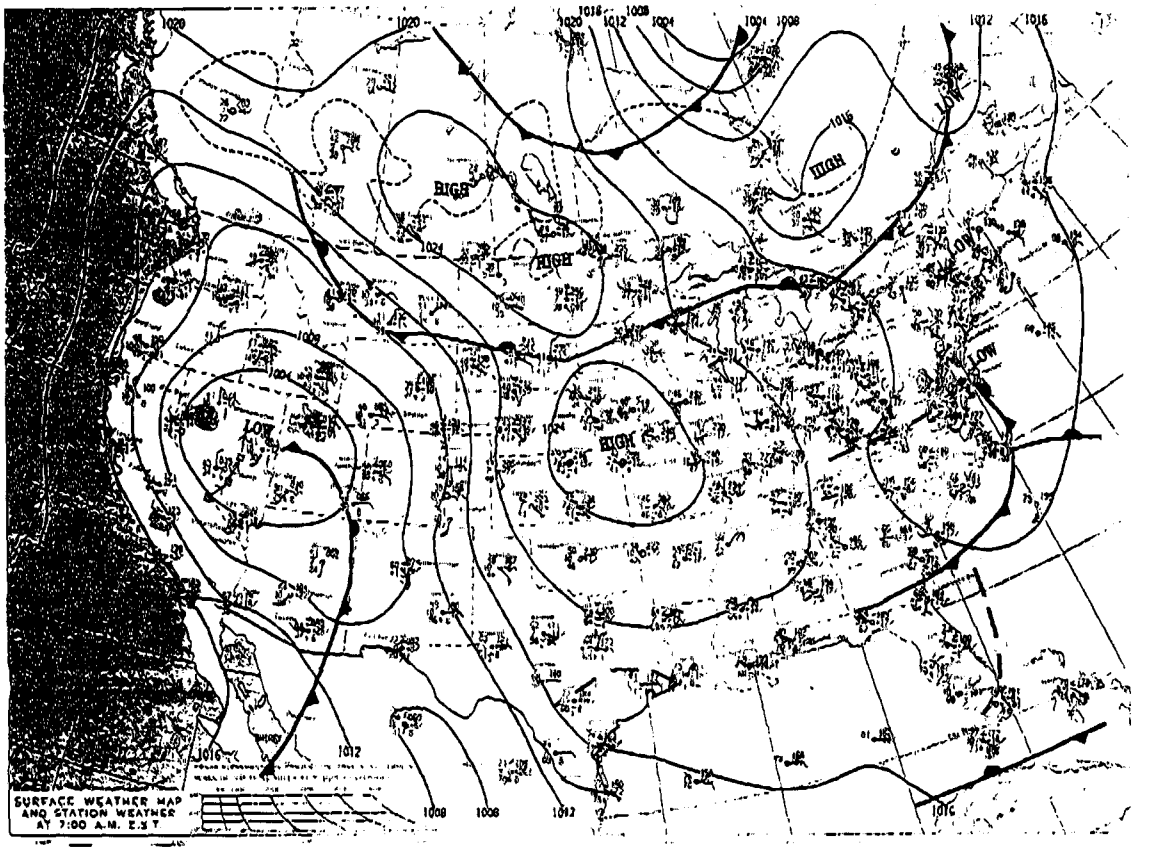

Fig. 3. Surface weather chart for 1200 UTC 5 May 1995. From the Daily Weather Maps published by the National Center for Environmental Prediction.6 May at 1200 UTC, and the occluded/cold front stretched southeast into eastern Colorado and central New Mexico. A dry line was evident in western Texas with dewpoint

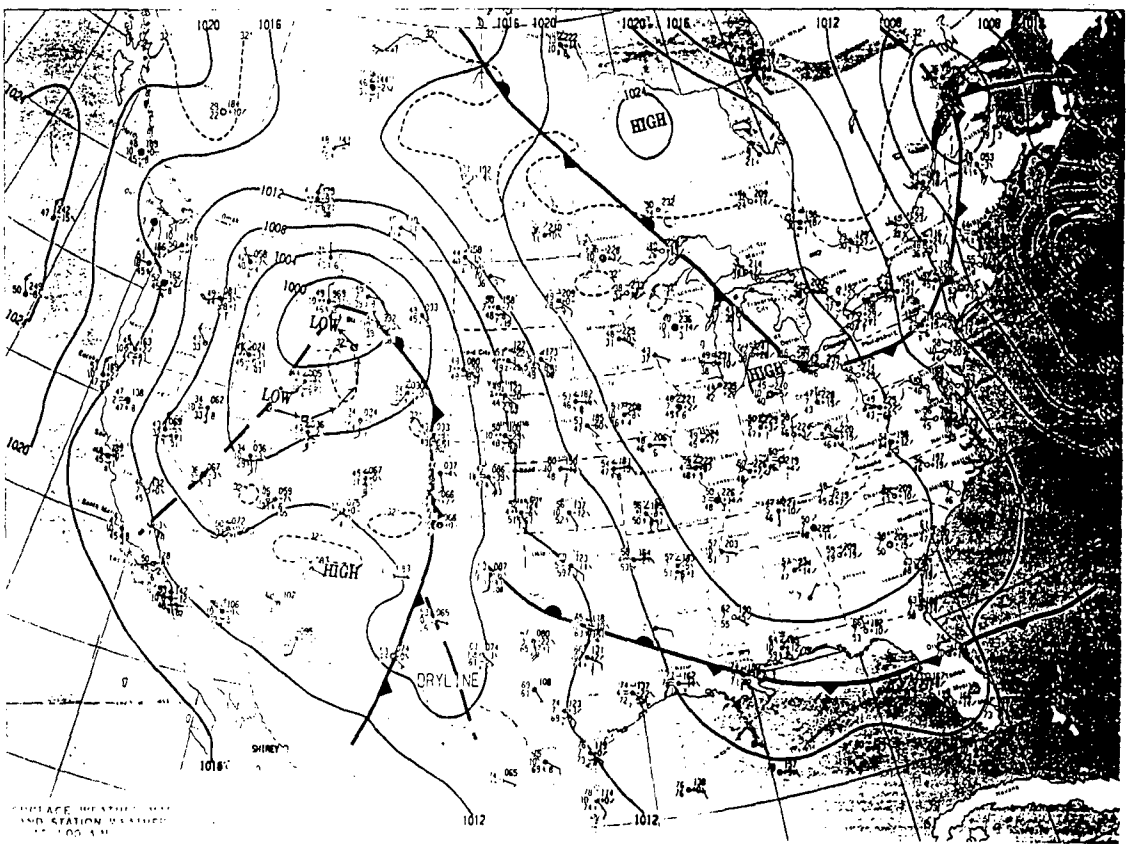

Fig. 4. Surface weather chart for 1200 UTC 6 May 1995. From the Daily Weather Maps published by the National Center for Environmental Prediction.

differences over 4°C. Widespread rainshowers and thunderstorms were now occurring throughout the Great Plains. The strongest storms were in northcentral Texas with thunderstorm tops of 12,800 meters.

By 7 May at 0000 UTC, a developing low in eastern Colorado was now the center of attention (not shown). The low in Montana began to fill and the attached front dissipated. Three fronts were now connected to the deepening low in Colorado. A warm front through northern Texas and western Oklahoma, a cold front extending south into New Mexico, and a weakening occluded front extending north into western Nebraska and western South Dakota were associated with the developing lee cyclone. The dryline was still present through the Texas Panhandle and into southwest Texas. With the weakening of the LLJ, precipitation decreased in the early evening. Only a small area of isolated thunderstorms and rainshowers were occurring in the Texas Panhandle and western Nebraska. The rain totals were less for the period from 6 May at 1200 UTC to 7 May at 1200 UTC across the Great Plains. Wichita Falls, Texas and Tinker AFB, Oklahoma both received 35 mm of rain for the period.

At 1200 UTC on 7 May, three surface low centers were associated with the cold front moving into eastern New Mexico and extreme western Texas (Fig. 5). One low was positioned in northeast Colorado, another in northeast New Mexico, and the third in eastern New Mexico. The warm front had moved farther north into Oklahoma and straddled the Oklahoma/Texas border to the east. The severe weather increased dramatically toward sunrise with the strengthening of the LLJ. Thunderstorm cells grew in intensity in central Texas and a wide complex of severe weather began organizing in western Oklahoma and western Kansas. Thunderstorm tops in the Texas and Oklahoma Panhandles extended past 16,764 meters.

North central Texas and southern Oklahoma were hit hard between 1200 UTC on 7 May and 0000 UTC on 8 May. An isolated supercell spawned a tornado in northern Texas that crossed into Oklahoma and grew to F3 intensity. This tornado caused $75 million in damage in Ardmore, Oklahoma alone.

The low center in eastern Colorado had deepened to 993 mb by 0000 UTC on

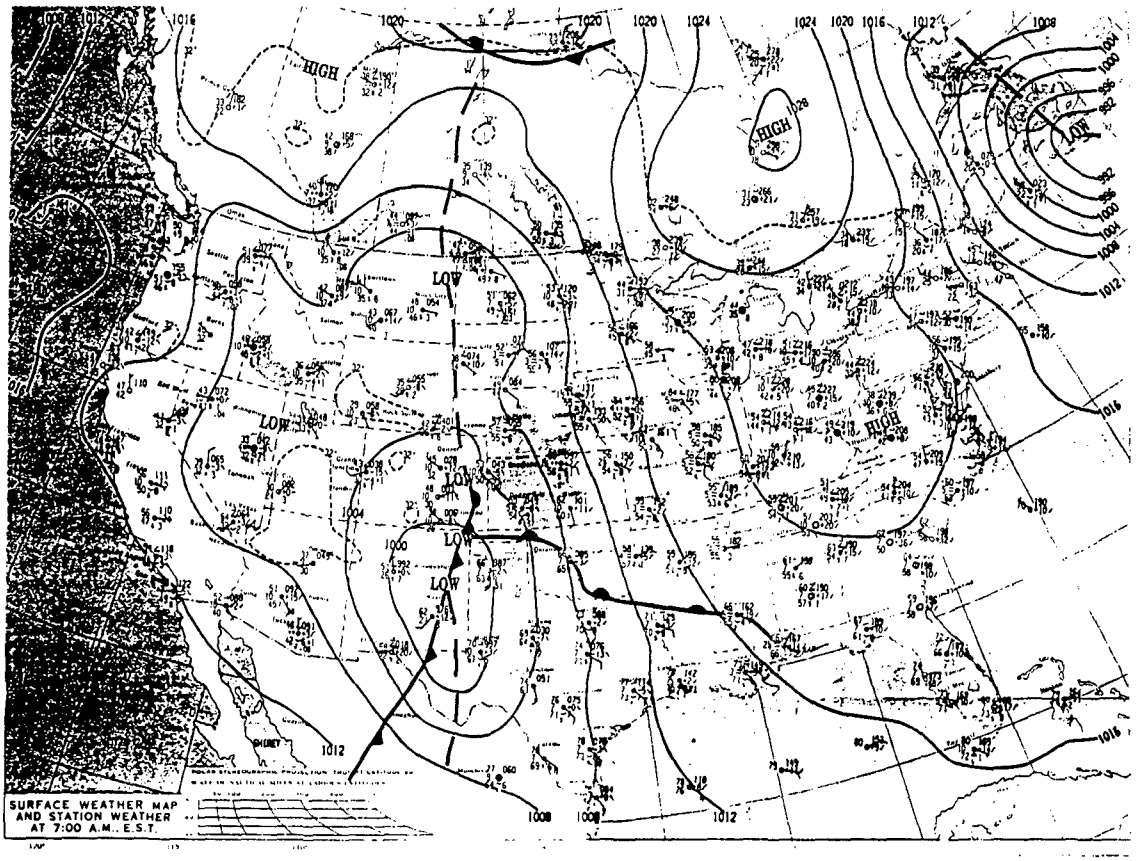

Fig. 5. Surface weather chart for 1200 UTC 7 May 1995 when the lee cyclone aided in forcing the LLJ development. From the Daily Weather Maps published by the National Center for Environmental Prediction.

8 May. Oklahoma and Texas were experiencing convection caused by lifting associated with an advancing cold front now past Amarillo and Midland, Texas moving into west central Texas. The warm front still extended east from the second low now in the northeast Texas Panhandle. Numerous thunderstorm watch areas were now in effect. These covered the southern Great Plains extending from western Texas through Oklahoma and into Kansas. Thunderstorms ahead of the cold front near Abiline, Texas topped out at 18,288 meters.

By 0600 UTC on 8 May, the cold front forcing was now evident based on the linear shape of the thunderstorms that had previously been scattered throughout the southern Great Plains. For the period, 7 May at 1200 UTC to 8 May at 1200 UTC, many stations in north Texas and Oklahoma experienced flooding from the thunderstorms. Over 51 mm of rain fell in Dallas, Waco, and Austin, Texas in just a few hours. Many Kansas locations received 51-64 mm, but Tulsa, Oklahoma was hardest hit receiving almost 112 mm during the 24 hour period.

The main low center was now on the Colorado/Kansas border and had deepened to 988 mb. The cold front extended south through central Texas having passed through Lawton, Oklahoma, Wichita Falls and San Angelo, Texas. A severe squall line well ahead of the front was spawning thunderstorms from northeast Arkansas into Louisiana and as far south as Houston, Texas. This same system was responsible for 305 mm of rain in New Orleans during the next 24 hours.

B. Stages of the Wind Event

The May 1995 case was selected because multiple factors influence the evolution of the LLJ. Djuric and Damiani (1980) presented the LLJ evolution in 5 stages. These stages consisted of cold air moving south before the LLJ was noticed, the initial appearance of southerly flow, the southerly flow spreading horizontally to the Gulf of Mexico, the humid air moving rapidly northward, and the LLJ retreating eastward ahead of an approaching cold front.

The lower-tropospheric wind development in this case can be described in 4 main stages. These stages are seen in the extent and strength of the jet core at 850 mb along with the location of the cyclone systems. Figure 6 shows the four stages using 850 mb isotachs and streamlines. Southeast flow over 10 m s^{-1} is first apparent at 1200 UTC on 5 May (Stage A). A jet core of 14 m s^{-1} is just developing over southwest Texas. In 24 hours (1200 UTC on 6 May), the LLJ develops in the vicinity of a STJ exit region and in response to height falls in a trough extending from a low center over Montana and the core speed reaches 21 m s^{-1} (Stage B). During the next 12 hours (0000 UTC on 7 May), the LLJ exhibits a decrease in speed and meridional extent (Stage C). At this time, the LLJ core in the southern Great Plains disappears. Lastly, at 1200 UTC on 7 May, the LLJ reaches its maximum horizontal extent and speed of 23 m s^{-1} as the newly formed lee cyclone strengthens (Stage D). Two cores are seen with one centered over Dallas, Texas and the other over Brownsville, Texas. For future reference, the four stages can be referred to as (with the Djuric and Damiani stages in parenthesis):

Stage A: The first appearance of southerly flow in southwest Texas at 1200 UTC on 5 May. (B)

Stage B: The LLJ appears over the southern Great Plains under a STJ streak with a cyclone system west of the Rocky Mountains at 1200 UTC on 6 May. (C)

Stage C: The LLJ shows a significant weakening at 0000 UTC on 7 May. (None)

Stage D: The LLJ reaches its maximum extent and speed as a lee cyclone develops east of the Rocky Mountains at 1200 UTC on 7 May. (D)

Djuric and Damiani did not examine the oscillating tendency of our Stage C.

C. Low-level and Upper-level Wind Maxima

The May 1995 case shows a migrating, lower-tropospheric wind maximum develop well ahead of a surface cyclone. The radiosonde sounding for Dallas-Fort Worth at 1200 UTC on 7 May is in the LLJ core (Fig. 7). The sounding shows a maximum

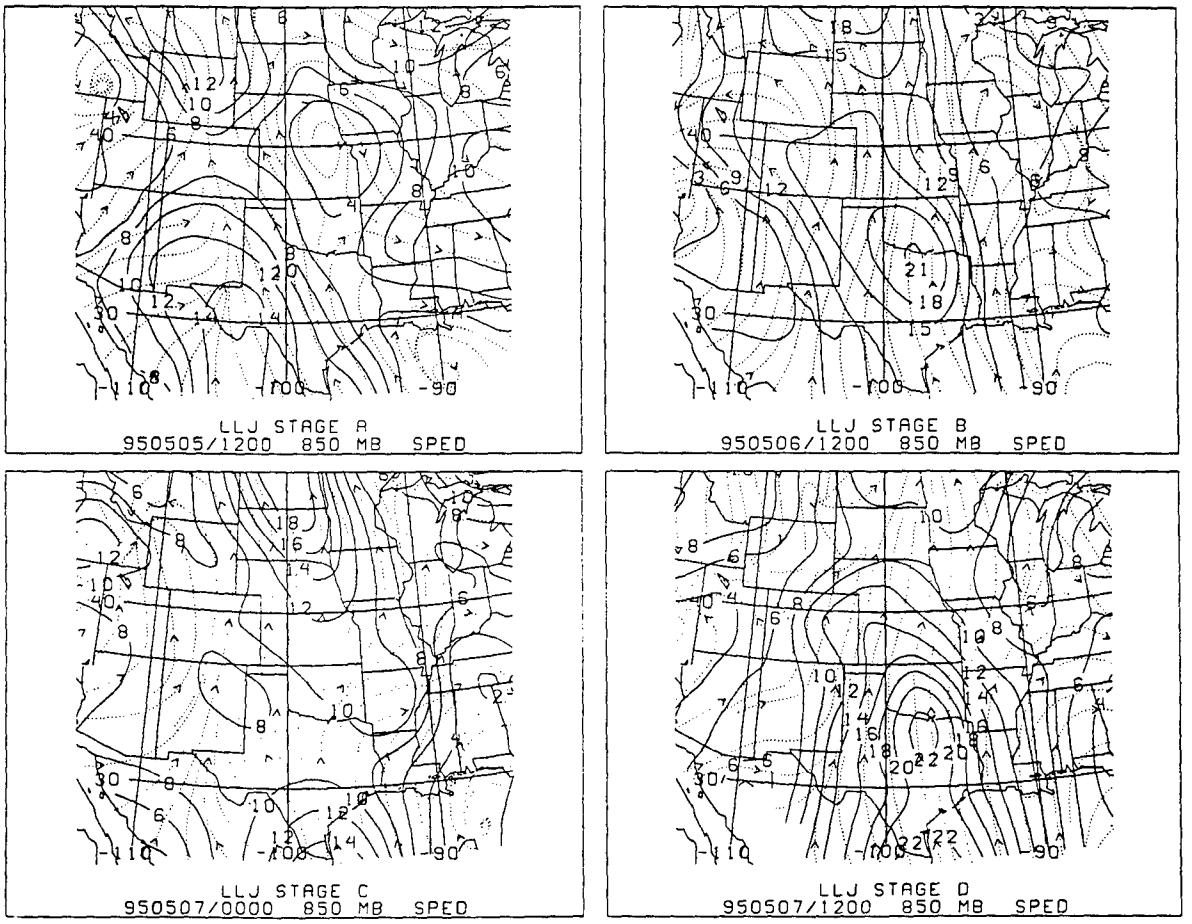

Fig. 6. Wind magnitude and streamlines at 850 mb; isotachs in m s^{-1} for stages A-D of the LLJ at 1200 UTC 5 May, 1200 UTC 6 May, 0000 UTC 7 May, and 1200 UTC 7 May respectively.

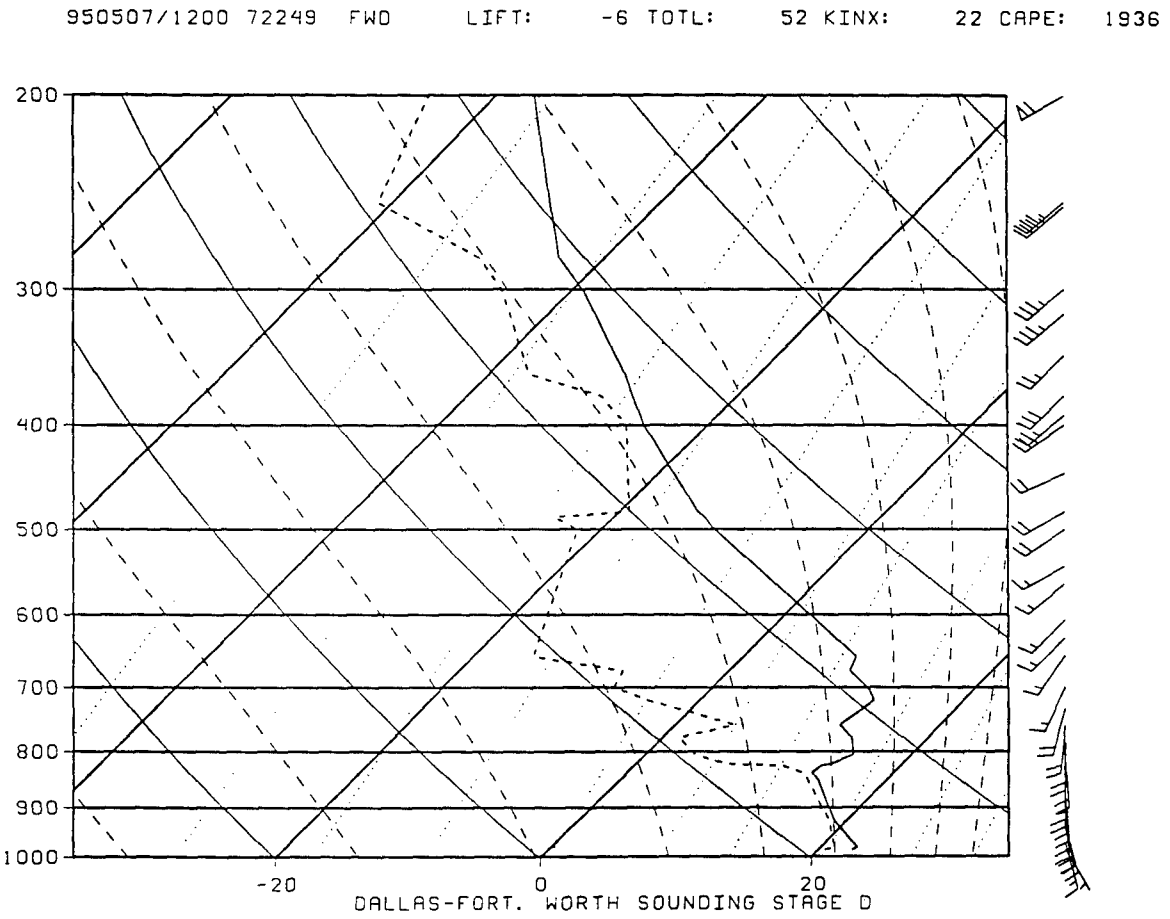

Fig. 7. Dallas-Fort Worth sounding at 1200 UTC 7 May 1995. The ambient temperature (solid lines) and ambient dew point (dashed lines) are plotted. Wind barbs on the right indicate speed in m s^{-1}. Three stability indices are included at the top. The LLJ occurs beneath the subsidence inversion based at 840 mb.

lower-tropospheric wind speed of 23 m s^{-1} near the 850 mb level beneath a subsidence inversion. At the base of the LLJ, a radiation inversion occurs near the surface. The wind decreases to 15 m s^{-1} and veers to the west-southwest above the inversion near the 550 mb level. This veering of winds with height causes a large angle between the mid-level wind direction (advecting dry air) and the low-level moist tongue axis. During the four stages of the wind event shown in Figure 6, the LLJ at 850 mb increases from a speed of 14 m s^{-1} in stage A to 23 m s^{-1} in stage D. At stage A, the LLJ initial direction is southeasterly. The jet begins to veer in northcentral Texas during stage B. Stations in the LLJ core show a 33-50% reduction in the LLJ maximum speed during stage C. Chapter V will try to explain the reason for fluctuating tendencies of the jet maxima during this stage.

At 300 mb, the polar jet stream (PJ) core stretches nearly south to north from Mexico into New Mexico with a speed of 55 m s^{-1} (Fig. 8). At 200 mb, the subtropical jet stream (STJ) speed approaches 60 m s^{-1} with a southwesterly direction into southwestern Texas. Time-height vertical sections throughout the southern Great Plains reveal the LLJ reaches its maximum speed at each location with the arrival of the ULJ streak. During each of the four stages, the LLJ appears to be coupled with the STJ exit region. Uccellini (1980) related the transverse circulations in the entrance and exit regions of jet streaks and the development of severe convection. All four locations, Lawton, Oklahoma, Corpus Christi, Waco and Dallas, Texas have a LLJ maximum of 21 m s^{-1} around 1200 UTC on 7 May with corresponding 200 mb speeds ranging from 45 to 57 m s^{-1} (Fig. 9). The LLJ speed decrease in stage C is noticeable at each of the four stations. The STJ speed increases over Texas starting at stage C, the time lee cyclogenesis begins. A statistical correlation relating the wind speed in the LLJ maximum and in the ULJ streak is as high as 0.85 at Dallas for the three day event.

A vertical section of wind magnitude between Del Rio, Texas and Cannon, New Mexico shows a boundary layer flow in its earliest development at stage A. A 14 m s^{-1} maximum is seen near 900 mb at Del Rio. During stages B and D, the vertical section between San Marcos, Texas and Salinas, Kansas shows the leading edge of the LLJ

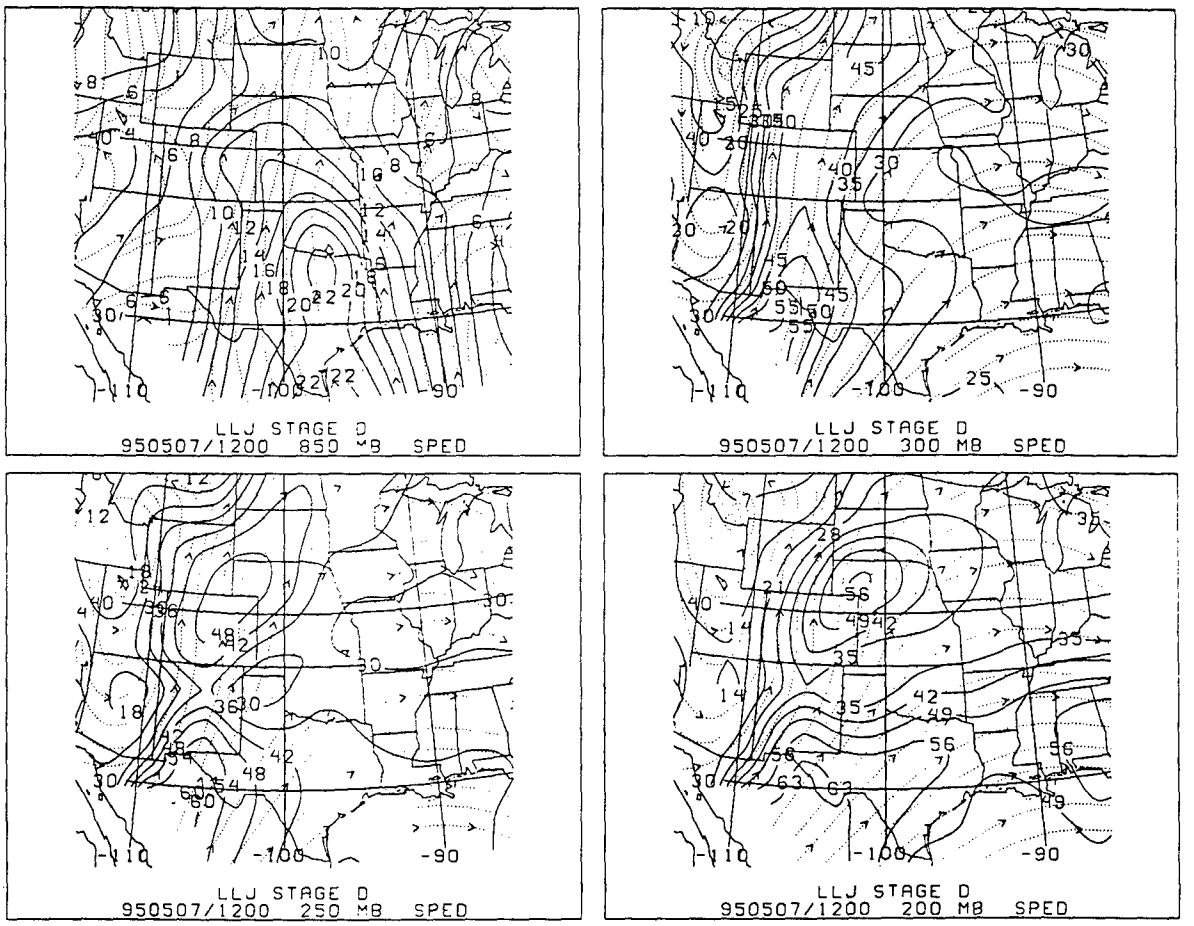

Fig. 8. Wind magnitude and streamlines (dotted lines) at 850 mb, 300 mb, 250 mb, and 200 mb on 1200 UTC 7 May 1995. This is the time of the LLJ's maximum strength and extent during the case. The polar front jet steak is best seen at 300 mb. The subtropical jet streak is best seen at 200 mb.

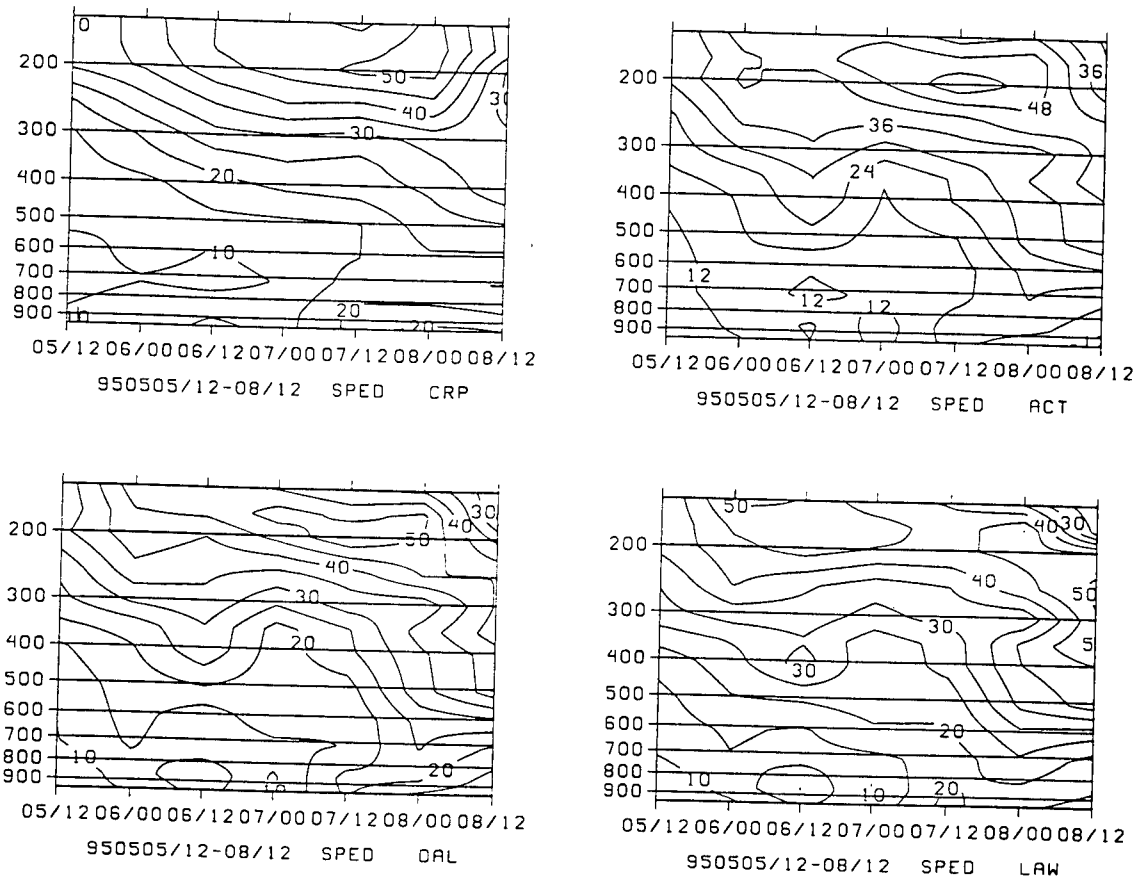

Fig. 9. Time-height cross section of wind magnitude for Corpus Christi, Waco, and Dallas, Texas and Lawton, Oklahoma from 1200 UTC 5 May 1995 to 1200 UTC 8 May 1995. The LLJ maximum occurs at 1200 UTC 7 May at all four stations.

extending north to Wichita, Kansas. At stage B, the core (20 m s^{-1}) of the LLJ from the southern most point to the northern most point is about 625 km long. Twenty-four hours later at stage D, the core (21 m s^{-1}) has grown to a length of 954 km. At this time, the STJ core is seen directly over the LLJ core (Fig. 10).

Another verification of the LLJ/ULJ relation is shown by the 850 mb and 200 mb isotach chart (not shown). In each of the four stages, the LLJ is coupled with a STJ streak. In stage A, the 12 m s^{-1} LLJ is coupled with the 50 m s^{-1} STJ isotach. The stage B LLJ of 21 m s^{-1} is coupled with the 48 m s^{-1} isotach of the STJ. In stage C, the LLJ of 12 m s^{-1} retreats to southern Texas as does the 54 m s^{-1} STJ core. In stage D, the 23 m s^{-1} LLJ core is underneath a 56 m s^{-1} STJ exit region. The large scale forcing associated with this relationship will be explored in Chapter V.

D. Low-level Temperature and Water Vapor Distribution

A warm, moist lower-troposphere is essential in creating favorable conditions for severe convection. The LLJ plays an important role in transporting heat and moisture into the convection areas. The transport generates convective instability in the lower half of the troposphere, lowers the level of free convection and raises the equilibrium level. The net effect is an atmosphere able to produce severe convective storms.

The 850 mb temperature chart shows a ridge of warm air associated with the newly developed southeast flow in stage A (Fig. 11). This ridge extends from western Texas to eastern Idaho, and a smaller ridge is present from east central Texas into southern Kansas. By stage B, the LLJ amplifies the ridge in the eastern Great Plains. In this case, the severe thunderstorms occurred south of the 10°C isotherm at 850 mb. The 10°C isotherm previously in northern Oklahoma now extends into northeast Kansas and northwest Missouri. By stage D, the LLJ has taken the 10°C isotherm into North Dakota having traveled over 1400 miles in a two day span.

Also of interest in the temperature distribution is the north to south gradient that strengthens as a cold front moves eastward toward Texas in stage D. To track the

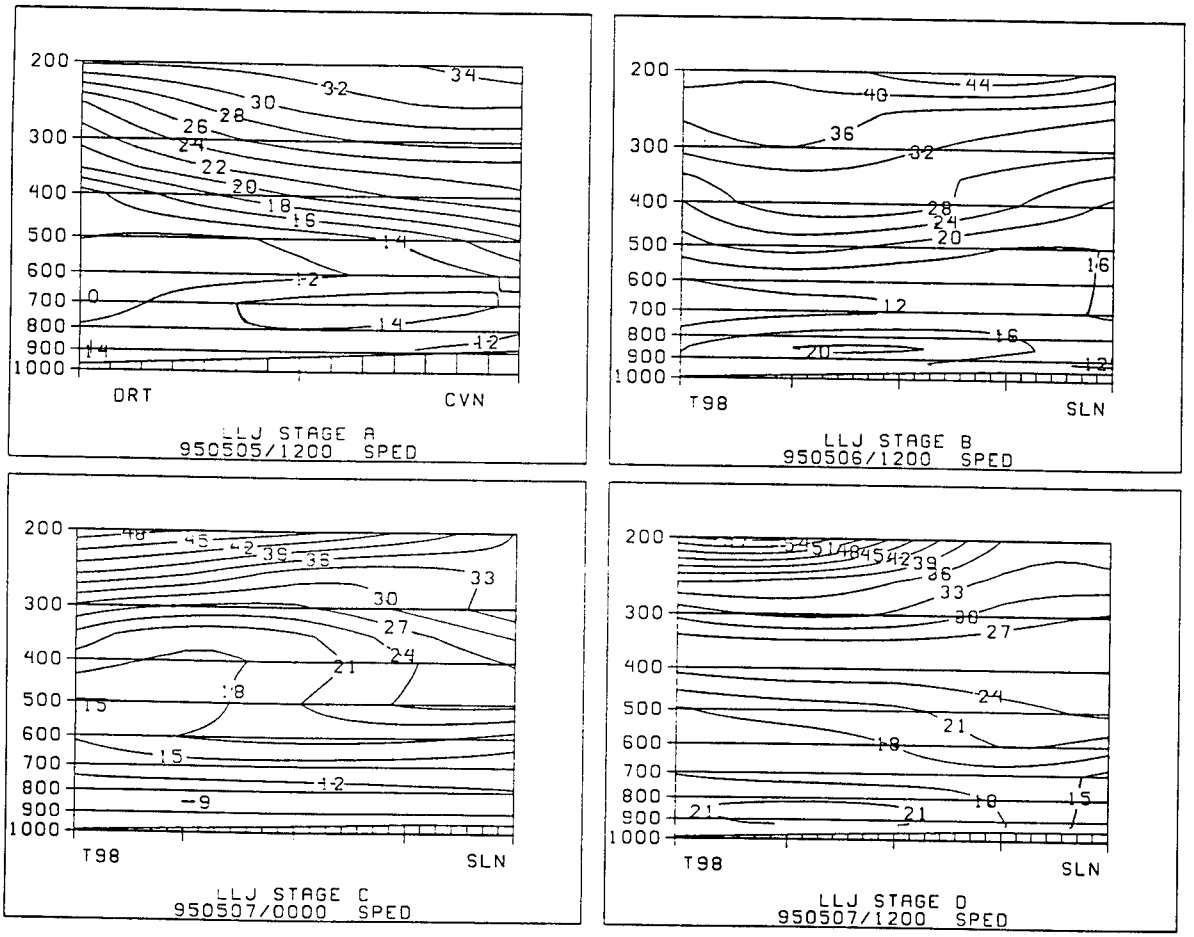

Fig. 10. Meridional cross section of wind magnitude during stages A-D of the LLJ. The LLJ maximum occurs in stage D over east central Texas and Oklahoma.

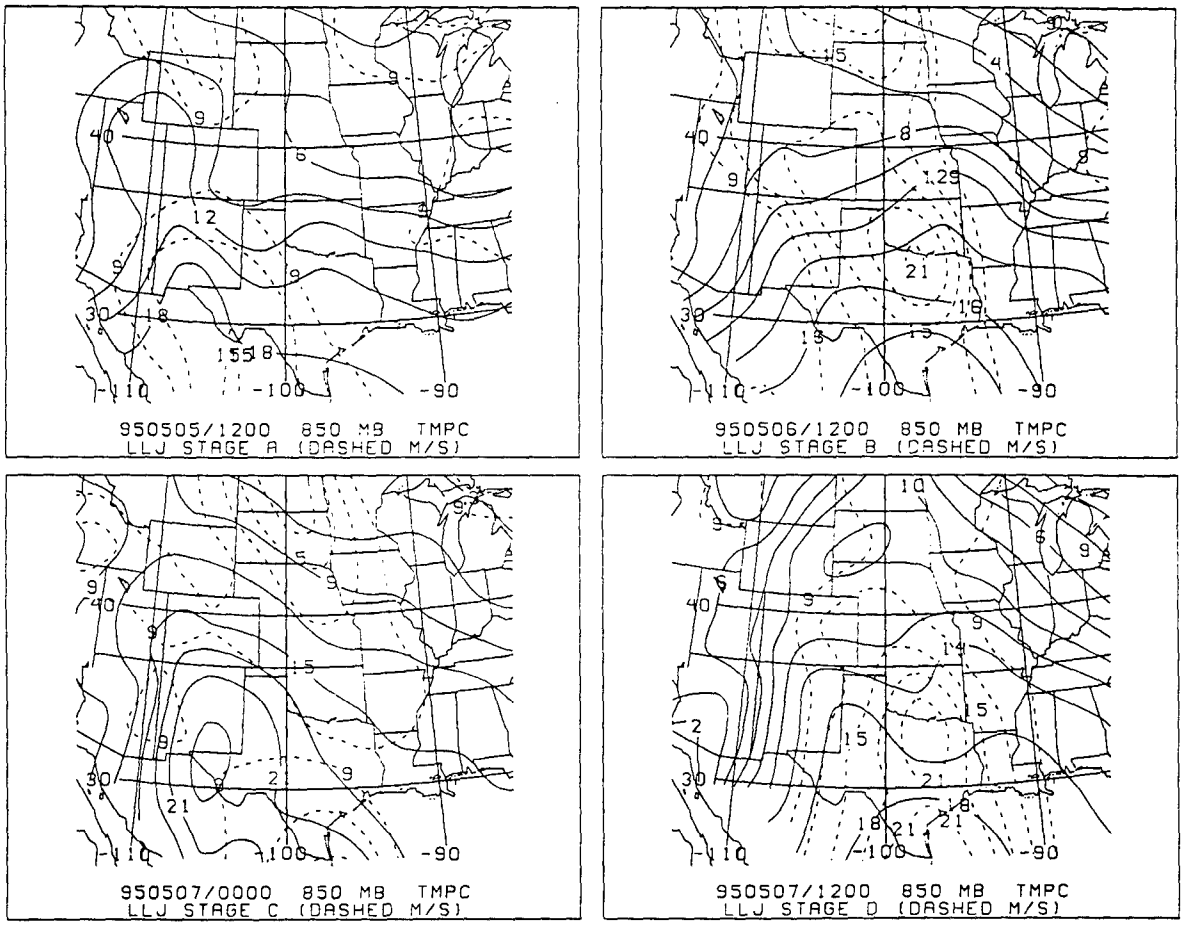

Fig. 11. Temperature (solid lines) and wind magnitude at 850 mb for stages A-D of the LLJ. Isotachs every 3 m s^{-1} starting at 9 m s^{-1} and isotherms every 2°C.

progress of the cold front, we follow the 850 mb temperature gradient between El Paso, Texas and Phoenix, Arizona. The difference increases from 8°C in stage A to 12°C in stage D. The cold air (2°C) in the base of the trough has progressed into southern Arizona in stage D.

Ample moisture was available during the studied event, and it moved north into the convective region as the LLJ strengthened. The remnants of the drier, Canadian air mass are still seen in the central Great Plains and the middle Mississippi Valley during stage A (Fig. 12). With the newly developed southerly flow off the Gulf of Mexico, the moist air has just begun to move northward. This creates a sharp north to south moisture gradient in the lower levels. At 850 mb, a 7 g kg^{-1} mixing ratio gradient exists between San Angelo, Texas (12 g kg^{-1}) and Tulsa, Oklahoma (5 g kg^{-1}). As the LLJ begins to strengthen in stage B, a moist tongue forms with the 10 g kg^{-1} isopleth moving into southern Oklahoma. By stage D, the 10 g kg^{-1} isopleth has moved into northeast Kansas. This is part of a well-developed moist tongue reaching into western Missouri. The previously mentioned gradient difference has reduced to 2 g kg^{-1}. With moisture, instability, and a forcing mechanism required for deep convection, the LLJ helped ensure the moisture portion of this requirement was available for the severe storms during the case.

E. Low-level Troughs and Ridges

Due to the quasi-geostrophic adjustment, height contours tighten within the LLJ core as a balanced flow is restored. This process shows the LLJ development is linked to an ageostrophic circulation. Chapter V will explore this circulation in the exit region of an upper-level jet streak.

Figure 13 shows 850 mb height contours along with wind speed at the same level. The initial southerly flow in stage A forms in southwest Texas with a 1400 gpm contour low center over Nevada and Utah. A large ridge is still intact over the eastern Great Plains as the 1540 gpm contour extends north into eastern Kansas. Twenty-four hours

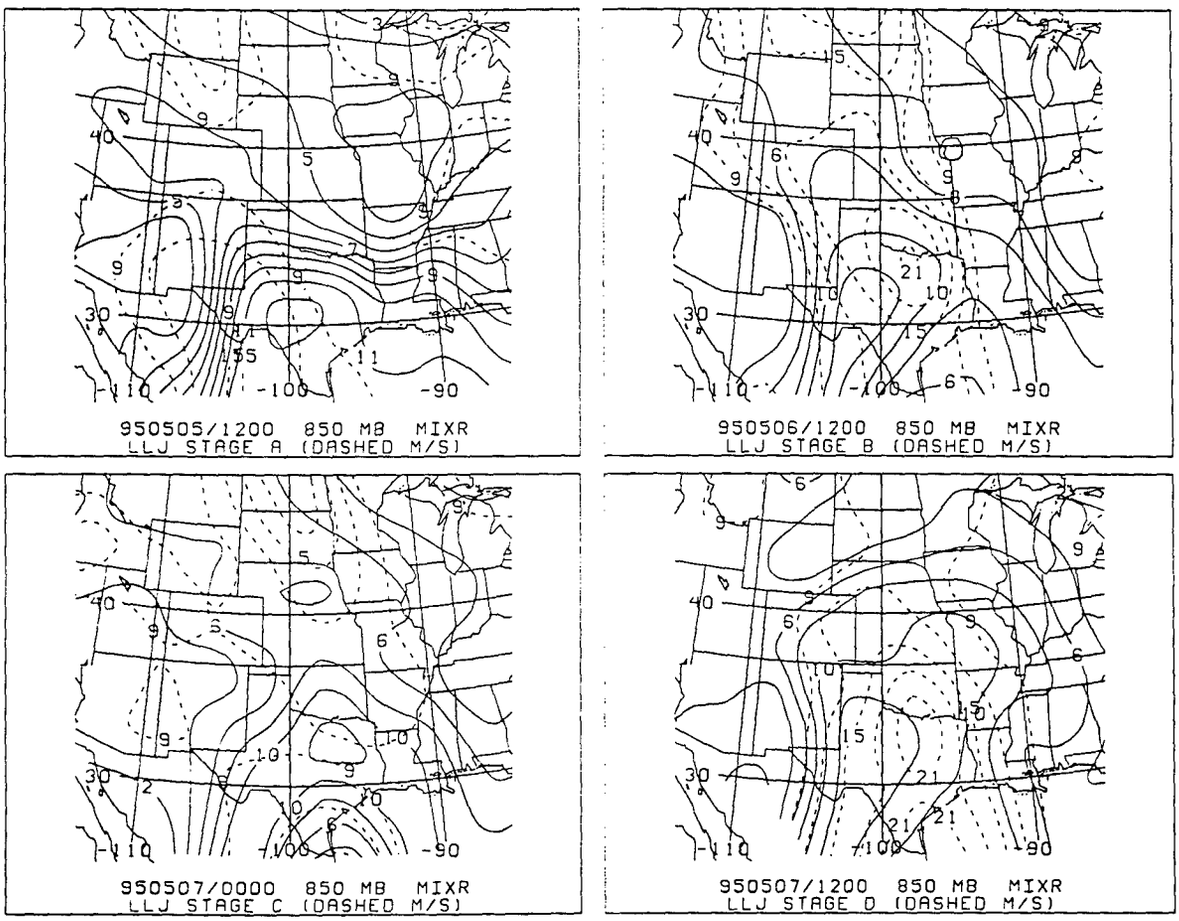

Fig. 12. Mixing ratio (solid lines) and wind magnitude at 850 mb for stages A-D of the LLJ. Isopleths of mixing ratio every 1 g kg^{-1}.

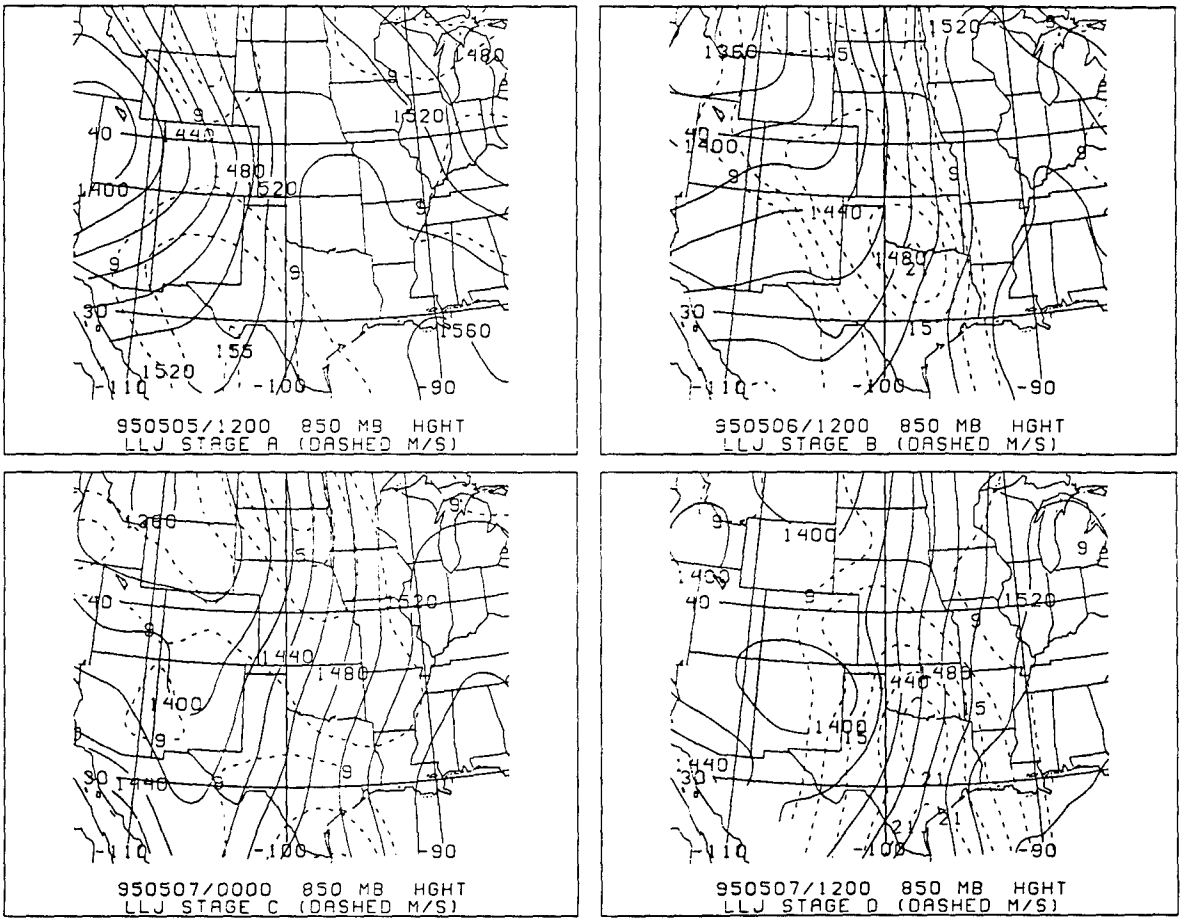

Fig. 13. Height contours (solid lines) and wind magnitude at 850 mb for stages A-D of the LLJ. The leeside cyclone appears in stage D.

later, the low has deepened to 1360 gpm and moved over western Montana. The LLJ core is located over the Texas and Oklahoma border with a speed of 21 m s^{-1} during stage B. During this stage, a height gradient between the northwest and southeast side of the core is 55 gpm. The ridge previously over the Great Plains has moved east of the Mississippi River and maintains its 1540 gpm contour. The LLJ core disappears from the 850 mb level during stage C even though a tight height gradient is apparent over the Great Plains. In stage D, a new low develops in the lee of the Rockies over New Mexico with a closed 1400 gpm contour. The LLJ core has moved only a few miles east since stage B, but its speed increased to 23 m s^{-1} while the height gradient across the LLJ increased to 95 gpm.

A similar relationship between height and wind speed exists between the 700 mb and 850 mb levels. In stage A, the low over Nevada and Utah has a 2980 gpm contour at 700 mb. The low has deepened in stage B to 2940 gpm and is vertically stacked above the 850 mb low. The cold front and associated trough is best seen at 850 mb in stage C though this trough does not appear at the 700 mb level. At the peak of the LLJ in stage D, a 2960 gpm closed-contour low has developed over Arizona at 700 mb. This low is farther west than the 850 mb low but is deep enough to help produce the dynamics necessary for a strong LLJ.

F. Low-level Properties on Isentropic Charts

For each of the four stages of the LLJ, the 301 K surface intersects the core of the LLJ. During the three day event, the LLJ core at 301 K occurs at a pressure between 930 mb and 780 mb (Fig 14). This shows the air flow through the LLJ increasing in altitude as it flows from south to north. In stage B, the southern portion of the core (18 m s^{-1}) is at 880 mb (1188 m) in central Texas. The northern portion of the core has ascended to 780 mb (2134 m) in southwest Nebraska. The LLJ in stages B and D occurs on the western side of a ridge in the isobars (on the 301 K chart). A trough in the isobars is evident to the west of the LLJ especially in stage B as the jet strengthens. Since isobars

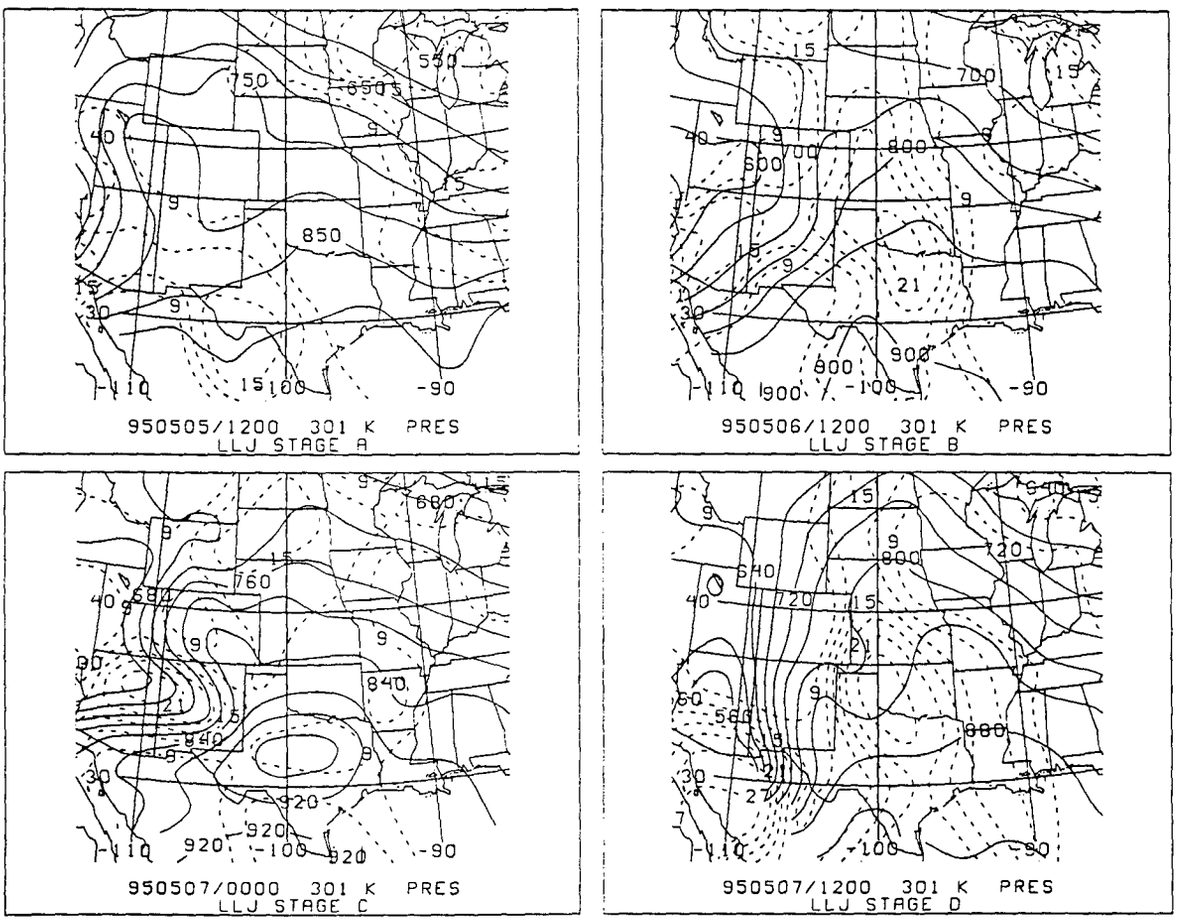

Fig. 14. Isobars (solid lines) and wind magnitude on 301 K isentropic surface for stages A-D of the LLJ. Daytime heating causes the 301 K surface to descend to 960 mb in stage C.

on isentropic surfaces represent isotherms, the ridge is warm, and the trough is cold. The isobars and isotherms on the 301 K surface have identical patterns of troughs and ridges.

On the 301 K surface, the LLJ is similar to the LLJ on the 850 mb surface. Figure 15 contains isotachs and streamlines on the 301 K surface during the four stages of the LLJ. This surface is nearly identical to the wind direction and speed on the 850 mb chart shown in section B. In stage A, the southeasterly flow first appears in southwest Texas at a speed of 15 m s^{-1}. By stage B, the LLJ core extends from central Texas to southwest Nebraska and begins to veer. The 301 K surface also shows the weakening of the LLJ in stage C, as the 12 m s^{-1} isotach retreats to southern Texas. At its peak in stage D, the LLJ core extends from southern Texas into northwestern Kansas with a maximum speed of 24 m s^{-1}. The 301 K surface ascends rapidly heading west over the southern Rocky Mountains.

The mixing ratio distribution on the 301 K surface shows a northward expansion similar to the 850 mb surface during the four stages as the LLJ strengthens (not shown). The 10 g kg^{-1} isopleth starts near Dallas, Texas in stage A and moves northward near Colombia, Missouri by stage D. A moist tongue is evident in each of the four stages providing a focus area for convection. The axis moves east during the stages from western Texas, to western Kansas, to eastern Kansas and into northeast Missouri. Each stage shows ample water vapor is available to fuel deep convection during the case study.

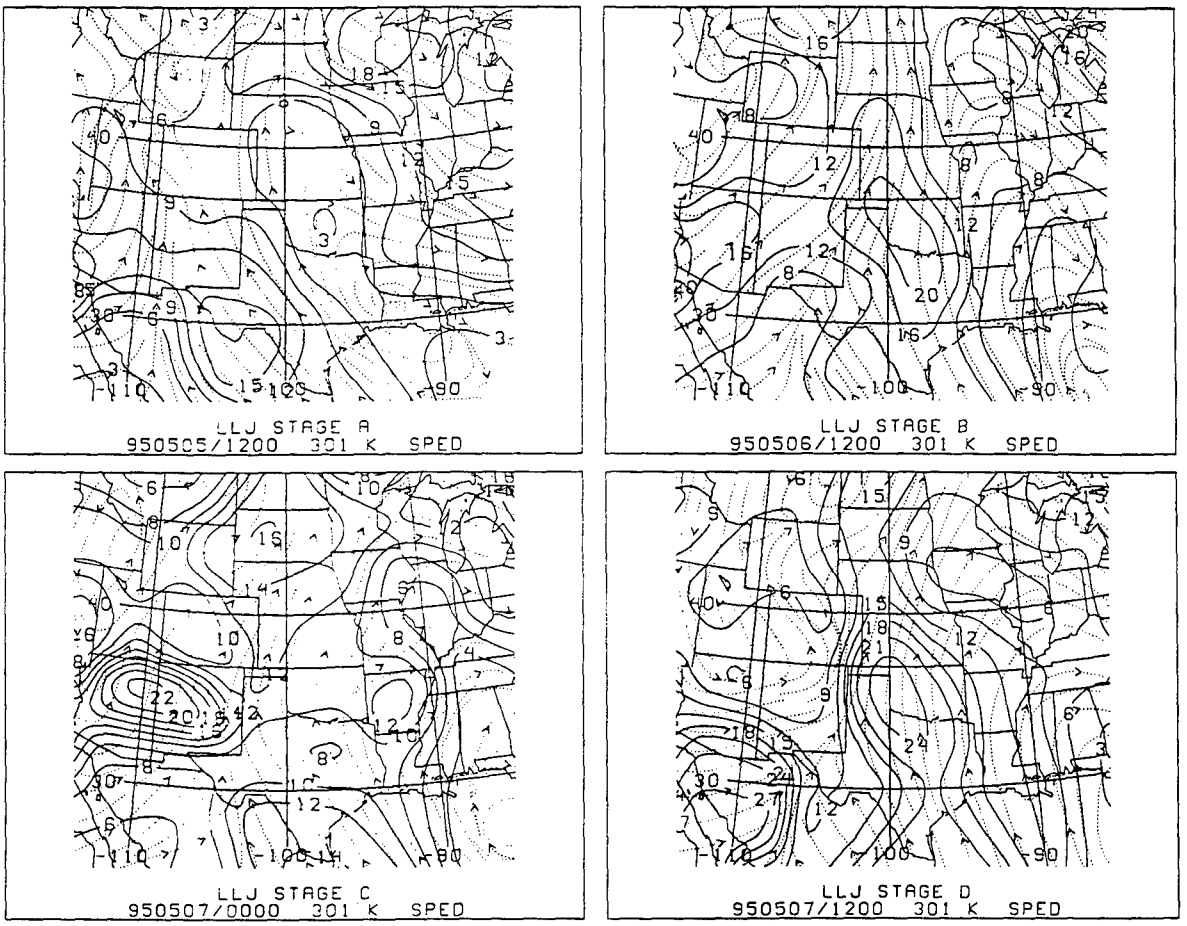

Fig. 15. Wind magnitude and streamlines (dotted lines) on 301 K isentropic surface for stages A-D of the LLJ.

CHAPTER V

LOW-LEVEL JET EVOLUTION AND INTERACTION WITH A SUBTROPICAL JET STREAK

Several mechanisms have been proposed concerning the development of the southerly LLJ that forms over the central United States. These mechanisms are classified into two main groups: boundary layer and synoptic-scale. In this case, a combination of synoptic-scale mechanisms is the main influence for the LLJ evolution over the southern Great Plains. It appears the combined effects of two upper-tropospheric jet streaks and lee cyclogenesis determine the behavior of the LLJ.

A. Upper-level Jet Streak Tendencies

In most cases over the Great Plains, the LLJ evolves in the active region between an upper-level trough over the Rocky Mountains and a downstream ridge. The case considered here, however, appears to stray from the usual pattern since the LLJ develops under the STJ streak exit region and strengthens as the lee cyclone forms. This large scale pattern forms a LLJ about 556 km southeast of Bonner's (1968) climatological maximum for the LLJ over northwest Oklahoma.

Figure 16 shows the 200 mb level where the STJ usually can be found. The exit region of the STJ streak induces an ageostrophic circulation, producing the southerly LLJ. As the southeasterly flow begins in stage A over southwest Texas, the STJ exit region is over northern Mexico and southwest Texas decreasing downstream from a maximum of 55 m s^{-1}. By stage B, the exit region moves over the southern Great Plains, and the LLJ develops beneath it over north central Texas and Oklahoma. During the apparent diurnal decrease of the LLJ in stage C, the exit region moves south into Texas. With the exit region occurring over southern Texas and no lee cyclone, the LLJ becomes weaker and disappears from the Great Plains. The LLJ reaches its maximum speed

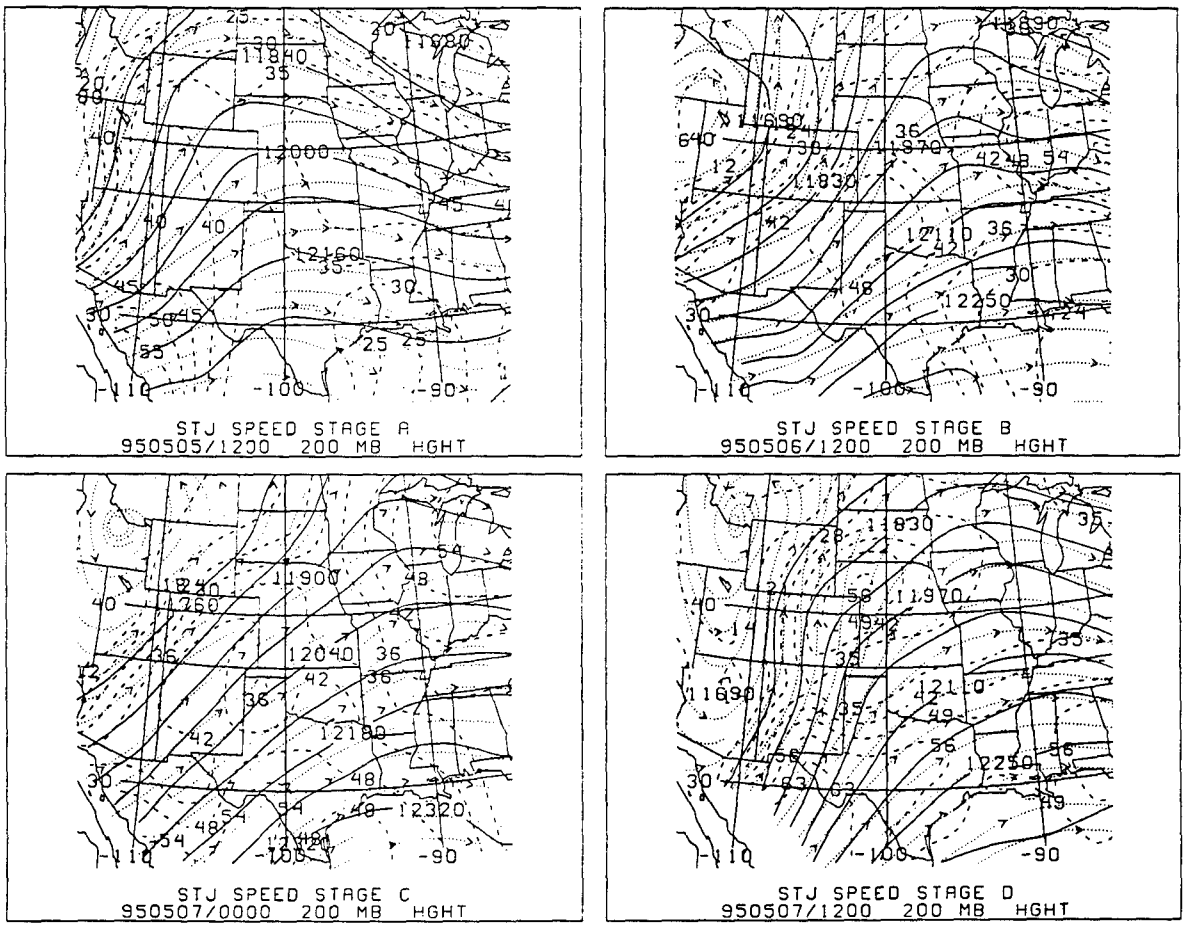

Fig. 16. Height, wind magnitude (dashed lines), and streamlines (dotted lines) at 200 mb during stages A-D of the LLJ. The subtropical jet occurs near the 200 mb level.

in stage D when the height contours show the 200 mb trough over eastern Arizona with one closed height contour. At this time, the streak reaches its maximum speed, and the exit region is positioned over central Texas again over the LLJ. Since the LLJ in stages B and D occur under the exit region of the STJ streak, this verifies the dynamic relationship between the two features.

Over the four stages of the LLJ, the STJ flows almost zonally across northern Mexico and over Texas. This is quite a contrast to the polar jet stream (PJ) position. As the upper-level trough digs south into Arizona in stage D, the PJ flows meridionally over the Rockies. It appears the diffluence between the PJ and the STJ has a significant influence on the LLJ. In stage C, the STJ migrates south over southern Texas. The upper-level divergence is at a minimum for at this stage with the large distance between the two jet streams. As the PJ moves east ahead of the trough in stage D, the diffluence reappears over the LLJ area. A strong area of upper-level divergence via advection of vorticity at this time leads to low-level convergence as part of the ageostrophic circulation covered in sections C and D. In stages A, B, and D, the LLJ appears on the western side of the 200 mb ridge axis. The tightest height contours occur to the west of the LLJ closer to the approaching cyclone.

B. Wind Divergence and Convergence Patterns

The development of the Great Plains LLJ is typically associated with lee cyclogenesis. Upper-level divergence is required for cyclone development and is followed by a reduction in surface pressure in an area of converging low-level winds. Both upper-level divergence and low-level convergence are required for surface cyclogenesis. In this case, the STJ streak provides upper-level divergence, and lifting above the LLJ provides the low-level convergence. We expect convergence and ascent in the front right portion of the LLJ exit region as part of the ageostrophic circulation induced by the STJ streak exit region. This ascent in the northern portion of the LLJ helps trigger convective development during this case.

Figure 17 shows divergence patterns for stages A-D of the LLJ at 850 mb. Negative divergence indicates low-level convergence in this figure. In stage A, the LLJ development is accompanied by a strong area of convergence over New Mexico and western Texas with a maximum value of $-4x10^{-5}$ s^{-1}. As in all the stages, the convergence occurs on the northern half of the LLJ. In stage B, convergence also occurs on the northern half of the LLJ over Oklahoma and Kansas. The influence of a upper-level jet streak over the Ohio Valley is seen at this time. Convergence occurs over the middle Mississippi River Valley in conjunction with the right rear quadrant of this 200 mb streak. As the LLJ retreats south in stage C, a broad area of divergence replaces the convergence. This is in response to the STJ streak exit region shifting south and realigning the low-level convergence pattern. The LLJ strengthens in stage D, and convergence reappears over Oklahoma and Kansas. The result of the low-level convergence in the northern part of the LLJ is lifting and precipitation which are both driven by the position of upper-level divergence caused by the STJ streak. Tornadoes and flooding rains were reported throughout the area with strong upper-level divergence during the case.

In upper-tropospheric jet streaks, parcel acceleration in the entrance region and deceleration in the exit region induces ageostrophic motions in the jet streak. We expect divergence in the right entrance and left exit regions of the jet streak from these motions. The 200 mb divergence pattern for the four stages of the LLJ is shown in Figure 18. These divergence patterns confirm the connection between the STJ streak exit region and the dynamic properties of the LLJ. An area of strong divergence ($6x10^{-5}$ s^{-1}) over western Oklahoma is positioned above the northern half of the LLJ and its band of convergence in stage B. The divergence takes place in the front left region of the STJ streak as studied by Uccellini and Johnson (1979). As the STJ streak moved northeast and strengthened from stage A to stage B, the LLJ shifted eastward and strengthened. In stage C, the divergence disappears over the southern Great Plains helping cause a decrease in the LLJ. The STJ moves over southern Texas repositioning the divergence maximum over north central Mexico. Without any low-level convergence, upper-level

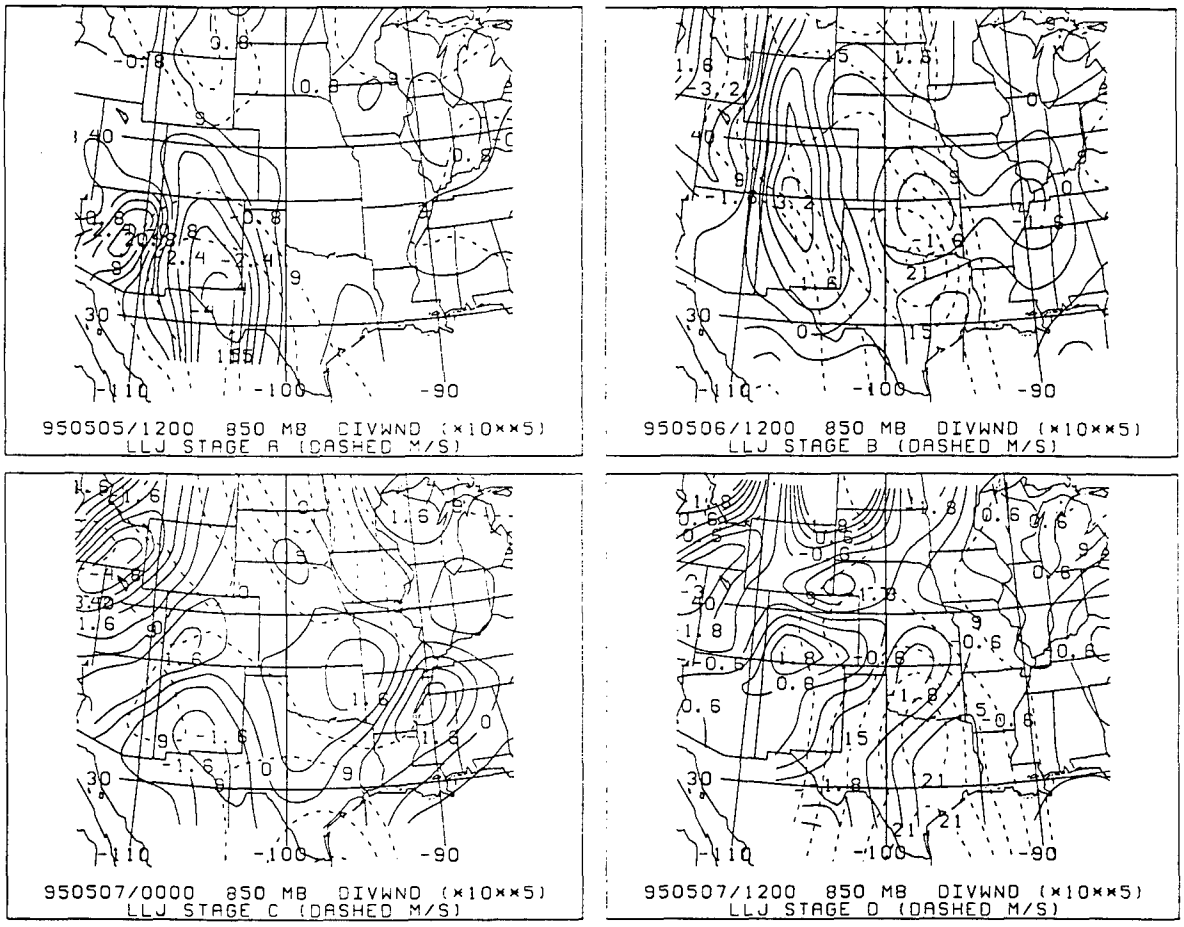

Fig. 17. Wind divergence and wind magnitude (dashed lines) at 850 mb during stages A-D of the LLJ. Convergence is shown by negative divergence values.

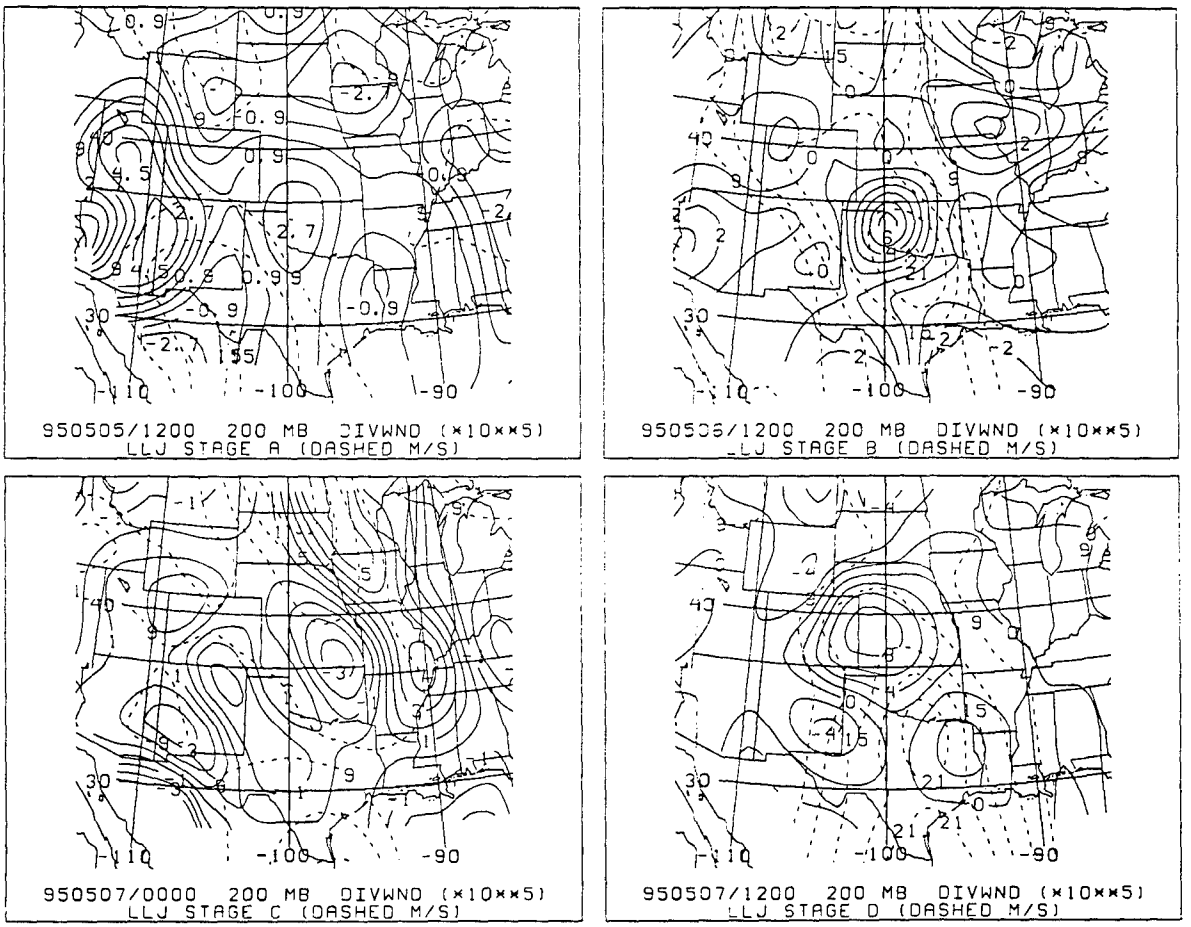

Fig. 18. Wind divergence at 200 mb and wind magnitude (dashed lines) at 850 mb during stages A-D of the LLJ.

divergence, or diffluence between the PJ and STJ, thunderstorm activity halts during this stage over the southern Great Plains.

The dynamical pattern redevelops in stage D with the PJ positioned near the STJ, and diffluence returning over the southern Great Plains. At this time, the LLJ reaches its maximum size and speed. A strong area of divergence ($8x10^{-5}$ s^{-1}) is positioned over western Kansas and above the northwest side of the LLJ. This divergence maximum appears to strengthen due to its location between the STJ streak and PJ streak flowing south to north over western Nebraska. The radar summary from 1135 UTC on 7 May shows a large thunderstorm complex covering the western half of Kansas directly underneath this divergence maximum and near the convergence maximum with the LLJ. The 200 mb divergence pattern in stage D is similar to Uccellini and Johnson's jet steak schematic. Strong divergence takes place in the front left region of the streak while convergence occurs in the front right region of the streak. Section D of this chapter will show how an indirect thermal circulation develops in the STJ streak forming the LLJ and producing low-level convergence necessary for convection underneath the upper-level divergence.

A meridional vertical section of divergence and isotachs is seen in Figure 19. During the LLJ development in stage A, moderate convergence develops along the northern edge of the southeasterly wind over western Texas and eastern New Mexico. Weak divergence is evident over the southern portion of the newly formed LLJ. A subsequent increase in the upper-level divergence occurs in stages A, B, and D as shown by Figure 18. The exception is in stage C when the STJ moves far south during the transition of large scale forcing. The increase in the upper-level divergence helps explain the continued presence of the low-level convergence in the northern regions of the LLJ in these three stages. Each low-level convergence maximum is positioned directly beneath the upper-level divergence maximum leading to the examination of the ageostrophic circulation caused by the STJ streak.

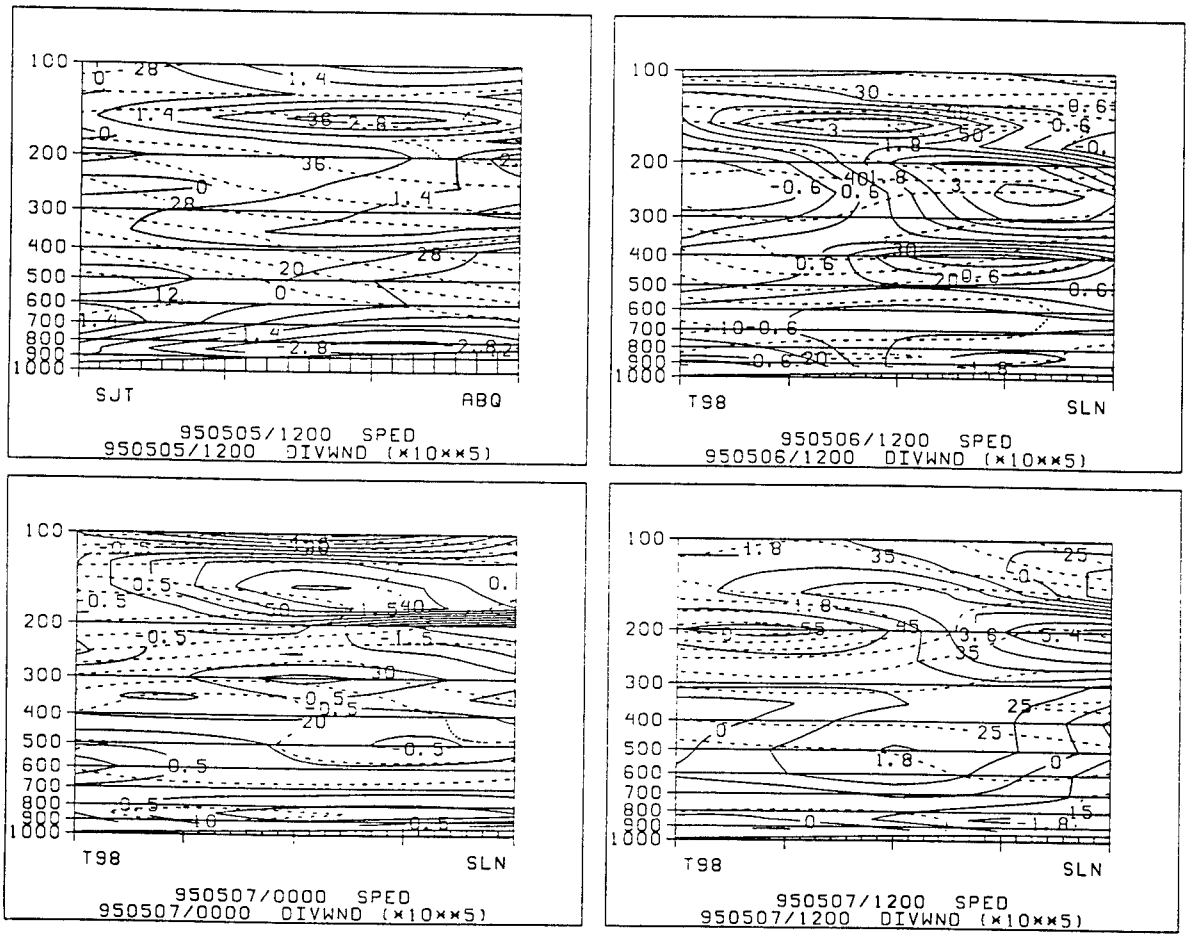

Fig. 19. Meridional vertical section of wind divergence and wind magnitude (dashed lines) during stages A-D of the LLJ.

C. Low-level Ageostrophic Wind

The May 1995 case contains large scale features similar to cases studied by Uccellini (1980). A trough over the Rocky Mountains and a ridge over the eastern third of the United States with upper-tropospheric jet streaks propagating over the Rockies produce a Type I LLJ. The Type II LLJ is diurnally oscillating and forms when a blocking ridge is in place over the Great Plains. This case is unique since the large scale pattern resembles Uccellini's Type I LLJ, but an oscillating LLJ develops similar to the Type II.

Temperature and vorticity advection by the ageostrophic wind play an important role in vertical motion, cyclogenesis, and weather system movement. When this flow is across contours toward lower pressures, the wind tends to strengthen. The cross-contour flow along with rising and sinking motions try to restore the atmosphere to thermal equilibrium.

The development of the LLJ as an isallobaric flow was studied by Uccellini and Johnson (1979) and Djuric and Damiani (1980). An ageostrophic wind with a large isallobaric component in the lower-troposphere develops due to an indirect circulation induced by an upper-tropospheric jet streak exit region. The ageostrophic wind tends to be perpendicular to the LLJ axis especially in the southern half of the LLJ core. The ageostrophic and isallobaric wind contribute to along stream accelerations for parcels entering and exiting the jet streaks. A complete explanation of the isallobaric wind is given by Carlson (1991, p. 370). Three equations aid the study of ageostrophic motions:

$$\mathbf{V}_g = (g/f)\mathbf{k} \times \nabla z \qquad (3)$$

The ageostrophic wind is found by subtracting the geostrophic wind ($\mathbf{V}_g$) from the total wind ($\mathbf{V}$).

$$\mathbf{V}_a = \mathbf{V} - \mathbf{V}_g \quad (4)$$

The last equation is for the isallobaric wind:

$$\mathbf{V}_i = -(g/f^2)\nabla_p(\partial Z/\partial t) \quad (5)$$

Equation 5 is the isallobaric wind where g is the acceleration of gravity, f is the Coriolis parameter and $\partial Z/\partial t$ is the height tendency.

1. Cross Isobar Ageostrophic Wind

Figure 20 shows ageostrophic wind and height at 850 mb for stages A-D of the LLJ. In stage A, the ageostrophic wind in the LLJ region flows across the height contours from the southeast. The ageostrophic maximum in the vicinity of the LLJ is about 11 m s^{-1} in southwest Texas. This wind is in response to a trough extending from the low center over eastern Nevada. In stage B, the ageostrophic wind is still southeasterly and flows across the contours in the southern half of the LLJ. The maximum ageostrophic wind associated with the LLJ occurs in the core, flowing along the contours with a magnitude of about 12 m s^{-1}. At this time, the strongest ageostrophic wind is in the trough over western Colorado close to the low in western Montana with a magnitude of about 20 m s^{-1}. In stage C, the ageostrophic flow becomes northeasterly toward the trough over central New Mexico. This appears to be a transition period between the forcing from the trough moving over the Great Plains in stage B and lee cyclogenesis in stage D. In stage D, when the LLJ reaches its maximum speed, the ageostrophic wind returns to the southeast across the contours directed toward the newly formed lee cyclone over New Mexico and Colorado. The convergence seen in stages C

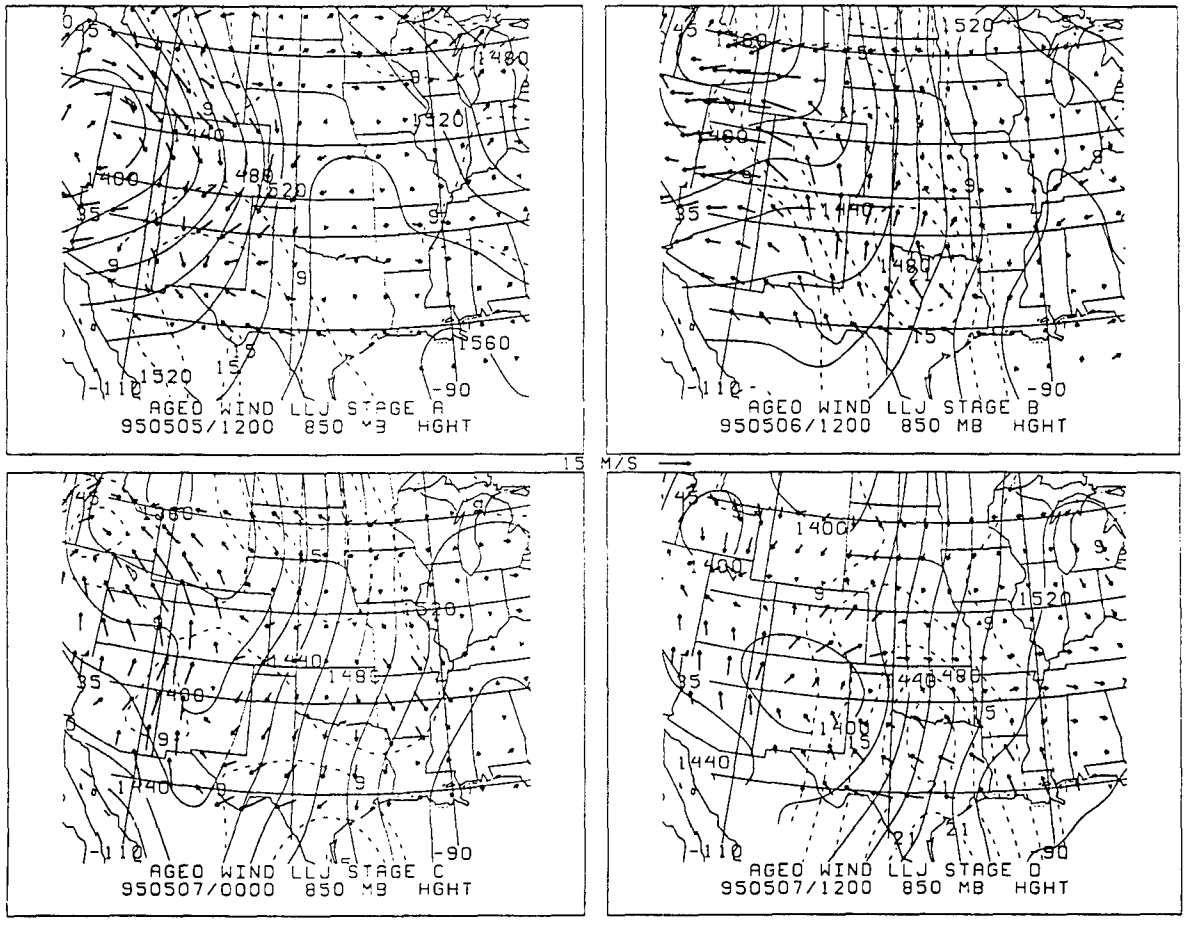

Fig. 20. Ageostrophic wind (arrows), height (solid lines), and wind magnitude (dashed lines) at 850 mb during stages A-D of the LLJ.

and D in New Mexico and the Texas Panhandle provides the mechanism for an increase in vorticity and contributes to lee cyclogenesis. The main concept from Fig. 20 is relating the cross-contour ageostrophic flow toward a trough or low center to the increase in the LLJ speed. In stages B and D, the LLJ develops and strengthens in an area of cross-contour ageostrophic flow. Section 2 relates this feature to the isallobaric wind and geopotential height gradients.

The ageostrophic wind in this case responds to two separate jet streaks. In stage B, the ageostrophic flow is directed toward the trough extending south from the low in western Montana driven by the PJ while the STJ streak is deepening the southern portion of the trough over the Rocky Mountains. The stronger LLJ in stage D has a cross-contour ageostrophic component toward the newly formed lee cyclone forced by the STJ.

2. Low-level Isallobaric Wind

Accelerations in the atmosphere are often represented by a cross-contour isallobaric flow into a low pressure area. When comparing the cross-contour flow of the ageostrophic wind in Fig. 20 to the isallobaric wind in Figure 21, we see the two winds are quite similar in areas away from highly curved flow near troughs or low centers.

Figure 21 contains the isallobaric wind and height at 850 mb during stages A-D of the LLJ. The time derivative for the change in height (Equation 5) necessary to compute the isallobaric wind is computed over the previous 12 hours. We expect the regions where the isallobaric flow is directed toward lower heights to experience an increase in geostrophic wind magnitude. As mentioned earlier, the drop in geopotential height gradients is linked to the strengthening of the LLJ. The Coriolis force changes the direction of the LLJ from the center of the height falls to a southerly direction. In our case, two separate low pressure areas influence the LLJ. The LLJ responds to a trough advecting northeast from a low over Montana, and lee cyclogenesis occurring under the STJ streak.

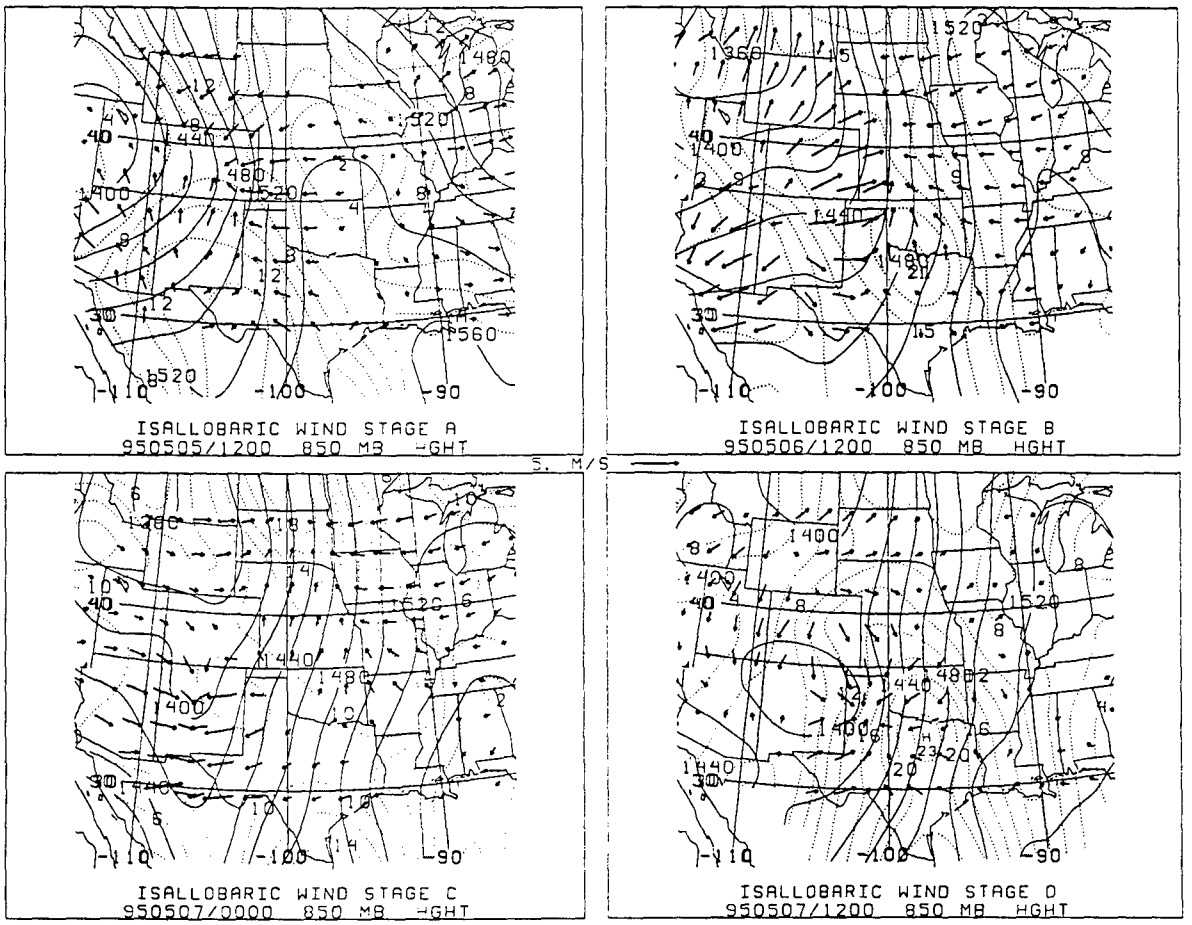

Fig. 21. Isallobaric wind (arrows), height (solid lines), and wind magnitude (dashed lines) at 850 mb during stages A-D of the LLJ.

In all four stages, the ageostrophic and isallobaric wind patterns are similar to each other especially over central Texas where the LLJ strengthens in stages B and D. Although, the magnitudes of the ageostrophic wind are 5 m s^{-1} to 10 m s^{-1} stronger in each of the stages. Such a result was also seen by Chen et al. (1994) in their study of the LLJ over southern China. In stage B, the larger isallobaric vectors in the northern LLJ core indicate stronger accelerations occurring in this portion of the streak. As the LLJ reaches its maximum in stage D, the magnitude of the isallobaric wind decreases. This is expected since acceleration (dv/dt) should be at zero when the wind (v) is at a maximum. Since the isallobaric wind is tied to the changes in the geopotential height gradient, this suggests the cross-contour ageostrophic winds are also related to changes in geopotential height gradients. Specifically in this case, the intensification of the LLJ in stages B and D is closely related to the short-wave trough advecting east over the northern Great Plains and lee cyclogenesis induced by a strong STJ streak.

Figure 22 shows the divergence pattern of the isallobaric wind at 850 mb for stages A-D of the LLJ. In stage B, strong convergence of the isallobaric wind occurs just ahead of the trough over the northern Great Plains. In stage D, the isallobaric convergence occurs just east of the newly formed lee cyclone over New Mexico. In both stages, the area of strong convergence occurs on the northwest side of the LLJ core similar to the total wind convergence patterns. The effects of the Coriolis force are seen since the LLJ occurs to the right of the acceleration associated with the isallobaric wind. During stages B and D, the LLJ is fully developed and attains speeds over 20 m s^{-1} over north central Texas and Oklahoma.

All the previous information in this section comes together when viewing Figure 23. This is a plot of the isallobaric wind and 12 hour height change at 850 mb for the four stages of the LLJ. Changes in geopotential height on a constant pressure surface are represented by isallohypses. Two separate pressure fall areas are easily identified using isallohypses. In stages A-C, heights fall ahead of the trough associated with the low over Nevada and Montana. The LLJ in stages A and B evolves partially in response to this isallobaric flow toward the height fall center ahead of the trough. Although the

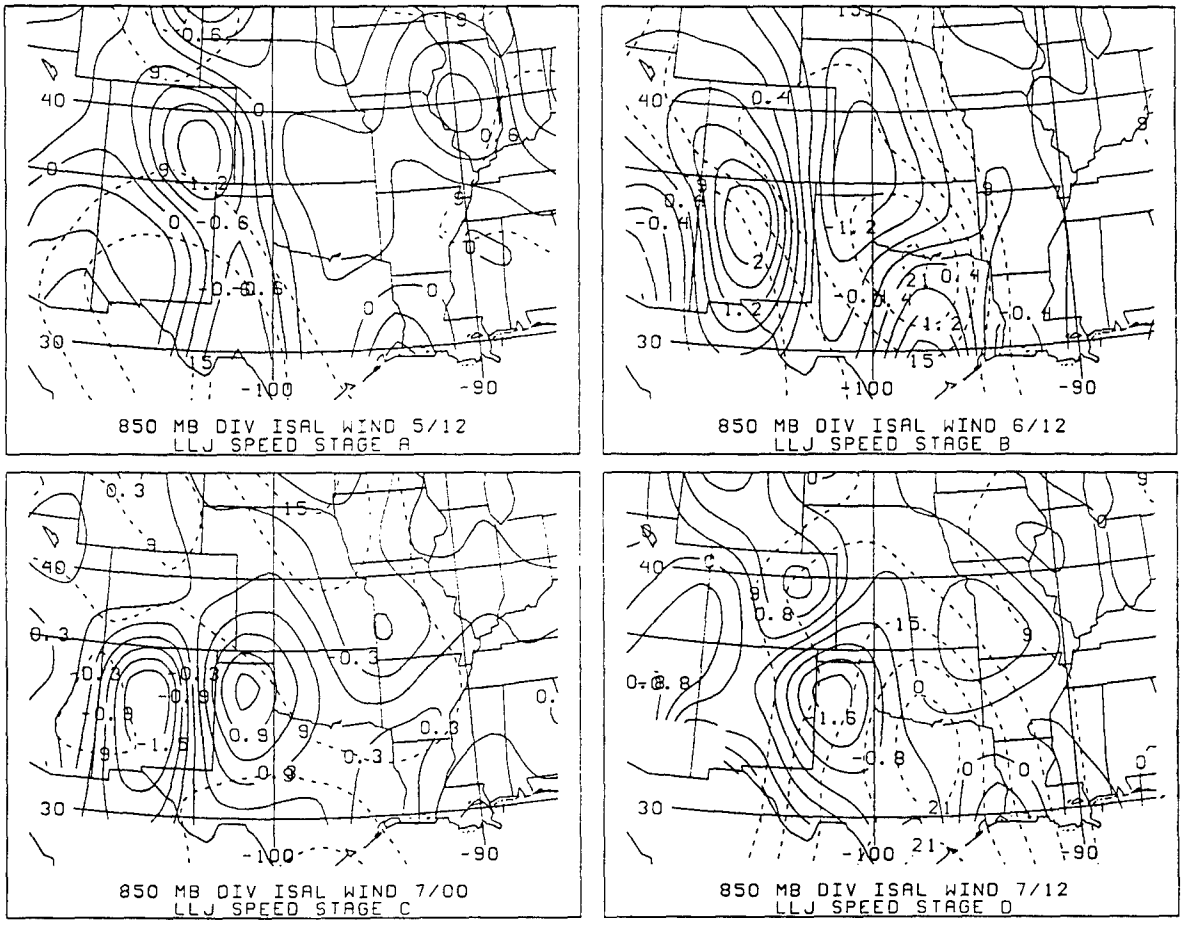

Fig. 22. Isallobaric wind divergence and wind magnitude (dashed lines) at 850 mb during stages A-D of the LLJ. Convergence is shown by negative values.

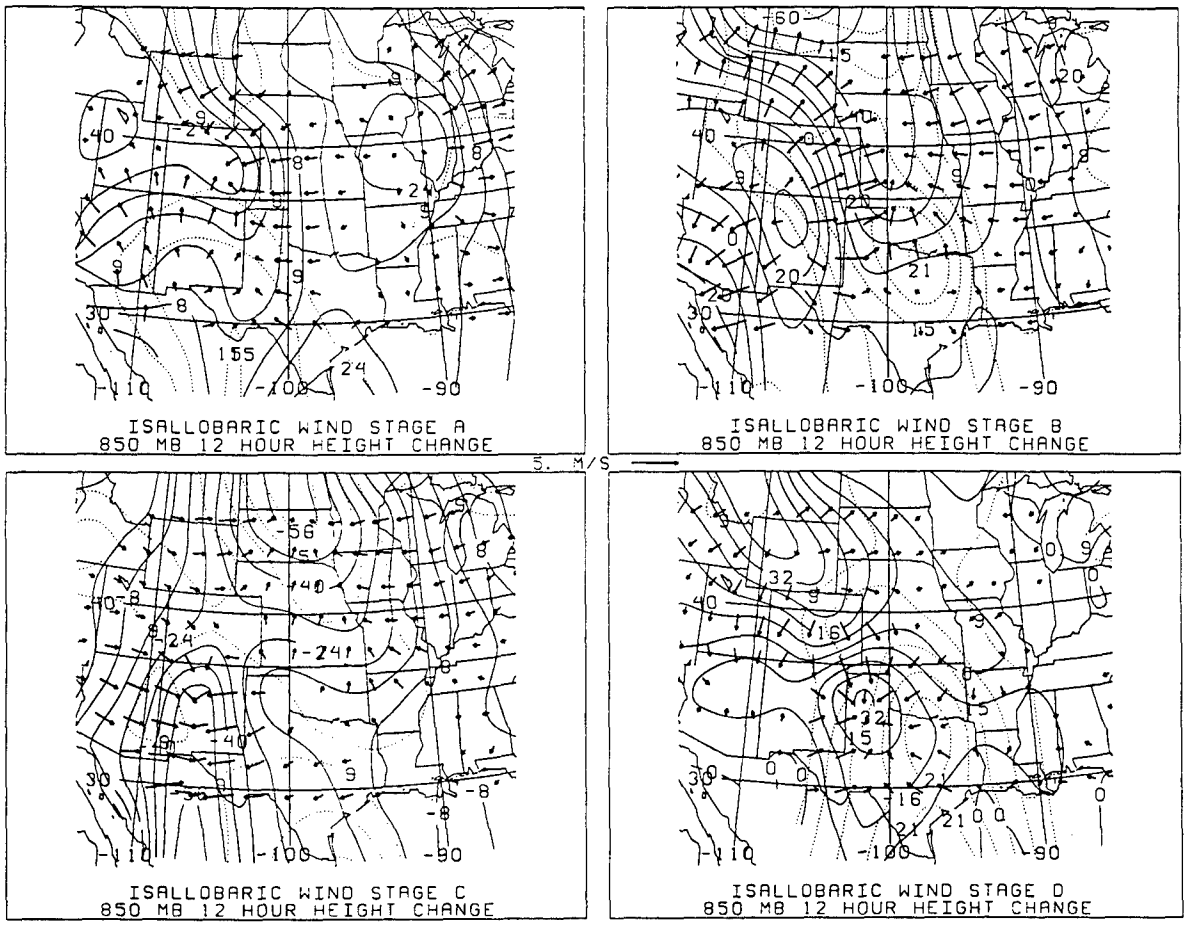

Fig. 23. Isallobaric wind (arrows) and 12 hour height change at 850 mb during stages A-D of the LLJ.

large scale pattern supports an Uccellini Type I LLJ, the transition period between the northern Great Plains trough and lee cyclogenesis contributes to a decrease in the LLJ in stage C. The weak isallobaric wind can be seen over northeast Texas and Oklahoma in the previous location of the LLJ. In stage D, the isallobaric flow resumes toward the area of cyclogenesis over Texas. Separate influences of the isallobaric wind are seen in stages B and D. The isallobaric flow over Oklahoma and Kansas toward the height falls over the northern Great Plains expands the LLJ northward in stage B. In stage D, the acceleration toward the height falls over the Texas Panhandle decreases the speed and extent of the LLJ in its northern portion.

Height falls of 10 to 30 meters occur over Oklahoma in stage B. The wind magnitude increases from 7 m s^{-1} to 18 m s^{-1} over the same 12 hour period from 0000 UTC to 1200 UTC on 6 May. These height falls correspond to the trough moving northeast over the northern Great Plains. Stage D shows height falls of 12 to 24 meters over north central Texas in to which to the wind magnitude responds by increasing from 9 m s^{-1} to 23 m s^{-1}. These height falls cause the isallobaric flow toward the newly formed lee cyclone over eastern New Mexico. The LLJ strengthening is supported by the increasing pressure gradient force from lee cyclogenesis. This lays the foundation to show the initial LLJ (stages A and B) is in the lower branch of an indirect circulation under a STJ streak exit region and strengthened by height falls over the Great Plains near stages B and D. The thermally indirect circulation (TIC) weakens in stage D as the STJ moves south, but the height falls associated with the developing lee cyclone strengthen the LLJ to its maximum extent and intensity.

D. Ageostrophic Circulation

The coupling of an upper-level jet streak and a low-level jet was studied by Uccellini et al. (1984). By taking a vertical section through an ULJ streak, they show a TIC near the coupled region. In the vicinity of the two jets, the warm air has a downward vertical component, and the cold air exhibits upward vertical motion. In the STJ exit

region, the ageostrophic component in the upper-troposphere is directed toward the anticyclonic side of the jet, representing the upper branch of the TIC. The lower-troposphere component is directed toward the cyclonic side of the jet, representing the lower branch of the TIC. Our case between 5-7 May 1995 contains a similar TIC near the exit region of a STJ streak.

Figure 24 is a meridional vertical section of the ageostrophic circulation near the two jet streaks. The ageostrophic wind in m s^{-1} is shown by the horizontal component of the arrows and omega in $\mu b\ s^{-1}$ is shown by the vertical component of arrows. It appears the along-stream variation of wind speed in the STJ exit region influences the circulation pattern more than the wind speed of the streak maximum.

Although the LLJ is just developing in stage A, the TIC is well established. Colder air over New Mexico shows an upward motion while the warmer air over San Angelo, Texas, has a downward motion and completes the circulation near the forming LLJ. In stage B, the strongest ascending motion occurs over the northern half of the LLJ core. During the weakening of the LLJ in stage C, the circulation cell disappears from the region as the STJ streak moves south only to return in stage D as the LLJ also reforms. The southerly branch of the circulation in stage D is not as defined as in stage B with the lifting of the approaching cold front effecting the sinking motion from the STJ streak. It appears the STJ and LLJ are coupled since the LLJ occurs in this return branch of the TIC. In spite of the weakening of the southern branch of the TIC, the LLJ is at its peak in this stage. This signifies the importance of the height falls occurring with lee cyclogenesis and the cross-contour ageostrophic flow intensifying the wind along the contours during this stage.

E. Vertical Motion

Figure 25 shows the vertical motion (kinematic omega) distribution at 850 mb during stages A-D of the LLJ. Vertical motion is of interest because of its influence on the precipitation process. Areas of upward vertical motion (negative omega) should

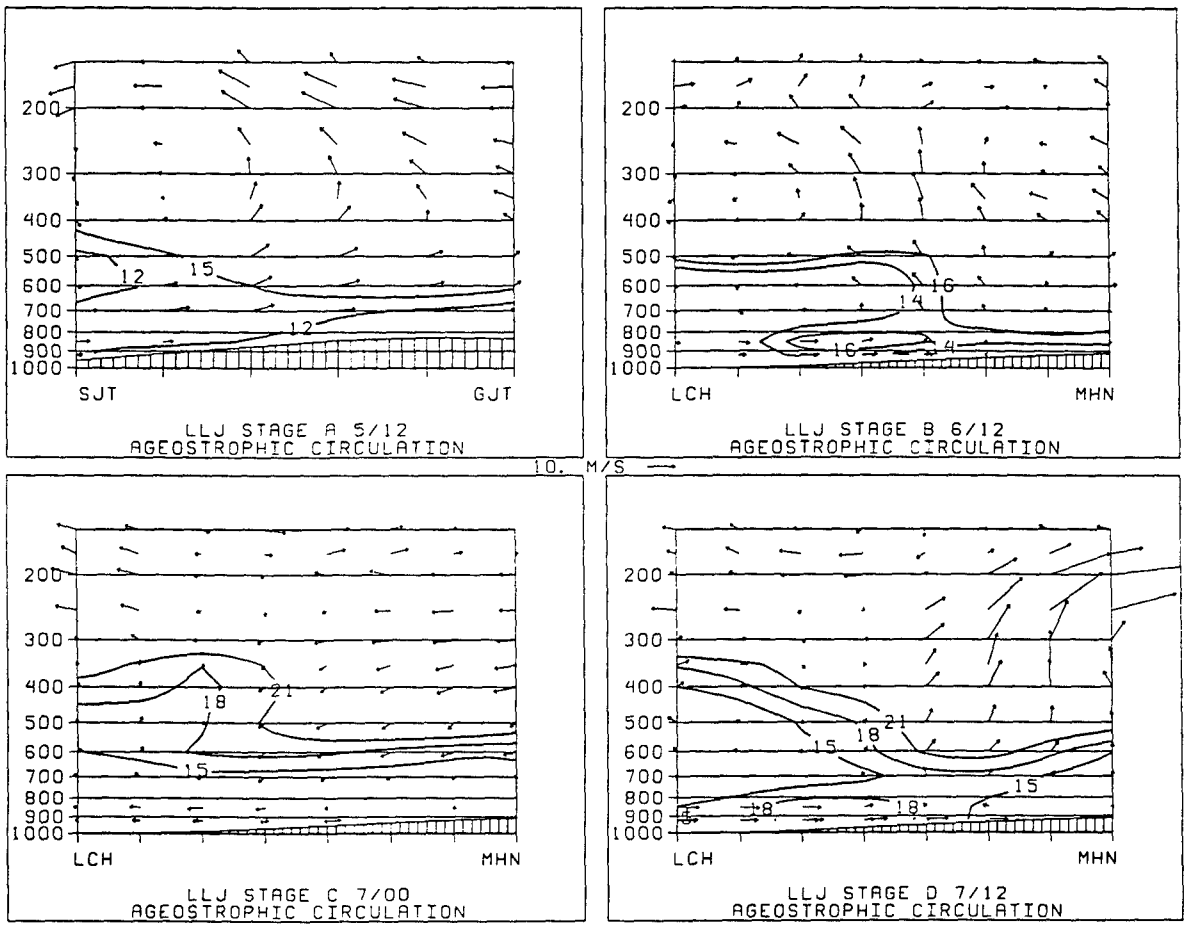

Fig. 24. Meridional vertical section of the ageostrophic circulation and wind magnitude (solid lines) during stages A-D of the LLJ. Horizontal component of the arrows is given by the ageostrophic wind (m s^{-1}), and the vertical component of the arrows is given by minus omega (μb s^{-1}).

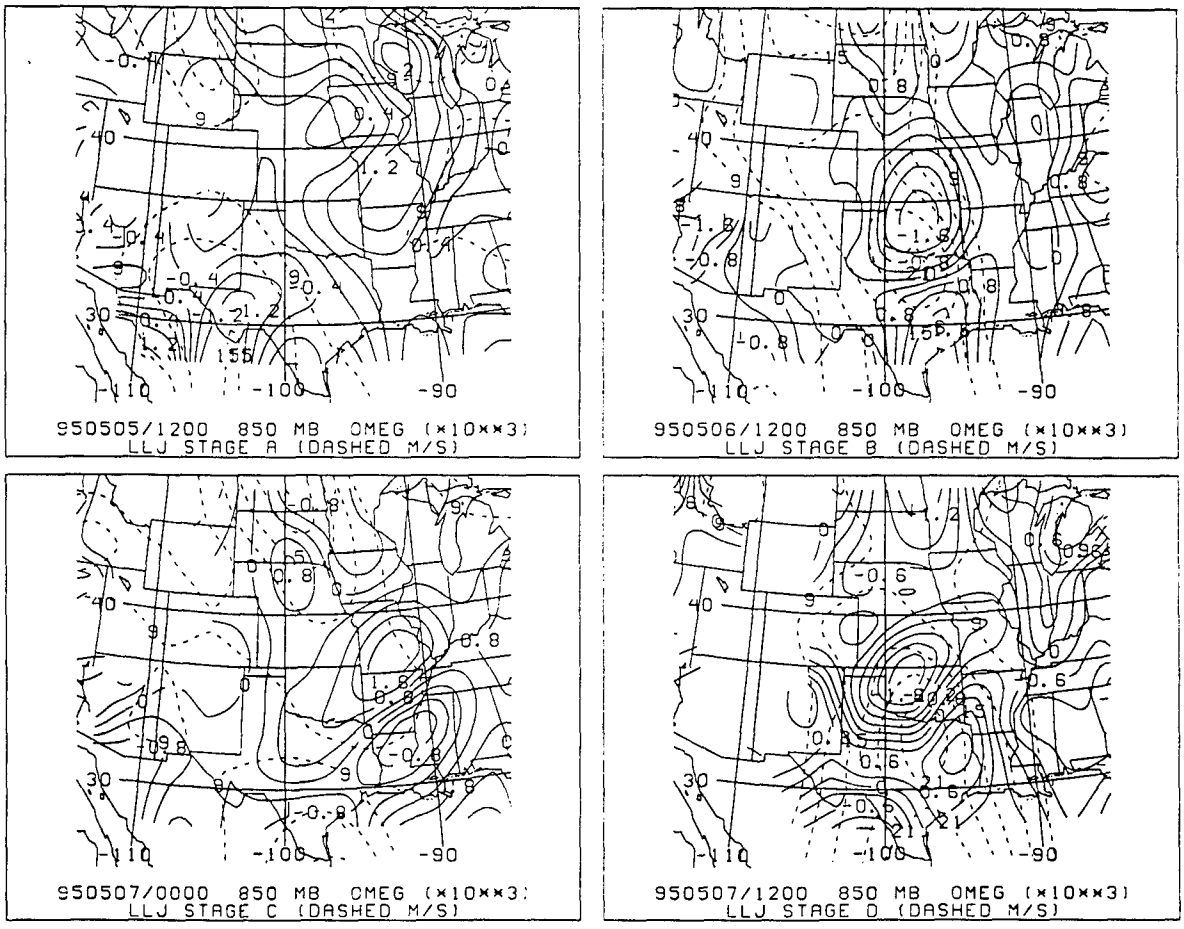

Fig. 25. Vertical motion (omega) and wind magnitude (dashed lines) at 850 mb during stages A-D of the LLJ. Upward vertical motion is given by negative omega values.

coincide with areas of convergence associated with the LLJ as shown in section B. Much of the ascent over the southern Great Plains can be attributed to the warm advection in the LLJ.

In stage A, an area of upward vertical motion is located over western Texas where the southerly flow is just developing. The area of ascent becomes well defined in stage B when the LLJ has developed. An area of $-2x10^{-3}$ $\mu b\ s^{-1}$ upward vertical motion is positioned over the northern half of the LLJ. Radar summaries around 1200 UTC on 6 May show numerous thunderstorms throughout the area with negative omega values. Over the next 12 hours, the significant upward vertical motion ceases in stage C over the southern Great Plains due to a few events. The STJ streak moves south, the LLJ disappears, warm advection decreases, and low-level divergence develops over the area. These are all related to the upward vertical motion over the southern Great Plains. With the changes in large scale forcing, this is a quiet time for convection without lifting in the area. The weakening of the LLJ during this transition of forcing mechanisms significantly decreases the transport variables. The severe weather resumes in stage D as the LLJ reaches its maximum. A second area of ascent occurs over southwest Texas and northeast Mexico to the northwest of a new wind speed maximum (21 m s^{-1}) over Brownsville, Texas. This explains the loss of descent in the southern vertical branch of the ageostrophic circulation cell in Fig. 24. Another large area of upward vertical motion is situated over the northern half of the LLJ in Oklahoma and Kansas. The blank data regions in this figure result from terrain reaching above the 850 mb level.

Figure 26 contains vertical motion at 500 mb during the four stages of the LLJ. This figure allows examination of ascent in the vertical column above the LLJ and below the ULJ streaks. Upward vertical motion occurs over the same locations as in Fig. 25, but omega values are much greater at the 500 mb level. This figure offers a better insight to the mechanisms in this case. The original low center over Idaho and Montana is evident by the large values of negative omega over the area in stage B. Height falls ahead of the trough associated with this low aid the development of the LLJ. The column of upward vertical motion is vertically stacked above the nose of the LLJ at this time. In

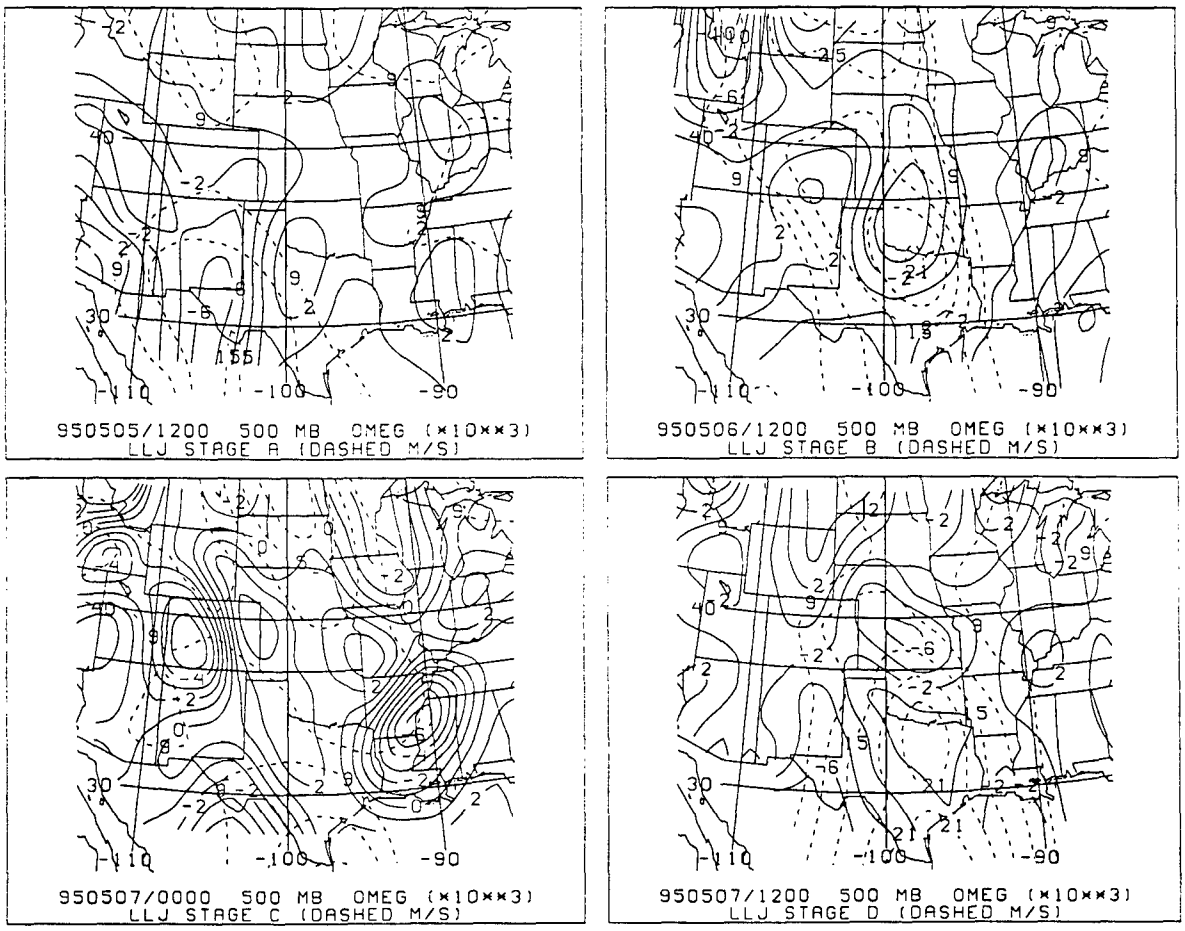

Fig. 26. Vertical motion (omega) at 500 mb and wind magnitude (dashed lines) at 850 mb during stages A-D of the LLJ. Upward vertical motion is given by negative omega values.

stage C, upward vertical motion associated with cyclogenesis appears over western Colorado. A strong line of thunderstorms over Mississippi and Arkansas accompanies the strong ascent over these states. In stage D, lifting ahead of the cold front occurs over western Texas and eastern New Mexico. The ascent with the low center in stage B has weakened and progressed eastward over Minnesota by stage D.

Although this study concentrates on the STJ influences on the LLJ, Figure 27 shows vertical motion during stages A-D of the LLJ at 300 mb near the level of the PJ. Upward vertical motion is not considered significant at 200 mb since the stability is usually high at that level. The most noticeable feature is the strong ascent over northwest Kansas in stage D. This is in the exit region of the PJ streak and contributes to the wide area of ascent over the Great Plains. Without the front left quadrant of the STJ streak exit region over the Brownsville LLJ, the ascent is not seen through the entire vertical column.

Figure 28 is a meridional vertical section of vertical motion (omega) for stages A-D of the LLJ. In stage A, the low-level winds are just beginning to increase, but a large area of ascent occurs underneath the exit region of the STJ over western Texas and eastern New Mexico. This is also an area of upper-level divergence between the PJ and STJ. At this time, the PJ flows southerly over eastern Arizona, and the STJ comes from the southwest over southern New Mexico. The LLJ core of 20 m s^{-1} extends over north Texas and Oklahoma in stage B. The combination of the LLJ and STJ streak increase the upward vertical motion to $-6x10^{-3}$ $\mu b\ s^{-1}$ over northern Oklahoma. The rear portion of the LLJ shows positive omega values which indicates downward vertical motion centered over San Marcos, Texas. This vertical motion pattern verifies the ageostrophic circulation within the STJ streak exit region. The warm air over southern Texas descends while the cooler air to the north ascends. The weakening of the LLJ has an astounding effect on vertical motion in stage C. With the dynamics of the STJ streak exit region shifting locations, the circulation cell breaks down in this stage. The STJ moving south and the lack of height falls helps decrease the circulation. The entire region displays a broad area of descent during a time of maximum heating. The LLJ extends farther north

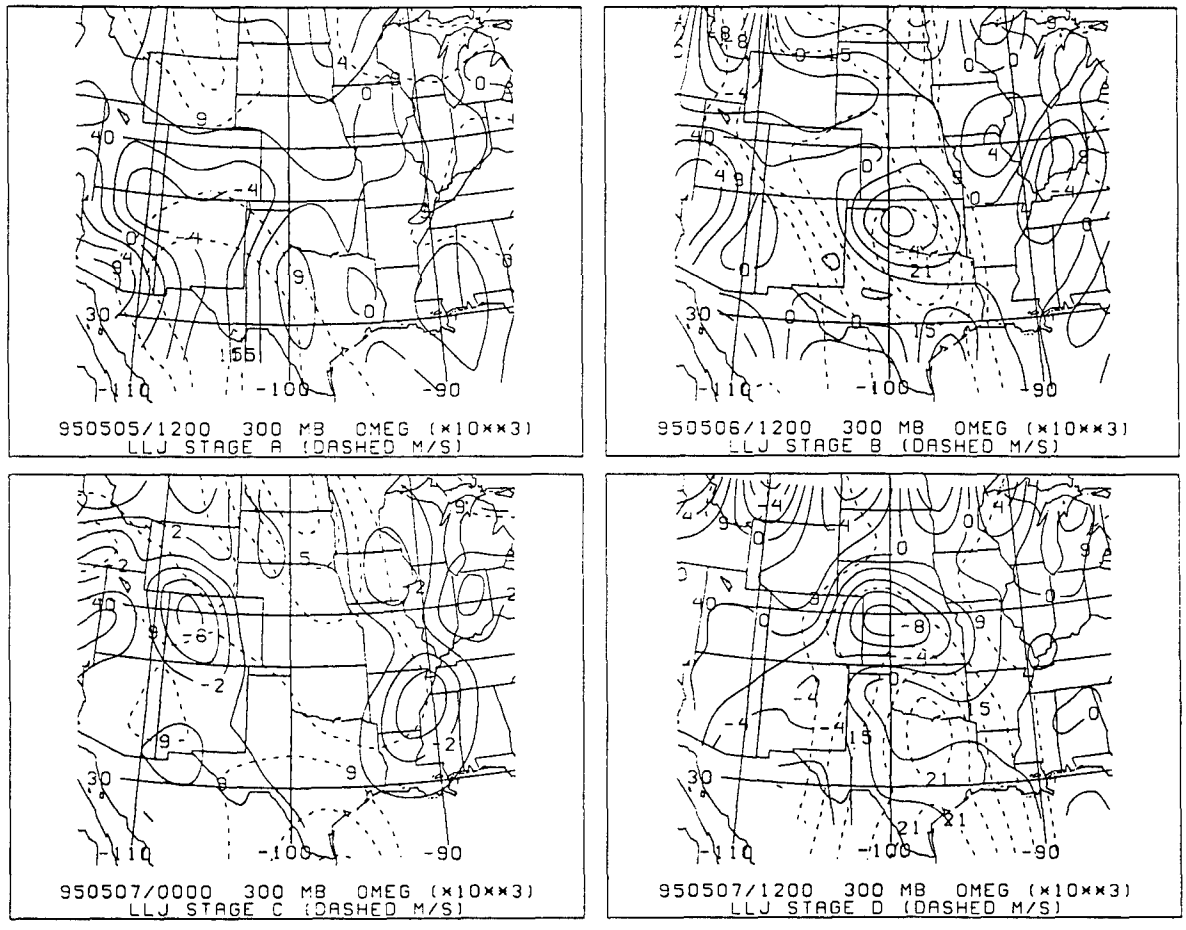

Fig. 27. Vertical motion (omega) at 300 mb and wind magnitude (dashed lines) at 850 mb during stages A-D of the LLJ. The polar jet stream is located near the 300 mb level.

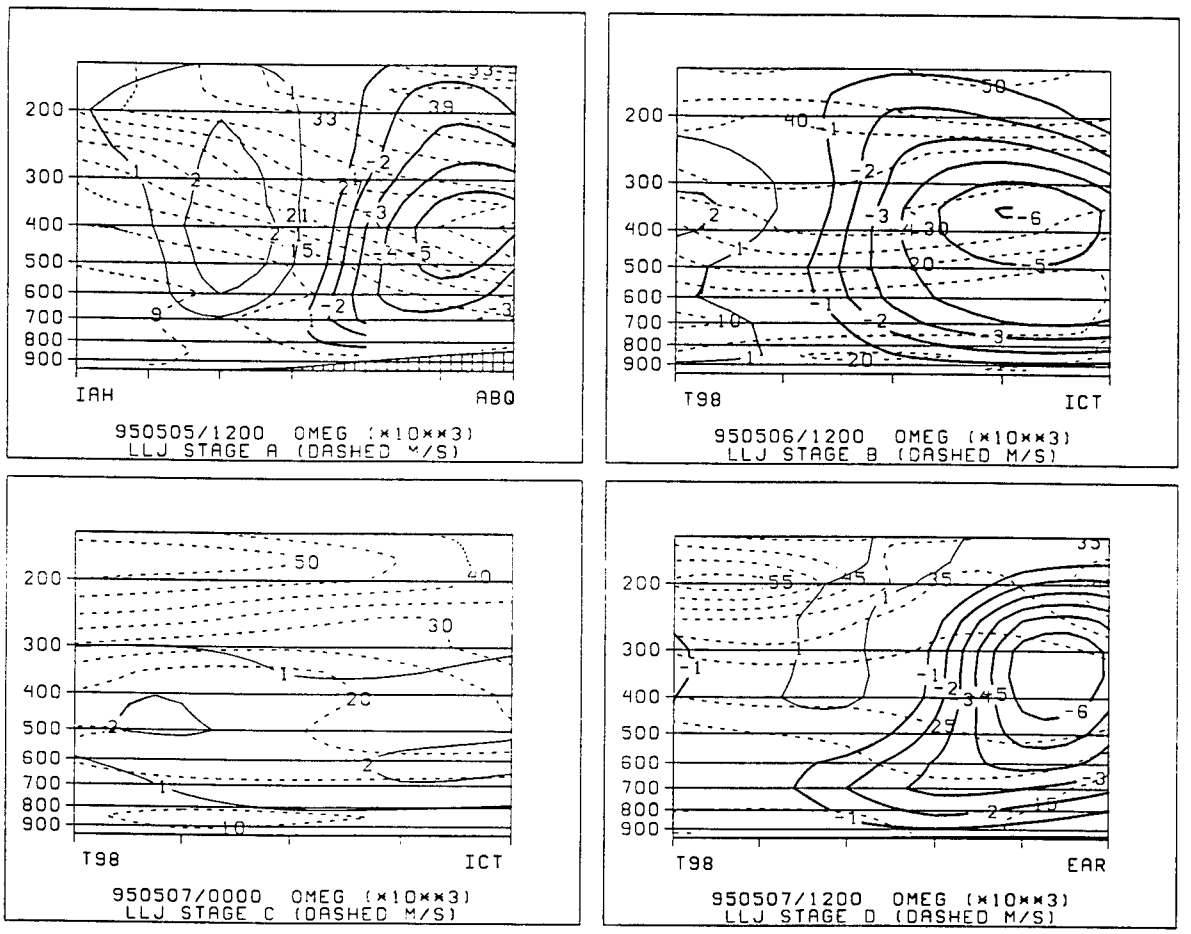

Fig. 28. Meridional vertical section of vertical motion (omega) and wind magnitude (dashed lines) during stages A-D of the LLJ. Thick solid lines indicated upward vertical motion.

in stage D and an area of upward vertical motion progresses north into Nebraska. Stages B and D show a strong ascent associated with the development of the LLJ. The incomplete TIC cell is noticeable during stage D. The southern vertical branch weakens, but the LLJ still strengthens due to the cross-contour ageostrophic wind and the isallobaric flow toward the height falls.

A zonal, vertical section of vertical motion for stages A-D of the LLJ is shown in Figure 29. The remnants of the cooler, Canadian air are evident in stage A. A wide area of descent (positive omega) still covers most of Texas. This is rapidly replaced by upward vertical motion in stage B as the LLJ transports warmer air north. The maximum of ascent occurs over the western side of the LLJ core. This is near the height falls ahead of a trough moving northeast over the northern Great Plains. The area of ascent occurs farther north in stage D since the LLJ has a greater northerly extent. The approaching cold front is evident in stage D over New Mexico. This large area of upward vertical motion is the lifting occurring just ahead of the front. These figures verify a relationship between upward vertical motion and the evolution of the LLJ.

1. Q-Vector

Q-Vector offers an alternative method to examine vertical motion in the atmosphere. Figure 30 shows Q-vector (arrows) for stages A-D of the LLJ. Q-vectors begin to converge over western Texas and southeastern New Mexico in stage A as the southerly flow evolves. In stage B, Q-vectors increase in magnitude and form a highly noticeable convergent pattern around the LLJ core. The area near the LLJ core is experiencing strong ascent and convective activity. This occurs in close proximity to the upward vertical motion maximum seen in Fig. 25. This well defined convergent pattern does not occur in stage C during the weakening of the LLJ, but reappears in stage D with the redevelopment of the LLJ.

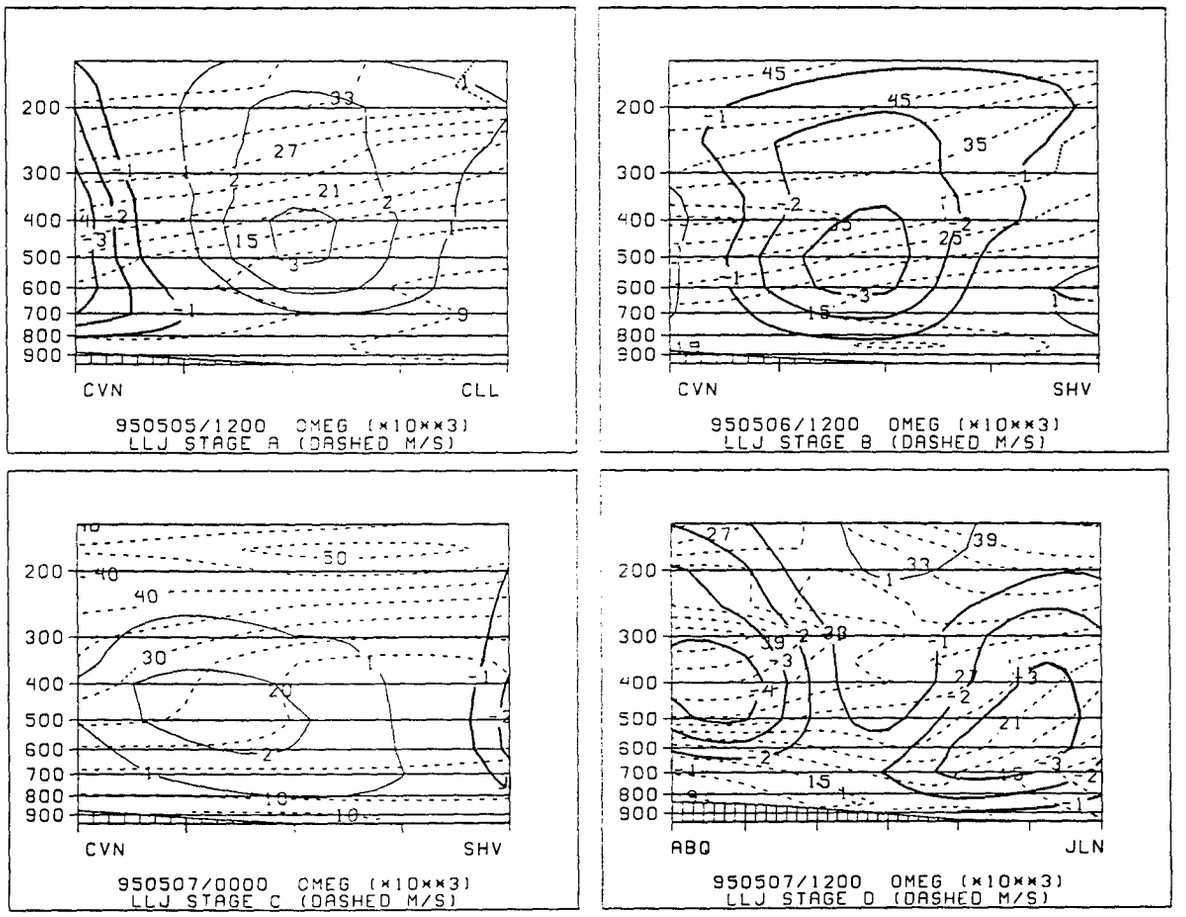

Fig. 29. Zonal vertical section of vertical motion (omega) and wind magnitude (dashed lines) during stages A-D of the LLJ. Thick solid lines indicated upward vertical motion.

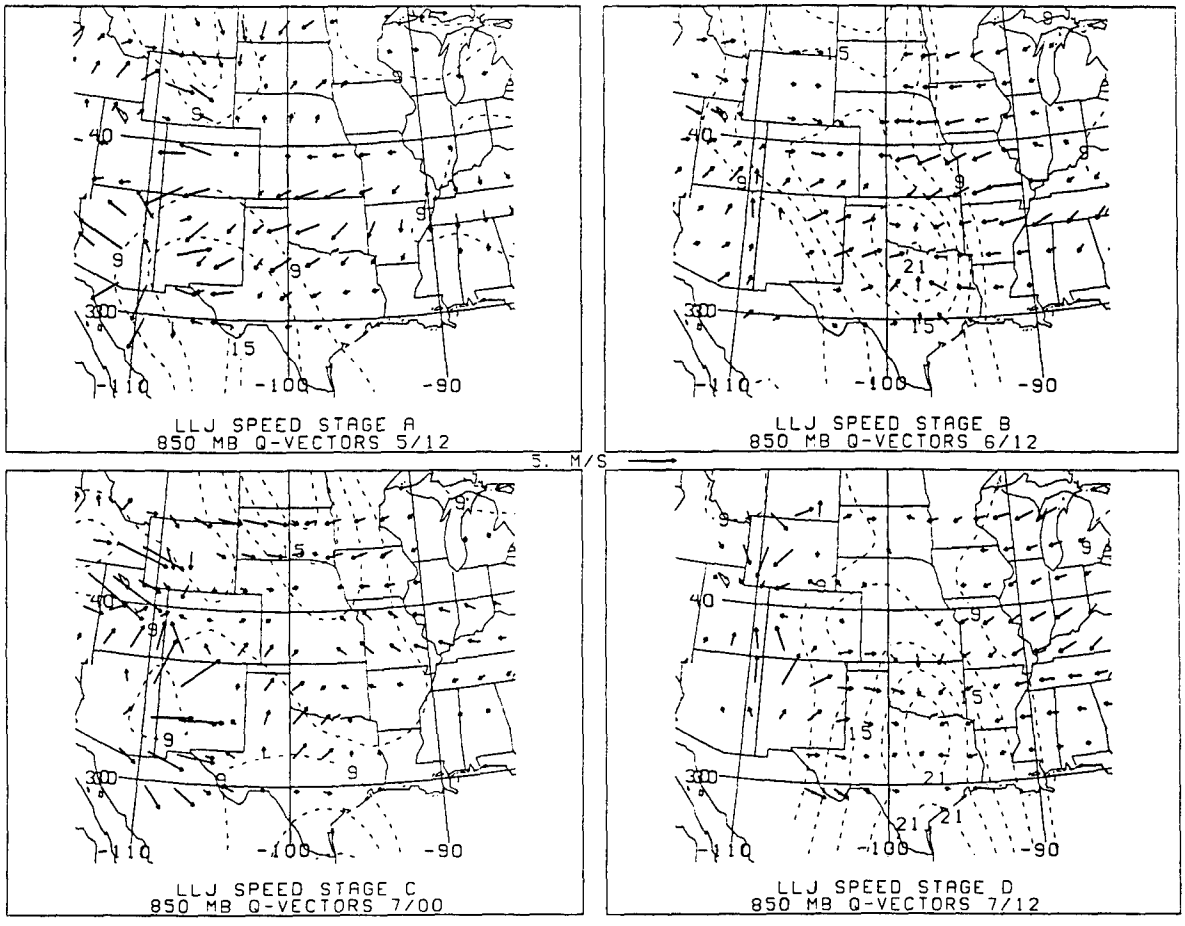

Fig. 30. Q-Vectors (arrows) and wind magnitude (dashed lines) at 850 mb during stages A-D of the LLJ. Convergence of Q-Vectors implies upward vertical motion.

2. Q-Vector Convergence

Hoskins and Pedder (1980) used Q-vectors to examine the ageostrophic motions in an upper-level jet streak exit region. The Q-vector is found using height and temperature values on constant pressure surfaces and combining vorticity and thermal advection terms found in the omega equation. Q-vectors represent winds trying to restore thermodynamic equilibrium and point in the direction of the ageostrophic wind in the lower levels. The balance is restored by changing the horizontal temperature gradients. In short, Q-vector convergence implies an area of upward vertical motion trying to restore the atmosphere to a thermal balance.

Figure 31 shows Q-vector divergence and convergence at 850 mb during stages A-D of the LLJ. In both stages B and D, the Q-vector convergence maximum occurs with the LLJ core. This convergence indicates lifting in the vicinity of the LLJ core and verifies the results shown by omega. The large values of upward vertical motion cease in stage C during the large scale forcing transition influencing the LLJ.

Figure 32 contains Q-vector divergence and convergence at 500 mb for stages A-D of the LLJ. This figure is included to show the lifting associated with cyclogenesis (western Kansas and Oklahoma Panhandle) and the approaching cold front (western Texas) in stage D. The ascent at the northwest side of the LLJ aides in both cyclogenesis and convection.

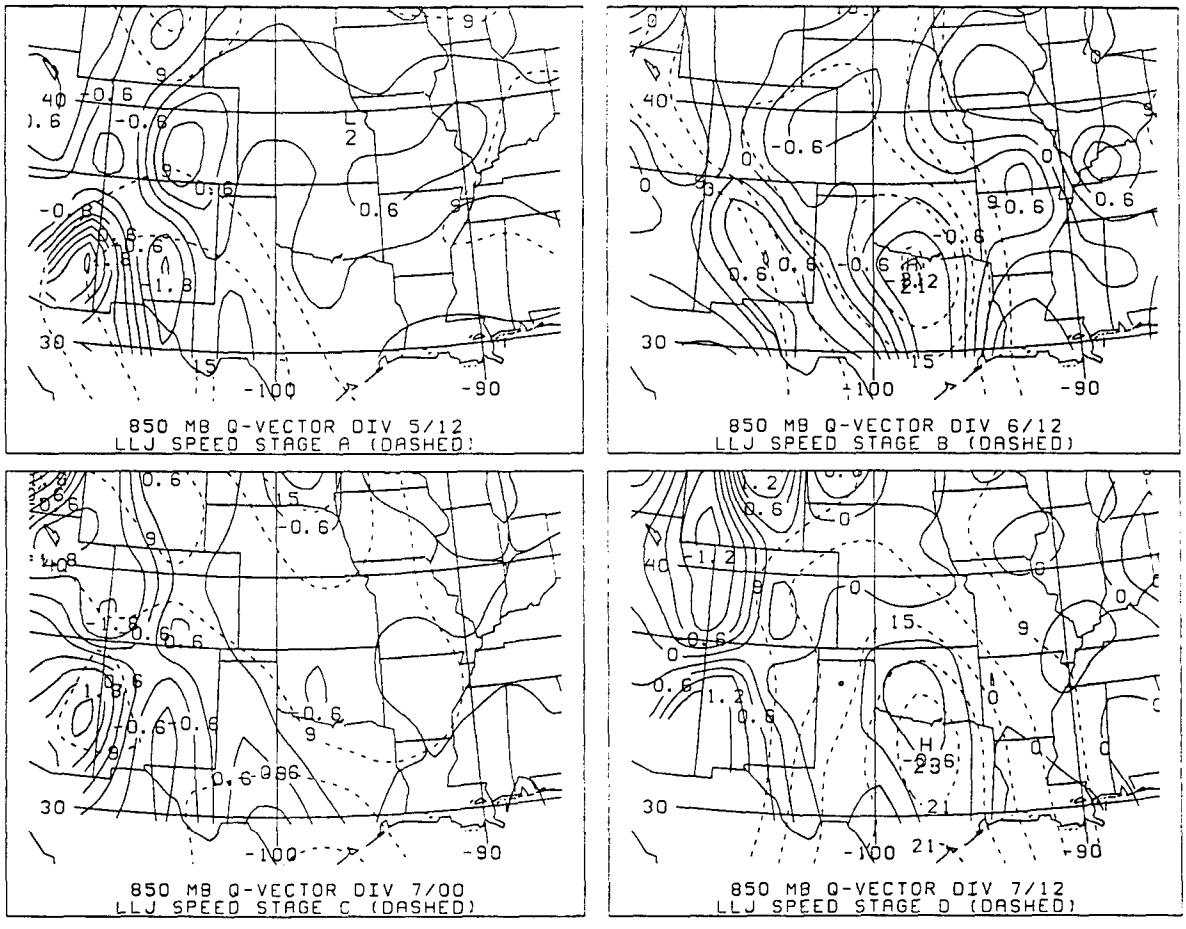

Fig. 31. Q-Vector divergence and wind magnitude (dashed lines) at 850 mb during stages A-D of the LLJ. Convergence of Q-Vectors implies upward vertical motion.

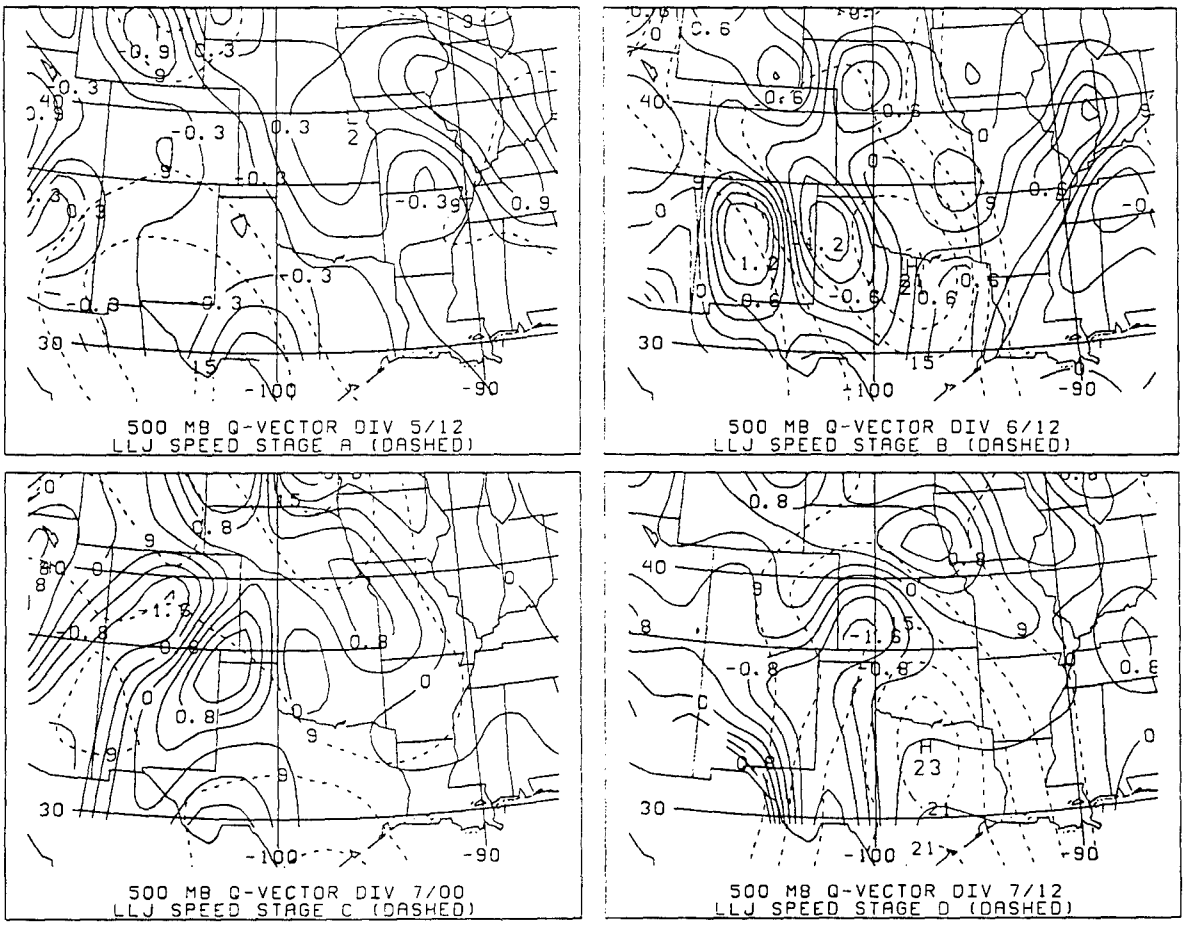

Fig. 32. Q-Vector divergence at 500 mb and wind magnitude (dashed lines) at 850 mb during stages A-D of the LLJ. Convergence of Q-Vectors implies upward vertical motion.

CHAPTER VI

TRANSPORT OF HEAT AND MOISTURE BY THE LOW-LEVEL JET

The LLJ that formed over Texas and Oklahoma was essential in transporting warm, humid air into developing convective regions covering the southern Great Plains. It is perhaps the most important forcing mechanism for heavy convective rainfall in the central United States. This chapter will show that the LLJ was vital in focusing temperature advection, mixing ratio flux, and θ_e advection into convective threat areas.

Table 1 displays the four transport variables studied in this chapter on the 850 mb and 301 K surfaces. The 301 K isentropic surface is found in the center of the LLJ core in the first four stages. Each table value is the maximum at each stage, only considering the southern Great Plains. When the LLJ strengthens in stages B and D, all four variables increase in value or maintain their previous amounts. The weakening of the LLJ in stage C has an astounding effect on all four variables. The most notable being the mixing ratio flux which decreases over 50 percent as the LLJ speed decreases. Stage E is included in Table 1 to elaborate on the effects of the transition of the LLJ in stage C. Stage E occurs at 0000 UTC on 8 May after a cold front has moved into west central Texas in close proximity to the LLJ. This scenario causes greater height falls forcing the LLJ evolution as the cyclone system moves into the southern Great Plains. This is in contrast to stage C when significant height falls are located in central New Mexico. The isallobaric wind decreases over Texas and Oklahoma helping decrease the strength of the LLJ. Chapter V contains the examination of different forcing effects on the LLJ during its four stages.

A. Temperature Advection

Warm advection contributed to severe convection and aided in cyclogenesis by creating an area of general ascent in eastern Colorado. Warm advection of at least 1.0×10^{-4} °C s^{-1} occurs in all four stages of the LLJ (not shown). In stage A, the warm

Table 1 Transport variables during stages A-E of the low-level jet.

850 mb	Stage A	Stage B	Stage C	Stage D	Stage E	Units
LLJ Speed	15.07	21.37	12.75	22.5	22.92	$m\ s^{-1}$
Temperature Advection	1.53	1.54	1.2	1.5	1.55	$10^{-4}\ °C\ s^{-1}$
θ_e Advection	4.95	6.02	4.16	4.78	5.45	$10^{-4}\ K\ s^{-1}$
Mixing Ration Advection	12.1	17.08	11.47	12	14.34	$10^{-8}\ g\ kg^{-1}\ s^{-1}$
Mixing Ratio Flux	15.35	22.75	11.46	26.85	27.78	$10^{-2}\ m\ s^{-1}$

advection of $1.0x10^{-4}$ °C s^{-1} coincides with the thunderstorms occurring in the western Texas Panhandle and eastern New Mexico. As the LLJ strengthens in stage B, an area of warm advection greater than $1.0x10^{-4}$ °C s^{-1} covers the entire southern Great Plains. This is in balance with the ascent required to release the instability throughout northern Texas, Oklahoma, and Kansas. Although the speed of the LLJ decreases in stage C, there is still an area of $1.2x10^{-4}$ °C s^{-1} warm advection remains over eastern Colorado and western Kansas supplying warm air and ascent to the area of cyclogenesis. Cold advection behind the approaching cold front is evident in stage C in southeastern Arizona. In stage D, the LLJ continues to supply warm air into the convective area with the greatest warming occurring over the Texas and Oklahoma Panhandles.

Figure 33 shows meridional and zonal vertical sections that allow us to examine the vertical structure of the temperature advection in relation to the LLJ. Although just developing in stage A, the LLJ begins feeding warm air into the convective region. The core speed of the LLJ in stage A has only reached 15 m s^{-1}, but the warm advection value of $0.9x10^{-4}$ °C s^{-1} extends north to Albuquerque, New Mexico. Because the southeasterly flow is just developing, the significant warm advection is confined to western Texas and eastern New Mexico. As the LLJ core expands in stage B, the warm advection increases significantly in coverage. A meridional vertical section indicates the geographical dependence of the warm advection maximum on the LLJ core. The warm advection maximum coincides with the LLJ core or lies just to the north of it (not shown). The zonal section for stage B shows the warm advection maximum extending from the LLJ core center in central Texas west toward Midland, Texas. The level of maximum warm advection ascends in stages C and D. In stage C, the maximum is $1.0x10^{-4}$ °C s^{-1} at 700 mb over northern Texas. By stage C, the warm advection has increased to $1.8x10^{-4}$ °C s^{-1} at 650 mb and moved north to northwest Oklahoma. In each of these stages, the rising maxima occur in the vicinity of the warm front that provides the additional ascent. The maximum over the warm front are much higher than the maxima located with the LLJ core while it resides near 850 mb.

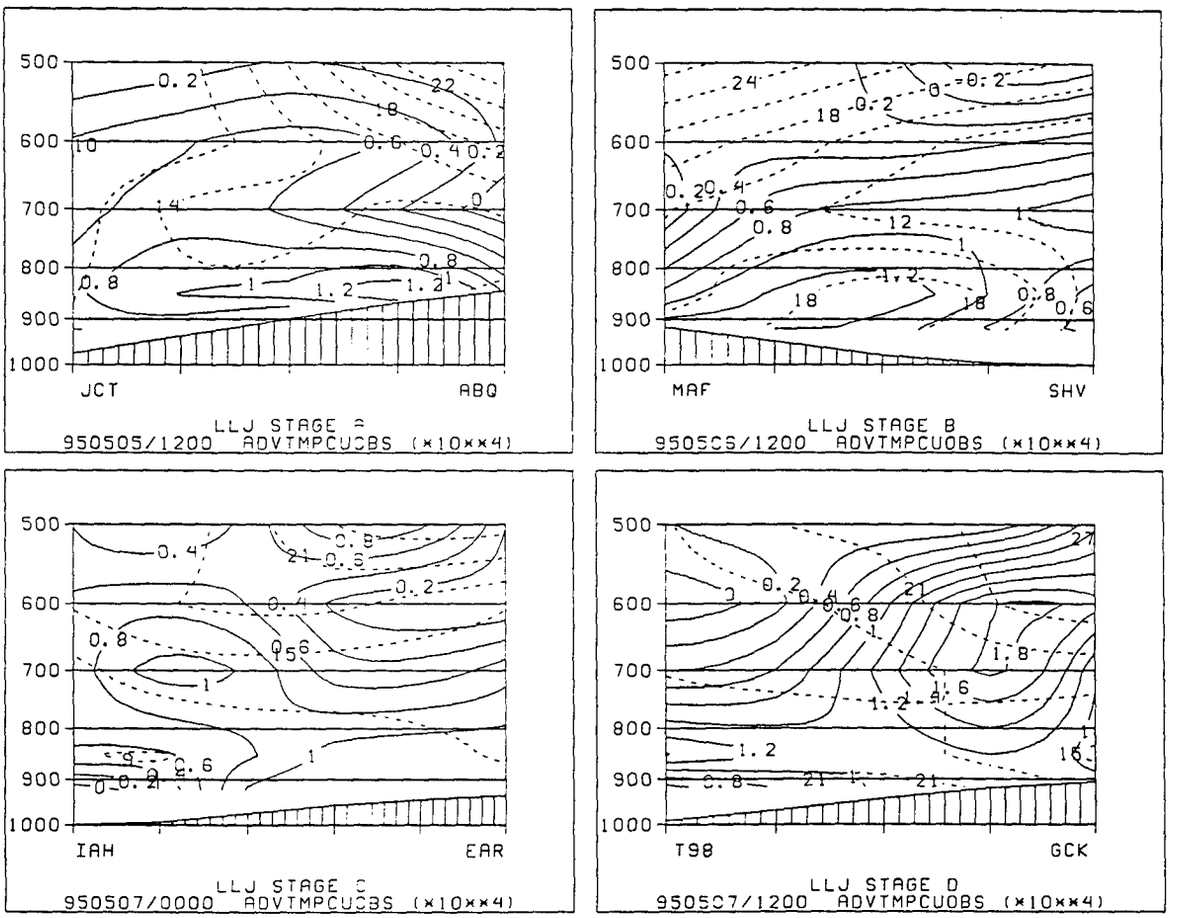

Fig. 33. Vertical sections of temperature advection by the observed wind and wind magnitude (dashed lines) between 1000 mb and 500 mb during stages A-D of the LLJ. Temperature advection units are °C s^{-1}.

After initializing the Eta model results for temperature advection with the radiosonde observations over the four stages of the LLJ, it appears the model computed certain aspects of the transport quite well (not shown). In stage A, the model output warm advection maximum is 360 km east of the radiosonde maximum in eastern New Mexico. This is due to the eastward placement of the LLJ maximum by the Eta model based on its accurate handling of higher terrain. The radiosonde 850 mb surface should intersect the ground in central New Mexico and eastern Colorado, but the gridded data of observations ignore the higher terrain. The Eta values decrease to zero as the elevation increases toward the Rocky Mountains while the radiosonde gridded observations appear as a continuous surface at 850 mb.

The Eta model hourly forecasts allow a step-by-step examination of the heat transport as the LLJ speed fluctuates. Figure 34 shows the southerly LLJ and warm advection begin to develop just after sunset. Initially at 0000 UTC on 6 May, the warm advection maximum of 0.9×10^{-4} °C s^{-1} is located in central Texas. This is near the northern edge of the LLJ core with a speed of 12 m s^{-1}. Within 4 hours, the warm advection increases to 1.6×10^{-4} °C s^{-1} and has moved north with the expanding LLJ core of 18 m s^{-1} into western Oklahoma. Thunderstorms begin to develop in this area over the next few hours. This indicates a significant dependence of an atmosphere conducive to convection on warm advection and shows importance of tracking the warm advection by the LLJ.

On the down side in three of the four LLJ stages, the Eta advection values are smaller than the radiosonde values at the initialization times. Unfortunately, as the model forecasts progress toward the 12 hour point, the warm advection maxima are overforecast and geographically displaced. In this case, the Eta model overforecast the values at the 12 hour point from 25 to 40 percent. Although the 12 hour output show deficiencies, the earlier output offers interesting insight on the hourly progression of the transport variables.

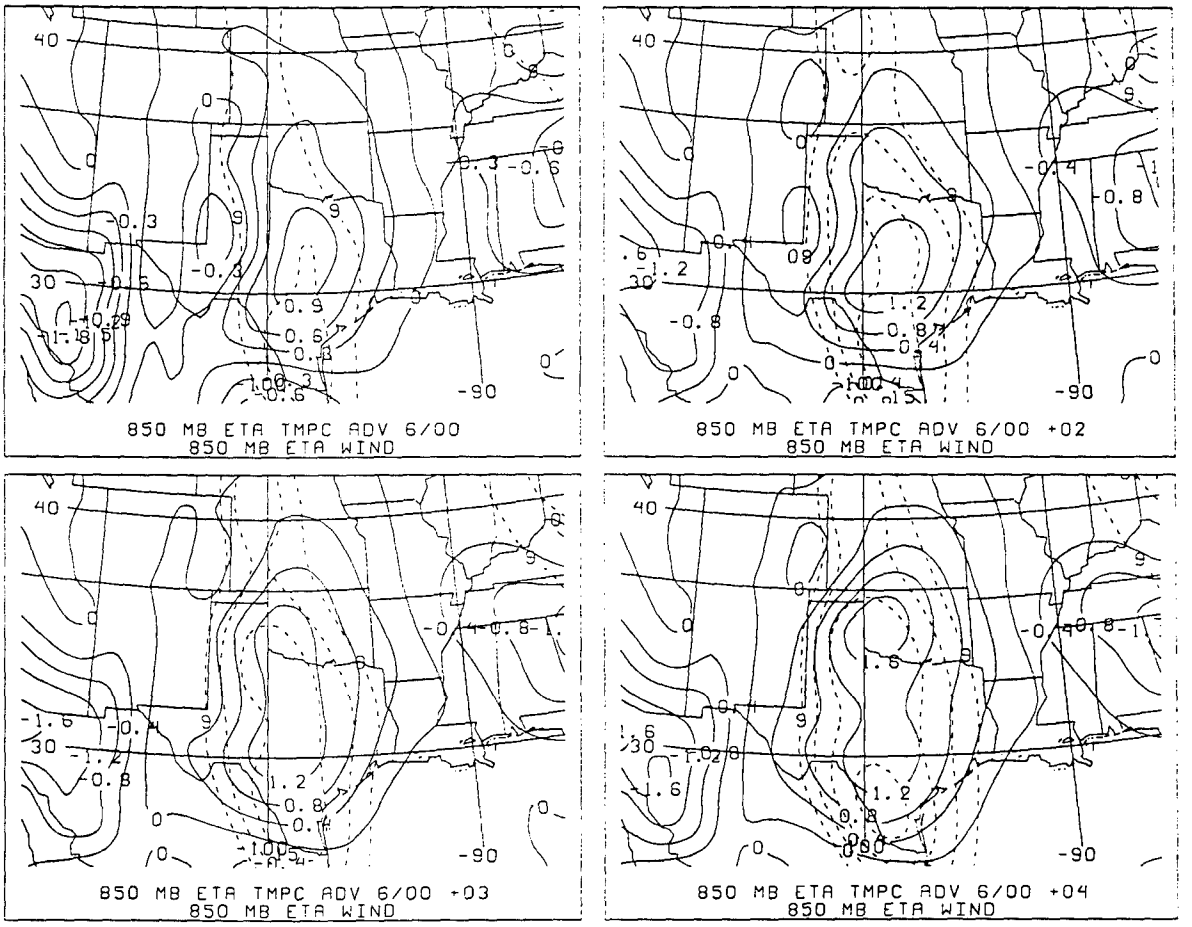

Fig. 34. Temperature advection by the observed wind and wind magnitude (dashed lines) at 850 mb using Eta model output. Panels 1-4 display output at 0000 UTC, 0200 UTC, 0300 UTC, and 0400 UTC on 6 May respectively. The temperature advection maximum progresses northward with the LLJ core.

B. Mixing Ratio Transport

During a cyclone event over the Great Plains, the LLJ supplies most water vapor to the convective areas. Since the humidity increase is confined below 700 mb, this moisture increase helps destabilize the atmosphere. As a result, the lifting condensation level and level of free convection descend, the amount of convective available potential energy increases, and the equilibrium level ascends. Mixing ratio flux and mixing ratio advection best display the LLJ influence on water vapor transport.

Figure 35 shows mixing ratio flux at 850 mb using Eta model output. At the first appearance of southerly flow in stage A, the mixing ratio isopleths bulge north toward the Texas Panhandle. The isopleths reach a maximum of $27x10^{-2}$ m s^{-1} 48 hours later in stage D when the south wind component is also at its maximum.

In all four stages, the flux maxima and LLJ core overlap over Texas. In three of the four stages, convection occurs on the western side of these overlap areas (Possibly tied to the intersection of the LLJ and STJ). This is not the case in stage C when thunderstorm activity has all but ceased due to the weakening of the LLJ. Over the three day event, the thunderstorm activity decreases after sunset and remains scattered until midnight. This is important since the LLJ weakens during the day but regenerates around 0200 UTC (9pm local) each evening before the thunderstorms intensify. As will be shown in Chapter VII, this is the best calculation of all the transport variables by the Eta model.

Vertical sections show the mixing ratio flux maxima are closely related to the LLJ core during stages A, B, and D (not shown). As the LLJ core loses shape in stage C, the isopleths of mixing ratio flux also scatter only to take shape again in stage D as the LLJ reaches its peak. The effect on mixing ratio flux can be seen by tracking the $10x10^{-2}$ m s^{-1} isopleth. In stage A, the isopleth begins its trek northward in western Texas, near Midland. After 48 hours, the LLJ transports the isopleth into central Nebraska and increases the moisture throughout the Great Plains. This is also seen in trajectories in

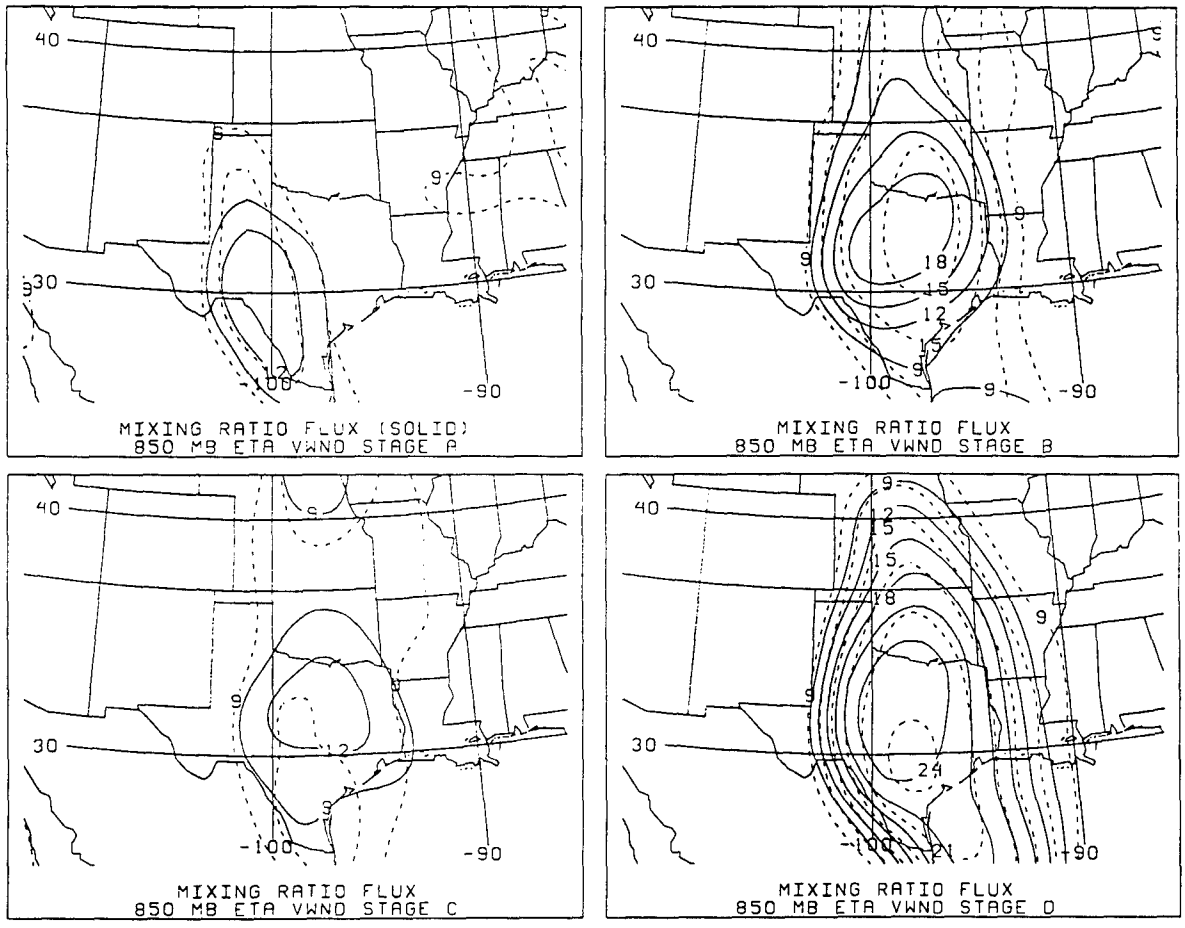

Fig. 35. Flux of mixing ratio by the southerly wind component and southerly wind component magnitude (dashed lines) at 850 mb using Eta model output. Panels 1-4 display output during stages A-D of the LLJ respectively. Flux units are m s^{-1}.

section D by tracking parcels from the Gulf of Mexico through the LLJ core and northward into the convective areas.

The vertical sections show that in contrast to the other transport variables, the mixing ratio flux maxima are located close to the surface during all four stages. The isopleths bulge upward near 600 mb in stage D in vicinity of the warm front in central Kansas, but the maximum stays below 900 mb through central Texas. This is understandable since the mixing ratio decreases rapidly with height below 700 mb.

Figure 36 shows mixing ratio advection at 850 mb using Eta model output. These advection patterns are similar to the advection patterns shown in section C. The southeasterly flow in stage A creates a θ_e advection maximum over the southern Texas Panhandle, supplying moisture necessary for convection that occurs in this area. In stages B and D, during the LLJ peak, the advection maxima coincide with the downstream portion of the LLJ. The transition period due to the changes in the large scale forcing in stage C again shows its influence by reducing the mixing ratio advection maximum from about 21×10^{-8} g kg^{-1} s^{-1} to about 13×10^{-8} g kg^{-1} s^{-1} in just 12 hours.

The Eta model hourly forecasts allow more insight on the LLJ transport effects (not shown). The mixing ratio advection maximum in stage A forms over the southwest Texas Panhandle. The southeasterly winds hold the maximum over this location until the LLJ develops in full force toward stage B. After sunset on 5 May, the LLJ began strengthening over south central Texas. Between 0100 UTC and 0700 UTC on 6 May, the LLJ increased from 14 m s^{-1} to 21 m s^{-1} and repositioned the mixing ratio advection maximum to eastern Oklahoma.

C. Equivalent Potential Temperature Advection

The advection of equivalent potential temperature (θ_e) best portrayed the influence of the LLJ on developing convective areas of all variables studied. θ_e advection is closely related to warm advection and moisture advection. Since θ_e is partially dependent on temperature, it is associated with the large-scale ascent caused by warm

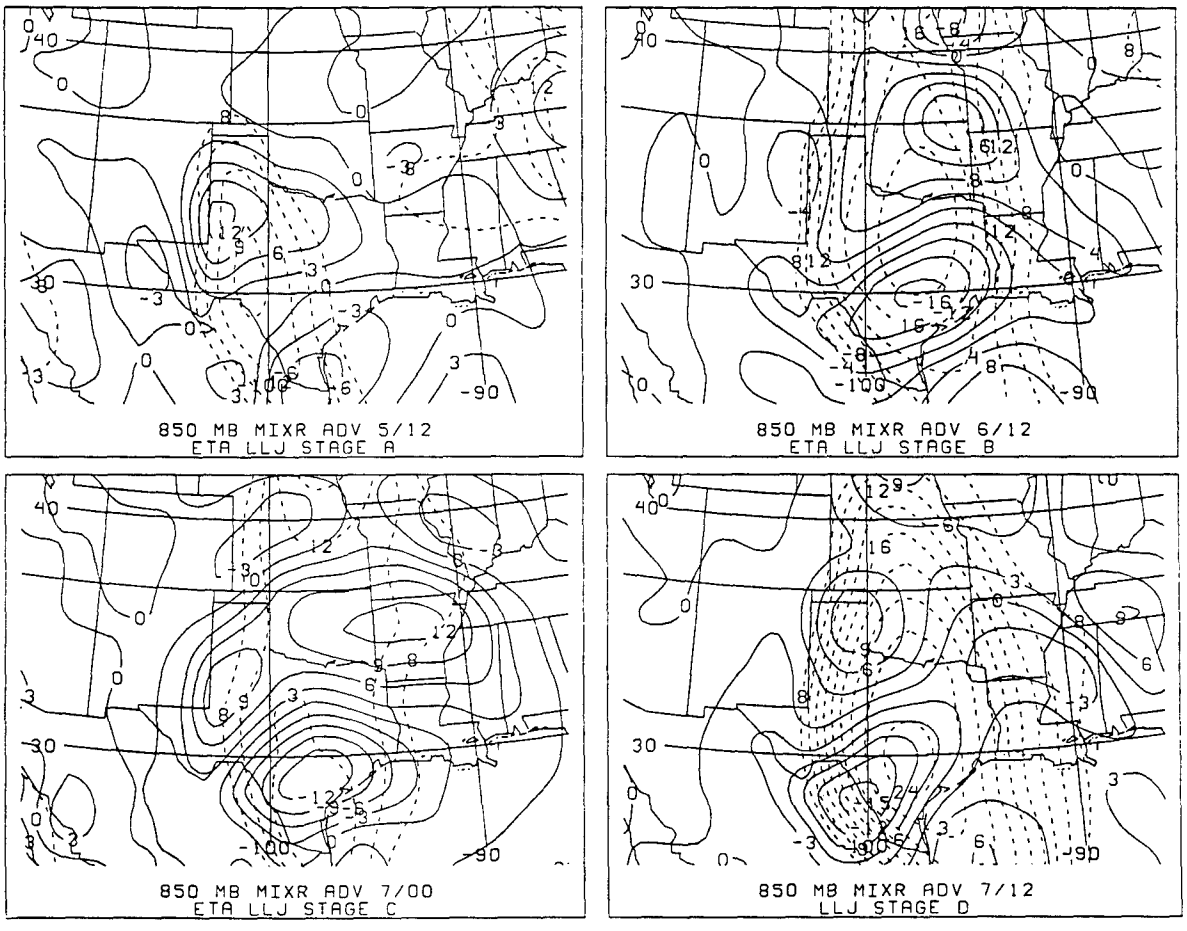

Fig. 36. Mixing ratio advection by the observed wind and wind magnitude (dashed lines) at 850 mb during stages A-D of the LLJ using Eta model output. Advection units are g kg^{-1} s^{-1}.

advection in the convective areas. Because θ_e is also a function of humidity, it is associated with the increase of precipitable water in convective areas shown by moisture advection.

Figure 37 shows θ_e advection of at least 3.6×10^{-4} K s^{-1} occurring in all four stages of the LLJ. In each stage, the θ_e advection maximum is located north of the LLJ core. In stage A, a maximum of 4.8×10^{-4} K s^{-1} is positioned near Lubbock, Texas northeast of the LLJ core. Thunderstorms are spread from Midland to Dalhart, Texas at this time. By stage B, the stronger LLJ of 21 m s^{-1} transports the θ_e advection maximum of 6.0×10^{-4} K s^{-1} north of Oklahoma City, Oklahoma. Again, convection is taking place throughout central Oklahoma in conjunction with the warm, humid air. The θ_e advection in stage C emphasizes the importance of the LLJ in transporting warm, humid air northward. The LLJ retreated over 500 km south and decreased in speed by 57 percent to 12 m s^{-1}. As a result, the θ_e advection decreased 40 percent to 3.6×10^{-4} K s^{-1}, and the convective activity reduced drastically around stage C. During the weakening of the LLJ at 0000 UTC on 7 May, only a few isolated thunderstorms were occurring just east of the θ_e advection maximum in western Arkansas. The 850 mb wind direction veered during this stage moving the maximum over the Oklahoma/Arkansas border. As the LLJ redeveloped in stage D, the maximum shifted over the northeast Texas Panhandle and western Oklahoma while increasing the θ_e advection maximum to 5.0×10^{-4} K s^{-1} and triggering numerous thunderstorms.

Vertical sections allow a more accurate examination of the lower tropospheric features. Figure 38 shows a combination of zonal and meridional vertical sections during the four stages of the LLJ. The newly formed southeasterly flow in stage A has focused the positive θ_e advection over the western Texas Panhandle. The maximum occurs near 850 mb over Lubbock, Texas in conjunction with the northerly extent of the LLJ core. Stage B shows the θ_e advection maximum's dependence for positioning on the LLJ core. The maximum appears adjoined to the LLJ core of 18 m s^{-1} since the LLJ core and θ_e advection maximum occur near 850 mb in close proximity to each other. The warm front's influence is evident in stage D of the LLJ core transports a θ_e advection ridge into

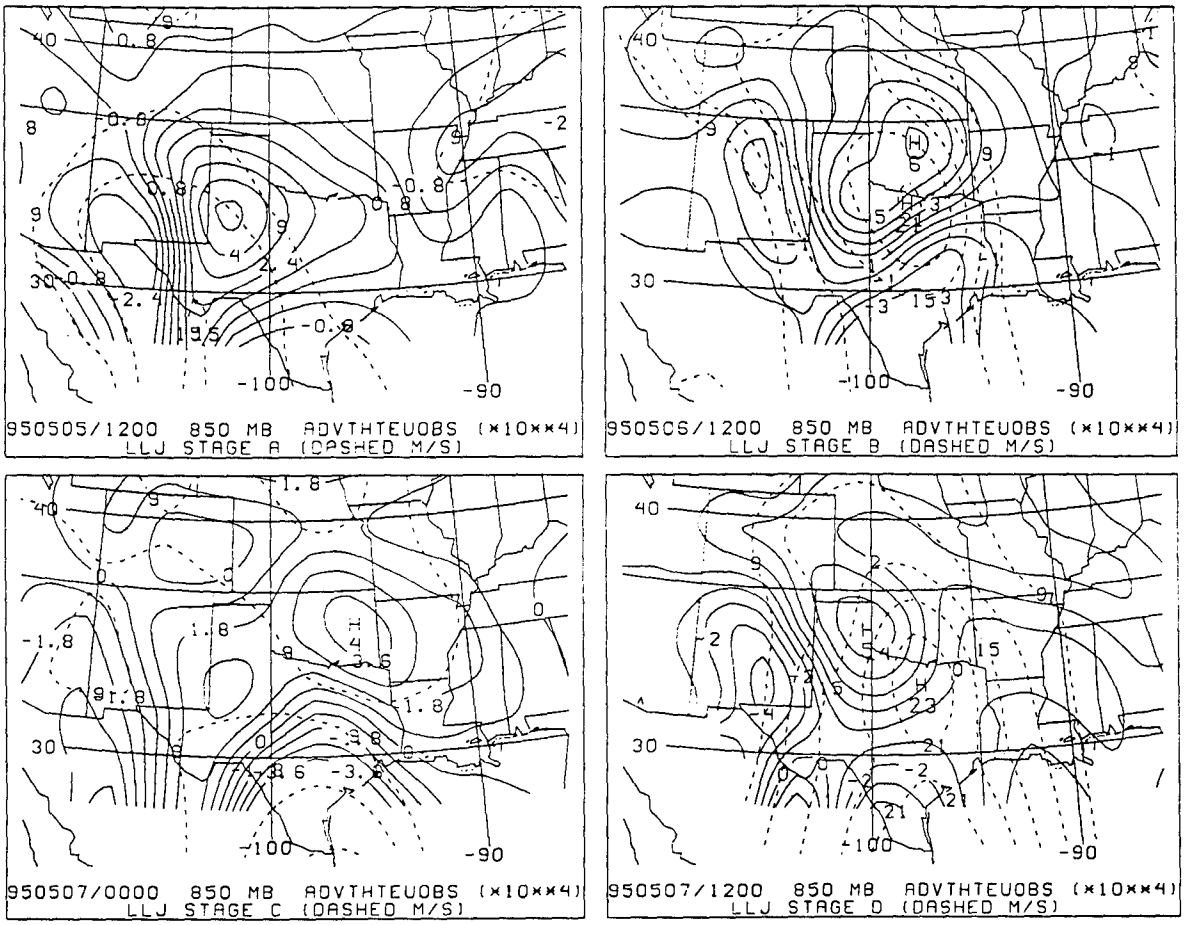

Fig. 37. Equivalent potential temperature advection by the observed wind and wind magnitude (dashed lines) at 850 mb during stages A-D of the LLJ. Advection units are °K s^{-1}. Thunderstorms develop in advection ridges during all four stages.

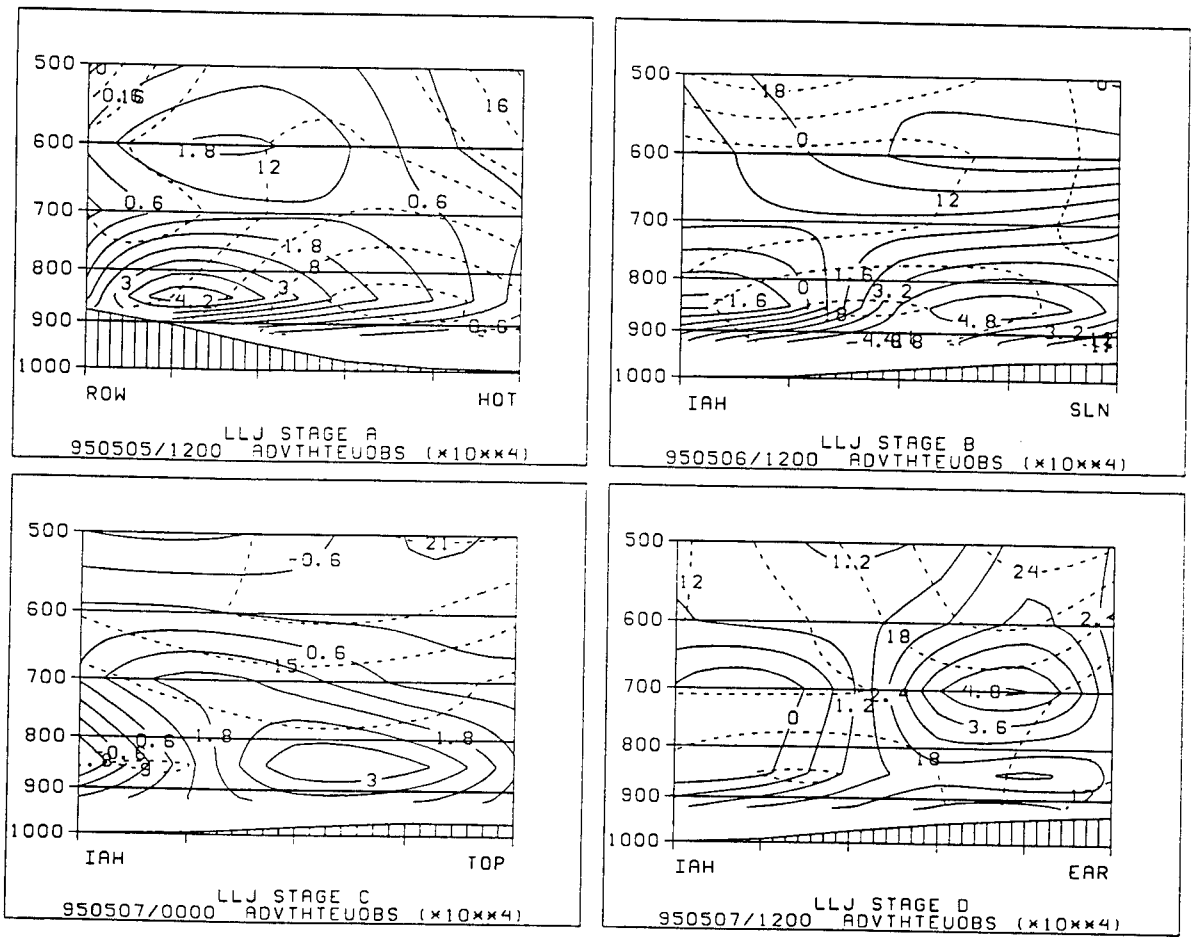

Fig. 38. Combination of zonal and meridional vertical sections of equivalent potential temperature advection by the observed wind and wind magnitude (dashed lines) during stages A-D of the LLJ between 1000 mb and 500 mb.

central Nebraska. The maximum has increased with the strengthening of the LLJ and ascends to 700 mb near the warm front and cyclone. The Eta model will show the importance of the θ_e advection ridge and its relationship to thunderstorm movement.

Hourly Eta forecasts accurately predict the location and values of positive θ_e advection over the first seven hours after each initial forecast but quickly lose effectiveness as the forecast times advance. At each initialization time, the model output is similar to the radiosonde values, but the model rapidly decreases the maximum values at 0800 UTC on both 6 and 7 May when the LLJ is strengthening. The comparison of forecast and initialized values show the model's inability to forecast after the seven hour point. At the LLJ's peak, 1200 UTC on 6 and 7 May, the Eta +12 hour forecasts are lower than the actual radiosonde values by 3.2×10^{-4} K s^{-1} and 1.2×10^{-4} K s^{-1} respectively. This underestimation at the +12 hour point held true for all four stages of the LLJ.

More important than the θ_e advection maximum in Figure 38 is the position of the θ_e advection ridge at 850 mb. The first seven hours of accurate Eta output allow us to verify a forecast technique for predicting thunderstorm development and movement (Glass et al. 1995). It appears the thunderstorms during the case develop in and move along positive θ_e advection ridges. Figure 39 shows the Eta θ_e advection forecasts at 850 mb between 0100 UTC and 0400 UTC on 6 May along with the LLJ speed and thunderstorm locations. A squall line developed near Dallas, Texas at 0000 UTC. This line of storms and the individual cells near San Angelo, Texas continued moving along the positive θ_e advection ridge. This technique for tracking the thunderstorm movement works during all four stages of the LLJ. Thunderstorms develop over the southern Great Plains and move in accordance to the positive θ_e advection ridge accurately forecast by the Eta model for at least the first 7 hours from the initialization of each stage. The LLJ again shows its importance in triggering and maintaining convection by arranging the lower tropospheric heat and water vapor it supplies to the convective areas.

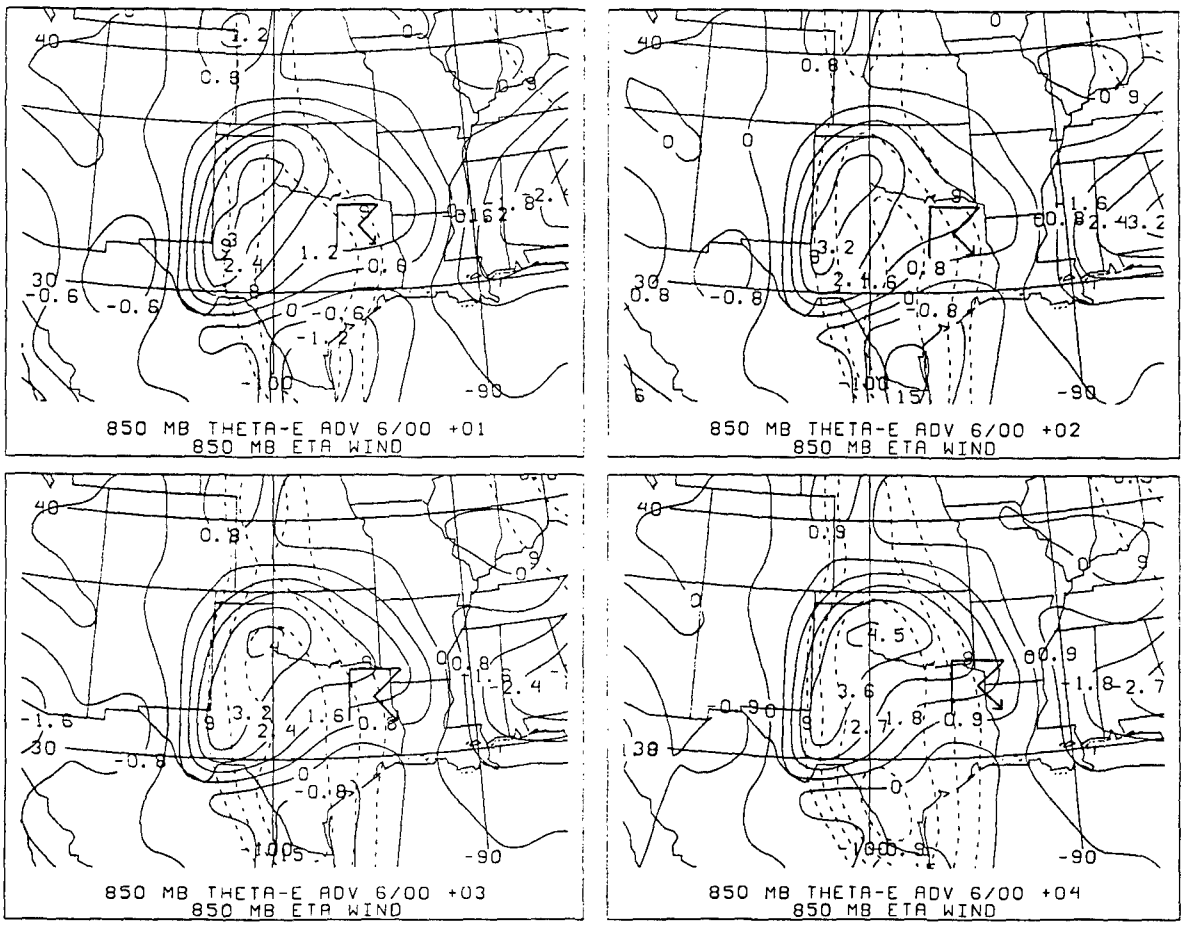

Fig. 39. Equivalent potential temperature advection by the observed wind and wind magnitude (dashed lines) at 850 mb using Eta model output. Panels 1-4 display output at 0000 UTC, 0200 UTC, 0300 UTC, and 0400 UTC on 6 May respectively. A squall line formed near Dallas, Texas and progresses eastward during the four panels along the positive advection ridge.

D. Transport on Isentropic Surfaces

The 301 K isentropic surface is found in the LLJ core during all four stages of the LLJ. This holds even as the LLJ flow ascends as part of the warm conveyor belt over the warm front in the central Great Plains. The LLJ starts below 900 mb in southern Texas and ascends to 750 mb in northern Kansas. This section focuses on the LLJ transport effects on this isentropic level.

In stage B, the LLJ transport generates a large area of warm advection over the Great Plains. A warm advection area of 1.4×10^{-4} °C s^{-1} extends from the LLJ core in northern Texas to the northern extent of the LLJ in South Dakota. Widespread rainshowers and thunderstorms cover this region of warm advection during the late morning hours on 6 May. The same is observed during stage D when a warm advection area of 2.0×10^{-4} °C s^{-1} is spread over the northern half of Texas. During both stages B and D, the LLJ core, warm advection, and thunderstorm activity appear intertwined. In the locations with thunderstorm activity, the most intense warm advection occurs between the 900 mb and 760 mb levels which is the same level where the LLJ resides.

The θ_e advection and mixing ratio advection patterns on the 301 K surface are nearly identical during the LLJ stages. It is apparent why Oklahoma was hardest hit by flooding rains during the study. A θ_e maximum covers Oklahoma during stages B, C, and D providing sufficient lift and water vapor necessary for deep convection. The LLJ transport of heat and water vapor kept the environment unstable for the three days during the case. In stages B and C, the maximum is positioned just north of the warm front, but it runs parallel to the cold front in close vicinity to the approaching cyclone in stage D. Figure 40 shows θ_e and pressure between the 300 K and 310 K isentropic surfaces. The meridional vertical section shows the θ_e maximum associated with the lee cyclone in stage D. We notice the large column of high water vapor and heat where lifting occurs in a vertical column. This is in sharp contrast to the other three LLJ stages where the θ_e maxima occur at 800 mb and below. The maximum located with the cyclone is the strongest in magnitude of the four LLJ stages.

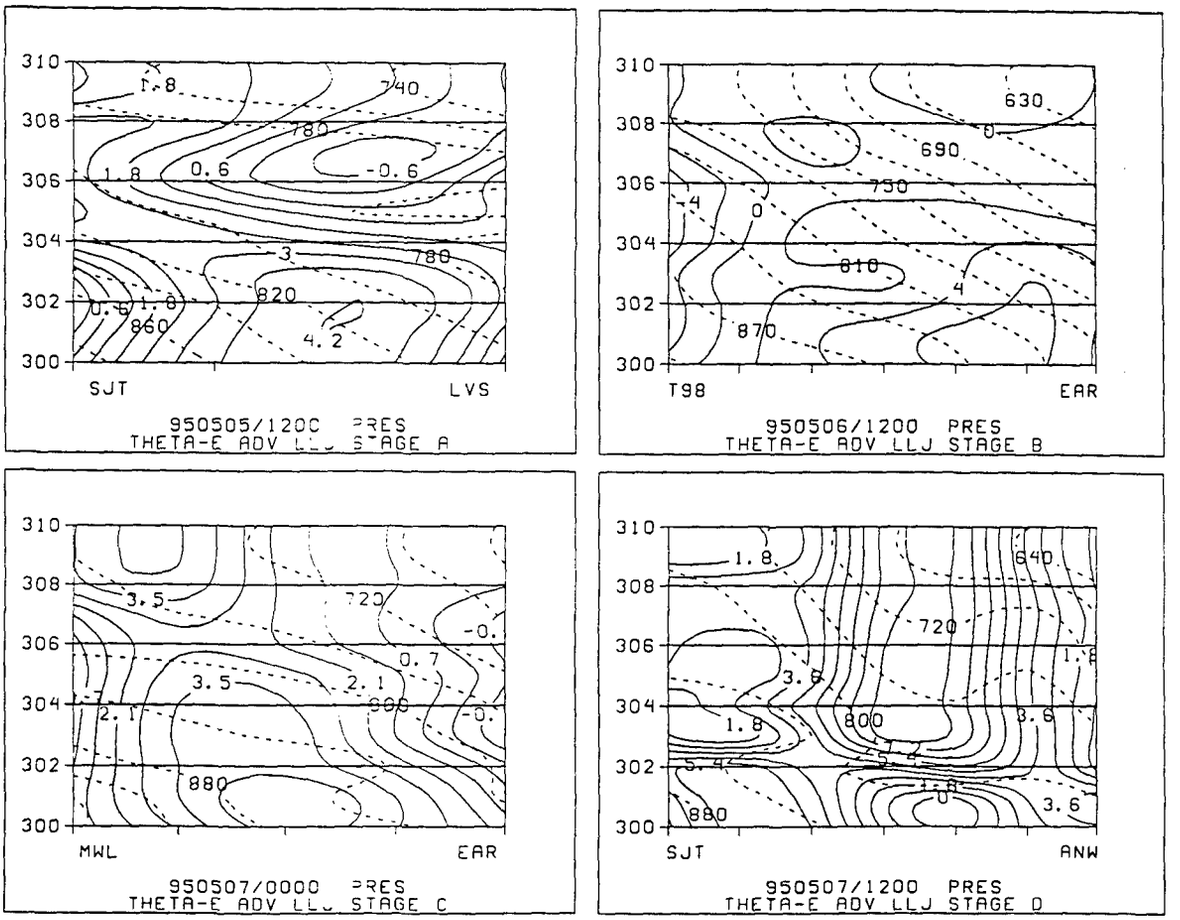

Fig. 40. Meridional vertical sections of equivalent potential temperature advection by the observed wind and pressure (dashed lines) between 300 K and 310 K isentropic surfaces during stages A-D of the LLJ.

Trajectories on the 301 K surface allow us to find the humid air source and track its progression through the LLJ cores. These trajectories are calculated using streamlines at the level of maximum wind 6 hours before and after the radiosonde observations. Figure 41 shows the trajectory results at 12 hour segments for this study. The trajectories in the eastern Gulf of Mexico remain under the anticyclonic influence of the high pressure that moved south behind a cold front a few days earlier. The western Gulf of Mexico appears to be the main water vapor source for the convective storms. All four trajectories in the western side of the Gulf of Mexico starting on 4 May travel over some portion of the Great Plains during this study.

Additional trajectory findings support the value of examining the low-level mixing ratio patterns to aid convective forecasting. The majority of air parcels in mixing ratio tongues of 9 g kg^{-1} or greater throughout Texas end in a rainshower or thunderstorm 12 hours later over Oklahoma, Kansas or Nebraska. In stages B and D, parcels initially positioned in the LLJ core end in mixing ratio advection maximums after 12 hours. As seen in the western trajectories, these parcels originally were stationed over the moist environment of the Gulf of Mexico and traveled into convective regions transported by the LLJ.

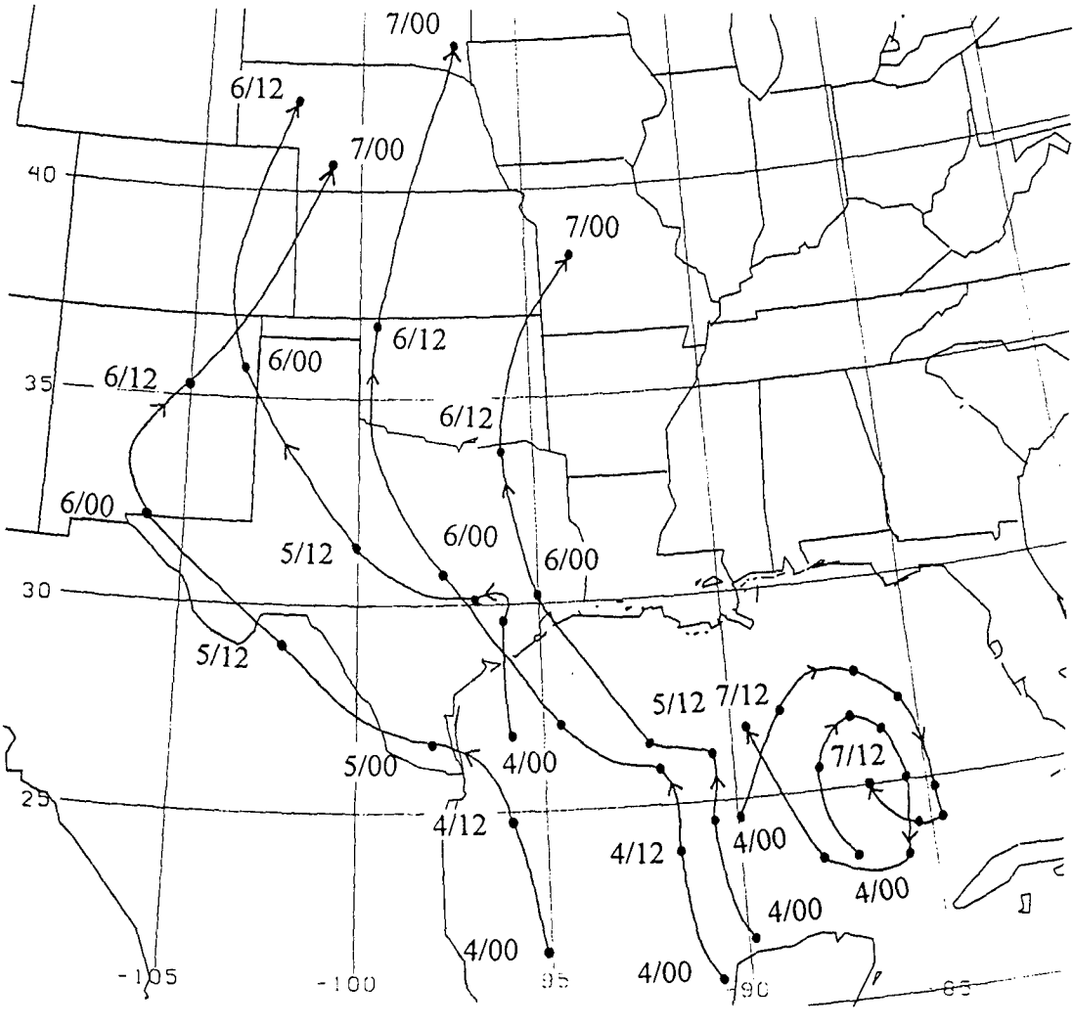

301 K ISENTROPIC TRAJECTORIES

Fig. 41. Parcel trajectories on the 301 K isentropic surface. All six trajectories begin at 0000 UTC on 4 May and progress at 12 hour segments represented by dots. Arrowheads indicate forward trajectory directions. The parcels in the east central Gulf of Mexico remain under anticyclonic influence during the four LLJ stages.

CHAPTER VII

ETA MODEL PERFORMANCE

The 80 km horizontal resolution, 38-level "Early" version of the Eta model offered supplementary output for this study. The 80 km version of the model replaced the LFM in June 1993 and the 48 km "Mesoscale" Eta model is being tested at the National Severe Storms Laboratory. This section presents a comparison of the Eta model output to radiosonde observations for the 3 day case study. This section will present results of the essential variables for the study.

A. Low-level Jet

Figure 42 shows the differences in wind magnitude at 850 mb between radiosonde observations and Eta model results for stages A-D of the LLJ. The high terrain in western Texas and eastern New Mexico affects the location of the LLJ core in stages A and B. The gridded radiosonde observations ignore terrain surfaces that occur at and above the 850 mb level. In stage A, this results in a LLJ core placed too far west over Mexico rather than over southwestern Texas by the radiosonde observations. Eta placement of the core just east of the higher terrain is more realistic than using the gridded observations at 850 mb. The two cores have different locations, but the effects on the transport properties are minor (shown in section C). The cores overlap in stage B and have speed values within 1 m s^{-1} of each other. Once again, the Eta speed values in this stage decrease sharply toward the higher terrain as it elevates above the 850 mb level. The model handled the speed change during the transition period in stage C well but extended the 12 m s^{-1} isotach into north central Texas. Also on the downside, the Eta overpredicts the core speed by 2 m s^{-1} in stage D and does not develop the separate maximum over Brownsville, Texas. The 18 m s^{-1} isotachs are almost identical, but the higher speeds exhibit a geographical discrepancy.

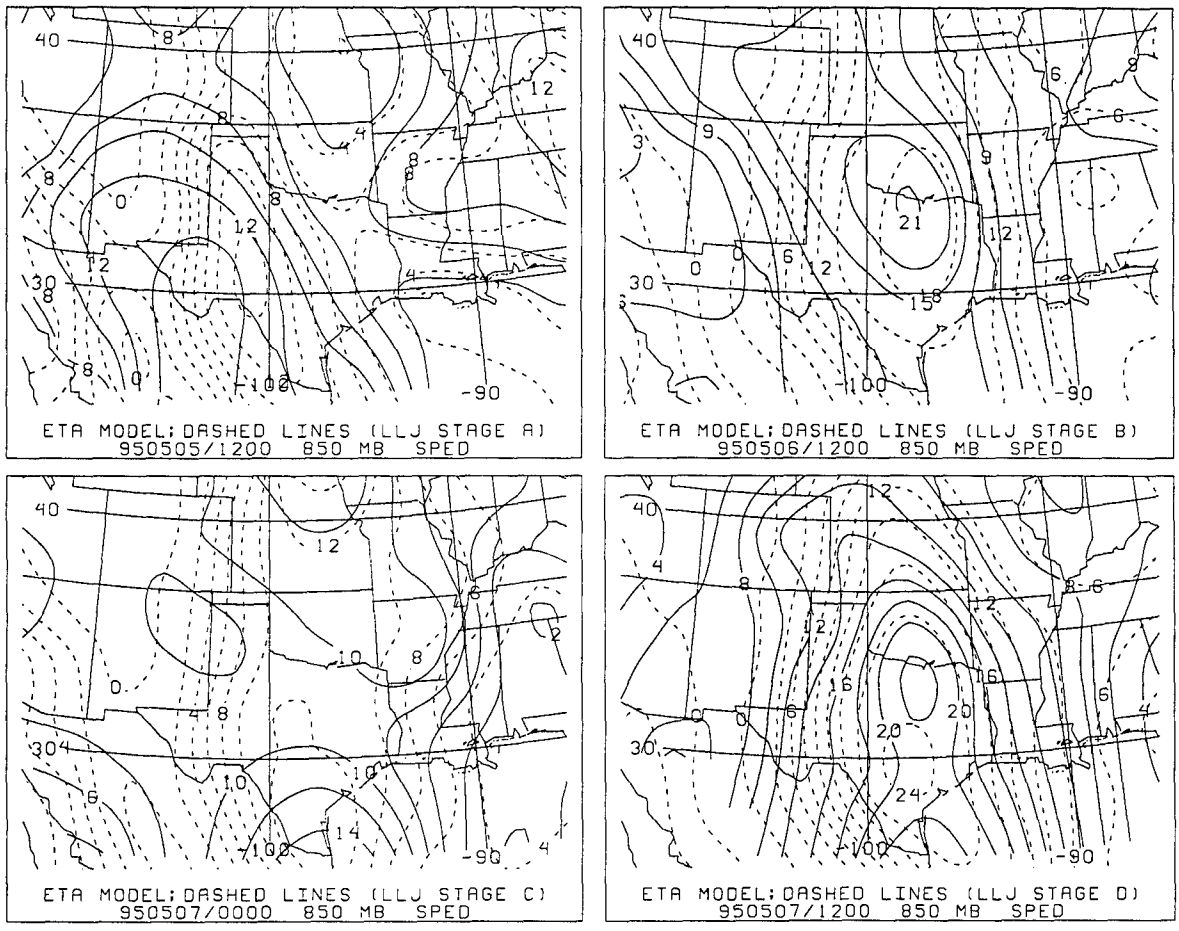

Fig. 42. Wind magnitude at 850 mb during stages A-D of the LLJ for radiosonde (solid lines) and Eta model output (dashed lines).

A plot of Eta output and radiosonde observations grids for the southerly wind component at 850 mb shows the strong southerly nature of the LLJ. The locations of maxima on this chart are almost identical to Fig. 42. This figure also reveals the model's failure to develop two separate maxima over Texas in stage D. The model places one core between the two observed cores over Texas. Overall, in all four stages, the cores overlap verifying the model's capability of predicting low-level wind magnitude and direction ahead of a developing cyclone system with only a few inconsistencies.

The Eta's ability to predict low-level wind divergence and convergence was not as good as the previous two variables. Although the wind magnitude and direction are quite similar between the outputs, the wind divergence shows a large variation in three of the four LLJ stages (not shown). In stage A, areas of maximum convergence at 850 mb from both outputs overlap in western Texas and southeast New Mexico. This occurs with the LLJ just developing at a speed of 15 m s^{-1}. As the wind speed increases in stages B and D, the distance between convergence maxima also increases. In stage B, the Eta maximum is centered over northeast Oklahoma. The radiosonde observations show two maxima, one centered over north central Oklahoma and a second over southeastern Missouri. This signifies the importance of the STJ streak in positioning the low-level wind convergence pattern. An eastward Eta maximum does not develop in stage B under the 200 mb jet streak right rear quadrant. In stage D, the radiosonde observations maximum is still located over north central Oklahoma, but the Eta maximum has moved over the Texas Panhandle.

For this case, the Eta output for wind magnitude and direction provided quality output, but the model's development upper-level features appears to have negative effects on the low-level wind convergence patterns. In comparison to an Eta model test over the Gulf Coast states (Janish et al. 1995), the Eta resolved three errors. The Eta output correctly forecast the LLJ strength in all four stages only missing the actual location in stage D when it failed to develop separate maxima over Texas. Vertical sections showed the upward slope of the LLJ from the Gulf of Mexico. Lastly, the Eta LLJ did not progress rapidly eastward ahead of the approaching cold front as in the Janish study.

B. Upper-level Jets

Figure 43 shows wind magnitude at 200 mb radiosonde observations and the Eta model output. The 200 mb level is closest to the STJ which plays a major role during this study in developing the LLJ and convective activity. Since the jet streak's location is pivotal in developing the lower branch of the ageostrophic circulation (Chapter V), this section will focus on the position of the upper-level streaks. During the study, the value of the streak's maximum wind speed proved not as important as the exit region location in forcing the lower-tropospheric wind.

In stage A, the two data sources contain many similarities between upper and lower level features. The STJ exit regions are shown near the same location over north central Mexico, western Texas, and southern New Mexico. The model shows some error in stage B improperly placing the STJ streak. The radiosonde streak moves over the southern Great Plains while the model streak remains over north central Mexico. Despite this discrepancy, the two 850 mb LLJ cores occur in close proximity to one another. The stage C comparison shows great similarities between the two data sources. The streaks are still over southwest Texas, and the trough over Utah is shown by both sources. The quality output continues in stage D for a complex pattern over the Great Plains, but minor differences in streamlines at the 200 mb level cause errors in the low-level convergence patterns.

Figure 44 contains divergence patterns for Eta model and radiosonde observations at 200 mb during stages A-D of the LLJ. The heaviest convection during the case occurs closest to stages B and D. The radiosonde observations show a divergence maximum in stage B occurs over extreme western Oklahoma, but the Eta maximum is farther east over Oklahoma City. Stage D is closest to the observed data for the four stages in similarities between the two sources. The jet streak maxima almost entirely overlap over western Kansas. Overall, these inconstancies instill a lack of confidence in using the model as a lone forecasting source. This emphasizes the fact that one should only use model output to supplement a forecast as one of many tools.

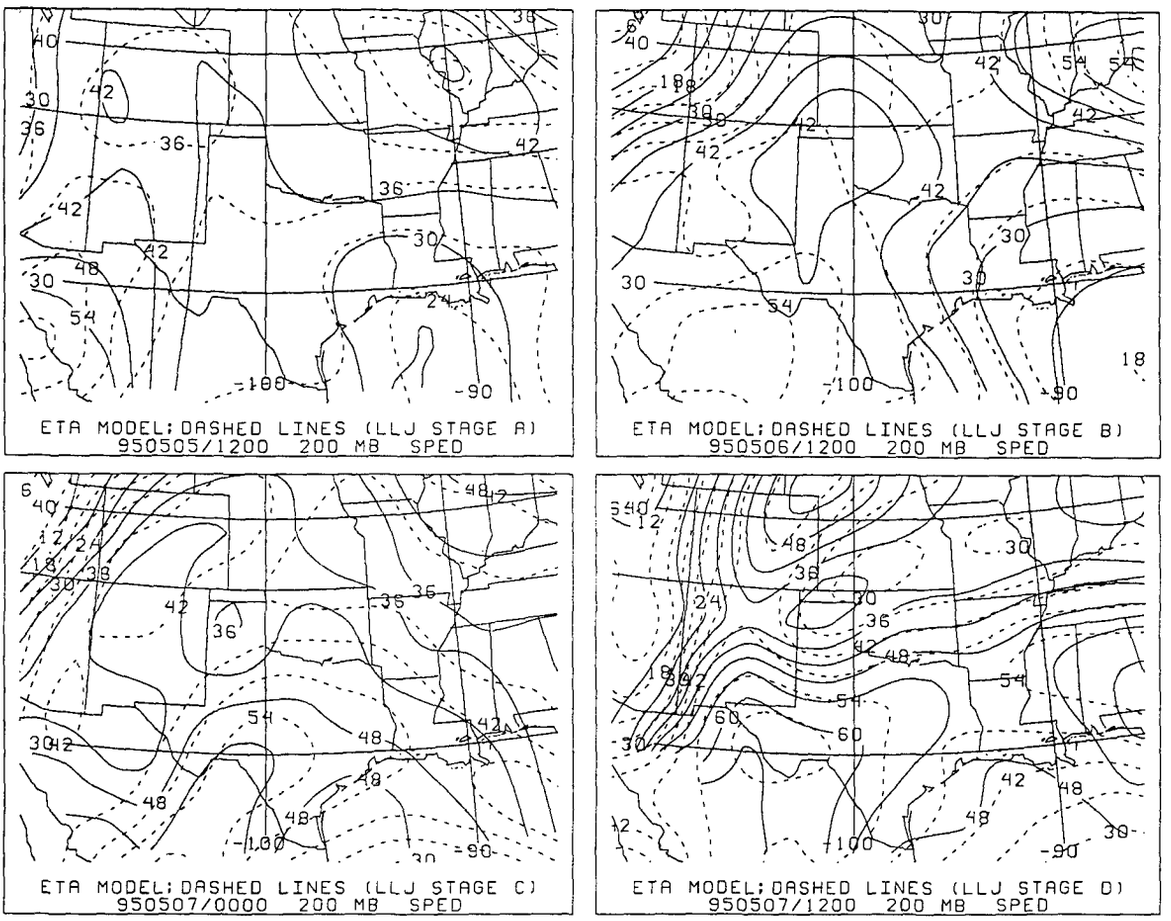

Fig. 43. Wind magnitude at 200 mb during stages A-D of the LLJ for radiosonde (solid lines) and Eta model output (dashed lines).

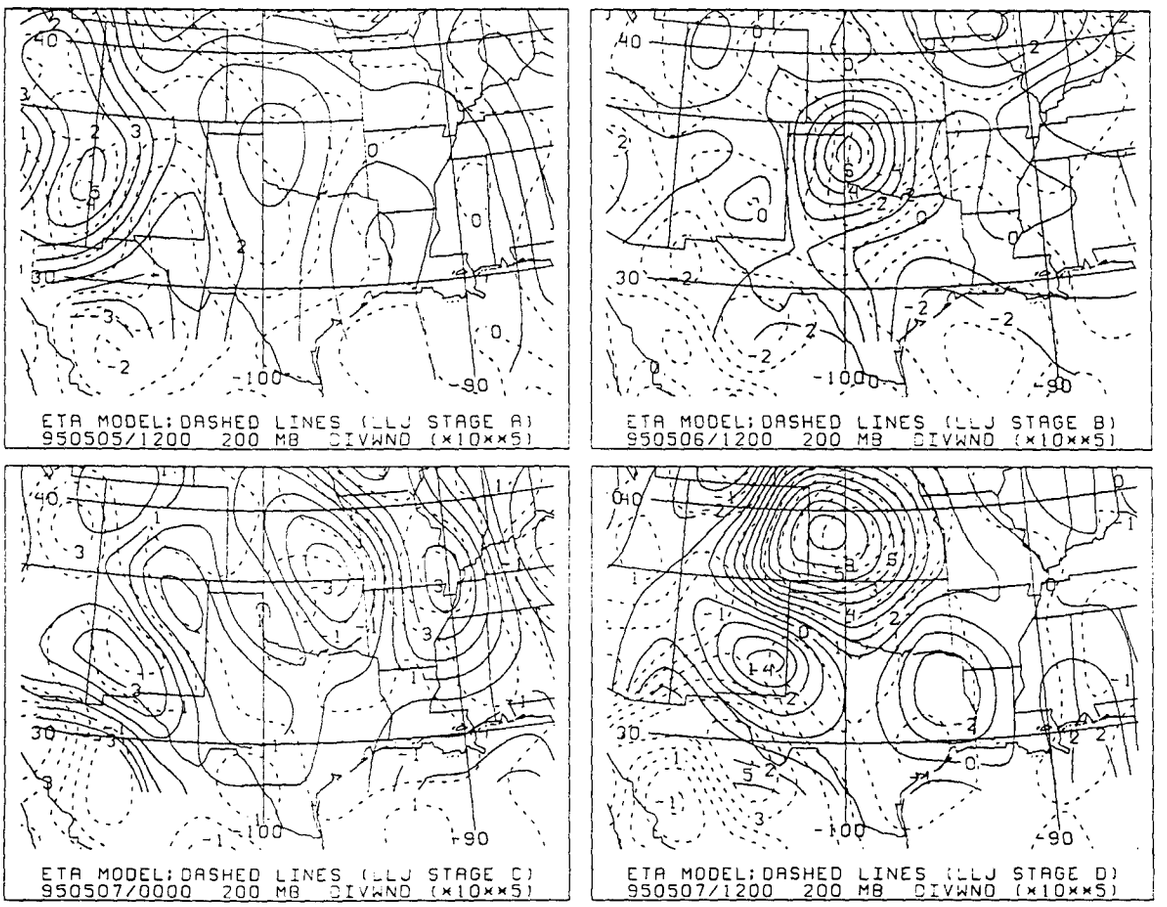

Fig. 44. Wind divergence at 200 mb during stages A-D of the LLJ for radiosonde (solid lines) and Eta model output (dashed lines).

C. Heat and Water Vapor Transport

Temperature advection patterns for Eta forecasts and radiosonde observations reveal the effects of slight differences in LLJ placement by the two data sources not shown. This is most evident in stage A where the Eta LLJ farther east created a temperature advection maximum over the Texas Panhandle. At this time, the radiosonde maximum is positioned over eastern New Mexico. The Eta's placement is the more accurate of the two due to terrain consideration by the model. Although the maximum values differ in stages B and D, both sources show a widespread area of warm advection over the southern Great Plains. The Eta failed to include cold advection behind the approaching cold front over Arizona and New Mexico in stage D, this did not influence the LLJ. Overall, the Eta deficiencies were minimal for temperature advection and developed the pattern of general ascent over the convective areas.

The model results were excellent for mixing ratio flux and for the southerly wind component. Mixing ratio flux patterns in stages A, B, and D were nearly identical between the two data sources. The only discrepancy occurred in stage C when the Eta failed to reduce the LLJ speed the full amount during its diurnal decrease. As a result, the Eta forecast for the flux maximum is stronger and displaced over north central Texas.

Figure 45 plots Eta model and radiosonde values of θ_e advection for stages A-D of the LLJ. Despite its minor flaws, the Eta output proves to be a valuable tool when viewing this variable (when viewed between +00 and +07 hours). All of the maxima overlap for θ_e advection but more importantly, the patterns are almost identical. The only significant difference was in stage B due to the STJ streak placement that formed the Eta LLJ east of the actual LLJ.

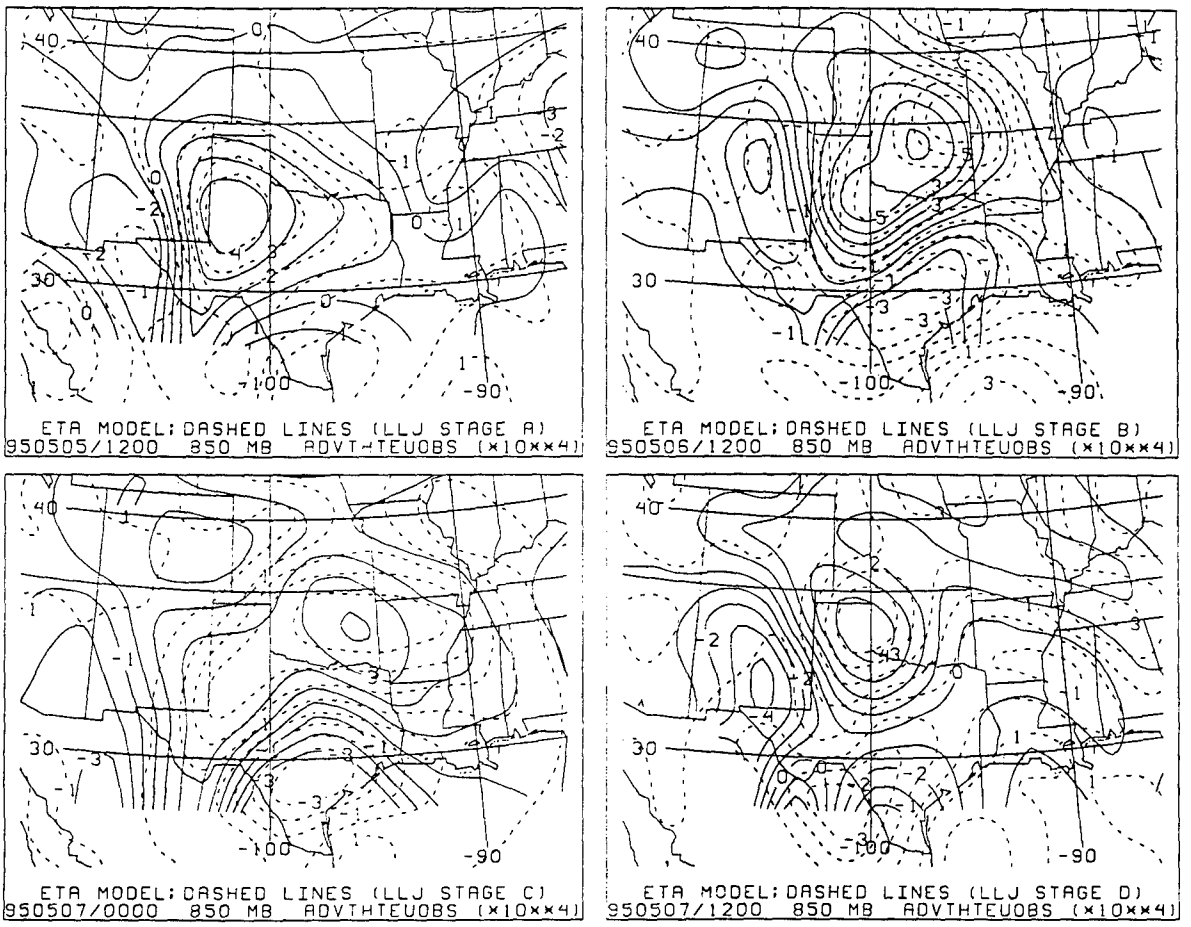

Fig. 45. Equivalent potential temperature advection at 850 mb during stages A-D of the LLJ for radiosonde (solid lines) and Eta model output (dashed lines).

CHAPTER VIII

CONCLUSIONS AND DISCUSSION

This study focused on the development of a LLJ with an apparent diurnal oscillation during 5-8 May 1995 over the southern Great Plains. The LLJ was forced by a subtropical jet streak exit region, by a weakening cyclone system west of the Rockies, and by a newly formed lee cyclone. Theories proposed by Uccellini and Johnson (1979), Djuric and Damiani (1980), and Chen et al. (1994) were used to examine these features. Eta model output provided a supplementary data source to examine the LLJ evolution and transport properties.

A. Summary of Conclusions

These main points surfaced during the study:

1. The diurnally oscillating LLJ exhibits a large scale pattern similar to Uccellini's Type I LLJ but oscillates like Uccellini's Type II jet. The speed maximum extends vertically near 700 mb, but its speed decreases by nearly 50 percent toward sunset much like a boundary layer jet. This time appears to be a transition between the large scale forcing of the STJ streak exit region and the isallobaric flow in response to lee cyclogenesis. The large decrease in the 200 mb diffluence between the PJ and STJ over the southern Great Plains seemed to initiate the weakening of the LLJ.

2. Isentropic trajectories and Eta model output showed the LLJ was essential in transporting warm, humid air from the Gulf of Mexico into the convective regions. The structure of the LLJ (southerly winds to about 750 mb) created a sharp contrast in air masses. Winds veered to the southwest and west above the LLJ, advecting cooler, drier air into the middle troposphere above the convective region.

3. The development of the LLJ was closely tied to the position of the STJ streak exit region. A vertical section through the exit region showed that the LLJ in

stages A and B increased as the lower portion of a thermally indirect circulation. The LLJ intensified due to the cross-contour ageostrophic wind that accelerated the southerly winds. In areas of cross-contour ageostrophic flow directed toward a trough or low center, the LLJ increased in speed. Away from highly curved flow, the ageostrophic and isallobaric winds are nearly equal. A strong subsidence inversion in the southern portion of the LLJ core shows the sinking motion as the southern branch of the circulation. Vertical sections of omega indicate ascent over the northern half of the LLJ and descent over the southern half of the core.

4. The LLJ evolved in response to multiple large scale forcing. Height falls associated with a trough and lee cyclogenesis strengthened the LLJ. The trough was moving east over the northern Great Plains, and the lee cyclone formed over New Mexico and Colorado. The isallobaric wind accounted for part of the speed increase. The 850 mb height gradient between the area of lee cyclogenesis and the LLJ core increased from 55 gpm in stage B to 95 gpm in stage D. Lee cyclogenesis did not lead to LLJ development in this case but strengthens the LLJ after it is already established. The STJ streak and trough over the northern Great Plains initiated the LLJ development.

5. Hourly Eta model forecasts showed the LLJ develop around 0200 UTC (9pm local time) each evening before convection activity intensified.

6. For θ_e advection at 850 mb, the Eta model accurately predicted the location and values of maxima over the first 7 hours. Eta model hourly forecasts of θ_e advection (within 7 hours of the initialization time) showed thunderstorms develop and progress along ridges of positive θ_e advection. Although the LLJ was still strengthening around 0800 UTC, the Eta showed the θ_e advection values decreasing. This was likely the cause of major differences between the 12 hour forecasts and observed values.

7. Eta model 12 hour forecasts of temperature advection were 25 to 40 percent higher than actual values for the four stages of the LLJ.

8. Low-level wind convergence patterns forecast by the Eta model faltered due to improper placement of ULJ streaks.

9. Eta model output of the southerly wind component and mixing ratio flux were very close to observed values.

B. Discussion of Research

The development and evolution of a low-level jet was studied as it transported heat and water vapor into convective areas over the southern Great Plains. The warm, moist lower-troposphere was necessary to create favorable conditions for severe convection. The LLJ was essential in transporting heat and moisture into the convection areas. The transport generated convective instability in the lower troposphere, lowered the level of free convection and raised the equilibrium level. Uccellini and Johnson (1979) found the LLJ forms in the lower part of a thermally indirect circulation underneath the exit region of an upper-level jet streak. Strong cross-contour ageostrophic winds developed under the subtropical jet streak exit region and accelerated the winds forming the LLJ.

Typically called a diurnal oscillation of a boundary layer jet, this case demonstrated a remarkable weakening of a LLJ in stage C making it unique. This was a transition time between large scale forcing mechanisms. The acceleration from the cross-contour ageostrophic wind and the isallobaric wind decreased. The trough over the northern Great Plains moved well north and lee cyclogenesis was just beginning. Also, the ageostrophic circulation induced by the STJ streak weakened as the streak moved over southern Texas. The physical properties of the streak classify it as a Type I LLJ (Uccellini 1980), but the nearly 50 percent decrease in speed and magnitude are similar to the Type II LLJ. This Type II LLJ is usually confined to the planetary boundary layer. The forcing from the STJ streak, a trough over the northern Great Plains, and a lee cyclone allowed such a jet to develop, but these large scale forces shifted in stage C to allow the decrease in the LLJ. The lee cyclone did not lead to the development of the LLJ as in most cases, but it strengthened the jet as cyclogenesis occurred.

VITA

Christopher Scott Donahoe w[redacted] to Mr. and Mrs. Ronald V. Donahoe. He graduated from Mascoutah Community High School, Mascoutah, Illinois in 1987. In 1991, he received a B.S. in Meteorology from St. Louis University. That year, he was also commissioned into the U.S. Air Force as a Second Lieutenant. He was stationed at Nellis Air Force Base in Las Vegas, Nevada from spring 1992 to summer 1994. While at Nellis, he also served a three month tour in Riyadh, Saudi Arabia in support of Operation Southern Watch. Beginning in August 1994, he was assigned to Texas A&M University under the Air Force Institute of Technology. After graduation, he will be working as a Weather Instructor for the Weather Training School at Keesler AFB, Mississippi.

[redacted]

REFERENCES

Black, T. L., 1994: The new NMC mesoscale eta model: Descriptions and forecast examples. *Wea. Forecasting*, **9**, 265-278.

——, D. G. Deaven, and G. DiMego, 1993: The step-mountain eta coordinate model: 80 km 'Early' version and objective verification. Technical Procedures Bulletin 412, NOAA/NWS, 31 pp. [Available from the National Weather Service, Office of Meteorology, 1325 East-West Highway, Silver Spring, Maryland 20910.]

Blackadar, A. K., 1957: Boundary layer wind maxima and their significance for the growth of nocturnal inversions. *Bull. Amer. Meteor. Soc.*, **38**, 283-290.

Bonner, W. D., 1968: Climatology of the low level jet. *Mon. Wea. Rev.*, **96**, 833-850.

Browning, K. A., and C. W. Pardoe, 1973: Structure of low-level jet streams ahead of mid-latitude cold fronts. *Quart. J. Roy. Meteor. Soc.*, **99**, 619-638.

Carlson, T. N., 1991: *Mid-Latitude Weather Systems*. Harper Collins Academic, 507 pp.

Chen, T-C., and J. A. Kpaeyeh, 1993: The synoptic-scale environment associated with the low-level jet of the Great Plains. *Mon Wea. Rev.*, **121**, 416-420.

Chen, Y-L., X. A. Chen, and Y-X Zhang, 1994: A diagnostic study of the low-level jet during TAMEX IOP 5. *Mon. Wea. Rev.*, **122**, 2257-2284.

Djuric, D., 1981: A numerical model of the formation and evolution of a low-level jet. *Mon. Wea. Rev.*, **109**, 384-390.

——, and M. S. Damiani, Jr., 1980: On the formation of the low-level jet over Texas. *Mon. Wea. Rev.*, **108**, 1854-1865.

——, and D. S. Ladwig, 1983: Southerly low-level jet in the winter cyclones of the southwestern Great Plains. *Mon. Wea. Rev.*, **111**, 2275-2281.

Glass, F. H., D. L. Ferry, J. T. Moore, and S. M. Nolan, 1995: Characteristics of heavy convective rainfall events across the Mid-Mississippi Valley during the warm season: Meteorological conditions and a conceptual model. Preprints, *14th Conf. Weather Analysis and Forecasting*, Dallas, Texas, Amer. Meteor. Soc., 34-41.

Hoskins, B. J., and M. A. Pedder, 1980: The diagnosis of middle latitude synoptic development. *Quart. J. Roy. Meteor. Soc.*, **106**, 707-719.

Janish, P. R., K. E. Mitchell, G. J. DiMego, S. J. Weiss, and S. W. Lyons, 1993: Impacts of Nested Grid Model changes and Eta Model performance on low-level moisture evolution during the return flow cycle. Preprints, *17th Conf. Severe Local Storms*, St. Louis, Missouri, Amer. Meteor. Soc., 512-515.

Martin, J. E., J. D. Locatelli, P. V. Hobbs, P-Y. Wang, and J. A. Castle, 1995: Structure and evolution of winter cyclones in the Central United States and their effects on the distribution of precipitation. Part I: A synoptic-scale rainband associated with a dryline and lee trough. *Mon. Wea. Rev.*, **123**, 241-264.

Mesinger, F., 1984: The sigma system problem. Preprints, *Seventh Conf. on Numerical Weather Prediction*, Montreal, Canada, Amer. Meteor. Soc., 340-347.

Mesinger, F., Z. I. Janjic, S. Nickovic, D. Gavrilov, and D. G. Deaven, 1988: The step-mountain coordinate: Model description and performance for cases of alpine lee cyclogenesis and for a case of an Appalachian redevelopment. *Mon. Wea. Rev.*, **116**, 1493-1514.

Miller, R. C., 1972: Notes on analysis and severe storms forecasting procedures of the Air Force Global Weather Central. Tech. Rep. 200 (Rev.), USAF Air Weather Service, Scott AFB, Illinois.

Uccellini, L. W., 1980: On the role of upper tropospheric jet streaks and leeside cyclogenesis in the development of low-level jets in the Great Plains. *Mon. Wea. Rev.*, **108**, 1689-1696.

——, and D. R. Johnson, 1979: The coupling of upper and lower tropospheric jet streams and implications for the development of severe convective storms. *Mon. Wea. Rev.*, **107**, 682-702.

——, P.J. Kocin, R. A. Petersen, C.H. Wash, and K. F. Brill, 1984: The Presidents' Day cyclone 18-19 February 1979: Synoptic overview and analysis of the subtropical jet streak influencing the pre-cyclogenetic period. *Mon. Wea. Rev.*, **112**, 31-55.

VITA

Christopher Scott Donahoe was born in San Angelo, Texas on 30 December 1968 to Mr. and Mrs. Ronald V. Donahoe. He graduated from Mascoutah Community High School, Mascoutah, Illinois in 1987. In 1991, he received a B.S. in Meteorology from St. Louis University. That year, he was also commissioned into the U.S. Air Force as a Second Lieutenant. He was stationed at Nellis Air Force Base in Las Vegas, Nevada from spring 1992 to summer 1994. While at Nellis, he also served a three month tour in Riyadh, Saudi Arabia in support of Operation Southern Watch. Beginning in August 1994, he was assigned to Texas A&M University under the Air Force Institute of Technology. After graduation, he will be working as a Weather Instructor for the Weather Training School at Keesler AFB, Mississippi.

The author's permanent mailing address is:

141 Chanel NE

Huntsville, Alabama 35811